КОЛЛОИДНЫЙ ЖУРНАЛ

COLLOID JOURNAL

(KOLLOIDNY ZHURNAL)

WITHDRAWN
POSTMASTER:
IF NOT DELIVERABLE NOTIFY
Chemical Abstracts
OHIO STATE UNIV., COLUMBUS 10, O.
AND POSTAGE WILL BE SENT
REC'D. APR 7 1958 C. A. LIBRARY
ABSTRACTOR:
PLEASE RETURN PROMPTLY TO
CHEMICAL ABSTRACTS
OHIO STATE UNIV., COLUMBUS 10, O.

IN ENGLISH TRANSLATION

~~VOL.~~ 19 1957 NO. 4

CONSULTANTS BUREAU, INC.
227 WEST 17TH STREET, NEW YORK 11, N. Y.
an agency for the interpretation of international knowledge

RUSSIAN AND GERMAN CRYSTALLOGRAPHY RESEARCH

IN COMPLETE ENGLISH TRANSLATION

THE GROWTH OF CRYSTALS—A Conference on the Growth of Crystals held by the Acad. Sciences, USSR, March, 1956, published in Russian June, 1957. Major Soviet contribution in this field. 43 important papers, 291 pages. Table of Contents on request.

Contents:

Introduction
I. General Questions
II. Theory
III. Experimental Research
IV. Growing of Single Crystals, Apparatus and Methods
V. Miscellaneous

only $15.00

SOVIET RESEARCH IN CRYSTALLOGRAPHY—Collection No. 5. Approx. 300–350 articles selected from all Russian chemical journals translated by Consultants Bureau, 1949–1955, comprising an estimated 1300 pages. To be published Feb. 1958. Single papers $7.50 each—Table of Contents on request. Price to be announced (approx. $150–$200) Contents—still tentative:

I. Structure determination, and structural change
II. Compound formation, and reaction studies in complex systems
III. Transformation, solubility, and phase diagrams
IV. Metals systems and their reactions
V. Experimental techniques and research methods
VI. Structure-sensitive properties
VII. Crystal growth and forms
VIII. General and theoretical papers

SPLITTING OF TERMS IN CRYSTALS, by Hans A. Bethe. The first publication in English of this important paper, originally published in German in 1929. Translated by Wendell Furry, who says of this work, "A classic in the field, by one of the world's most important theoretical physicists—of great interest to students of solid-state physics." **70 pages. $3.00**

All Consultants Bureau translations by *bilingual scientists*. Books are staple bound in durable paper covers; includes all diagrammatic and tabular material integral with the text; text is clearly reproduced by multilith process from IBM "cold type". For Tables of Contents to books, and for free catalogs of our Russian translations, address Dept. S, specifying field of interest.

CONSULTANTS BUREAU, INC.
227 WEST 17th STREET, NEW YORK 11, N. Y. — U.S.A.
Telephone: ALgonquin 5-0713 • Cable Address: CONBUREAU, NEW YORK

COLLOID JOURNAL

(KOLLOIDNY ZHURNAL)

Journal of Theoretical and Applied Physics and
Chemistry of Colloids

Volume XIX

(Number 4, July-August, 1957)

Editor

A. V. Dumansky

Editorial Board

P. N. Antipov-Karataev, B. V. Deryagin, B. A. Dogadkin (Deputy Editor), A. V. Dumansky,
V. A. Kargin, S. M. Lipatov, P. A. Rebinder, I. P. Serdobolsky (Secretary), M. P. Volarovich

Publication of the Academy of Sciences of the USSR

IN ENGLISH TRANSLATION

Copyright, 1957

CONSULTANTS BUREAU, INC.
227 West 17th Street
New York 11, N. Y.

Printed in the United States

Annual Subscription	$ 80.00
Single issue	20.00

Note: The sale of photostatic copies of any portion of this copyright translation is expressly prohibited by the copyright owners. A complete copy of any paper in this issue may be purchased from the publisher for $ 7.50.

SIGNIFICANCE OF ABBREVIATIONS MOST FREQUENTLY ENCOUNTERED IN SOVIET PERIODICALS

FIAN	Phys. Inst. Acad. Sci. USSR.
GDI	Water Power Inst.
GITI	State Sci.-Tech. Press
GITTL	State Tech. and Theor. Lit. Press
GONTI	State United Sci.-Tech. Press
Gosenergoizdat	State Power Press
Goskhimizdat	State Chem. Press
GOST	All-Union State Standard
GTTI	State Tech. and Theor. Lit. Press
IL	Foreign Lit. Press
ISN (Izd. Sov. Nauk)	Soviet Science Press
Izd. AN SSSR	Acad. Sci. USSR Press
Izd. MGU	Moscow State Univ. Press
LEIIZhT	Leningrad Power Inst. of Railroad Engineering
LET	Leningrad Elec. Engr. School
LETI	Leningrad Electrotechnical Inst.
LETIIZhT	Leningrad Electrical Engineering Research Inst. of Railroad Engr.
Mashgiz	State Sci.-Tech. Press for Machine Construction Lit.
MEP	Ministry of Electrical Industry
MES	Ministry of Electrical Power Plants
MESEP	Ministry of Electrical Power Plants and the Electrical Industry
MGU	Moscow State Univ.
MKhTI	Moscow Inst. Chem. Tech.
MOPI	Moscow Regional Pedagogical Inst.
MSP	Ministry of Industrial Construction
NII ZVUKSZAPIOI	Scientific Research Inst. of Sound Recording
NIKFI	Sci. Inst. of Modern Motion Picture Photography
ONTI	United Sci.-Tech. Press
OTI	Division of Technical Information
OTN	Div. Tech. Sci.
Stroiizdat	Construction Press
TOE	Association of Power Engineers
TsKTI	Central Research Inst. for Boilers and Turbines
TsNIEL	Central Scientific Research Elec. Engr. Lab.
TsNIEL-MES	Central Scientific Research Elec. Engr. Lab.—Ministry of Electric Power Plants
TsVTI	Central Office of Economic Information
UF	Ural Branch
VIESKh	All-Union Inst. of Rural Elec. Power Stations
VNIIM	All-Union Scientific Research Inst. of Meteorology
VNIIZhDT	All-Union Scientific Research Inst. of Railroad Engineering
VTI	All-Union Thermotech. Inst.
VZEI	All-Union Power Correspondence Inst.

Note: Abbreviations not on this list and not explained in the translation have been transliterated, no further information about their significance being available to us. — Publisher.

CHANGES IN THE STRUCTURE, DEGREE OF DISPERSION, AND YIELD VALUE OF PEATS AS THE RESULT OF COMPLETE FREEZING

M.P. Volarovich, K.F. Gusev, S.N. Markov and V.P. Tropin

The physicomechanical and physicochemical properties of moist peat are changed considerably by complete freezing. It is known [1, 2] that frozen peat after thawing gives up water much more easily, but has lower strength and higher moisture absorption in the air-dry state. This is caused by coagulation of the peat during freezing and subsequent thawing. It was of interest to study this effect by a combination of x-ray, dispersion and rheological analysis methods. The x-ray structure analysis was carried out by a procedure described previously [3]. The photographs were taken with the aid of a tube with a copper anticathode in a special x-ray camera of high resolving power [4] over a period of 8 hours, the β-lines not being filtered off. The x-ray diagrams were used to give microphotometric curves with the aid of a "Magnephot" microphotometer obtained from Hungary [5], adapted for this purpose.

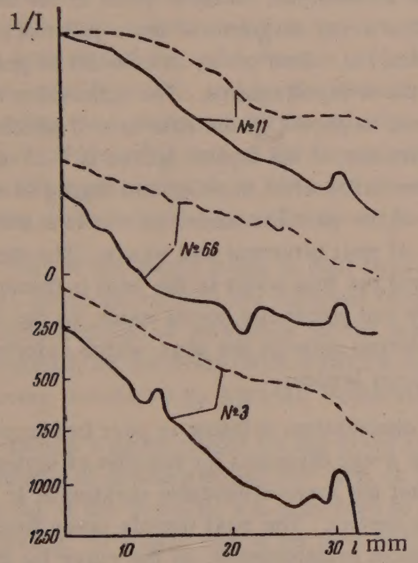

Fig. 1. Microphotometric curves based on x-ray diagrams of upper No. 66 peat and bottom peats Nos. 3 and 11. Continuous lines represent the original peats; the broken lines, after freezing.

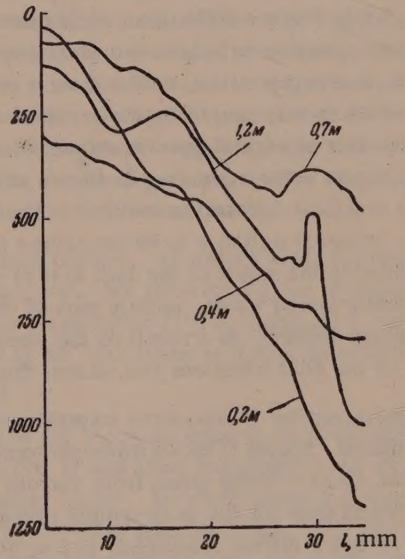

Fig. 2. Microphotometric curves from x-ray diagrams of peats taken from depths of 0.2; 0.4; 0.7 and 1.2 meters.

Figure 1 shows microphotometric curves taken from x-ray diagrams of upper pine – cotton grass peat No. 66 with degree of decomposition R = 65%, and wood – reed No. 3 (R = 50%) and reed No. 11 (R = 35%) lower peats, both in the original states and after freezing. The abscissa axis shows the distances from the center of

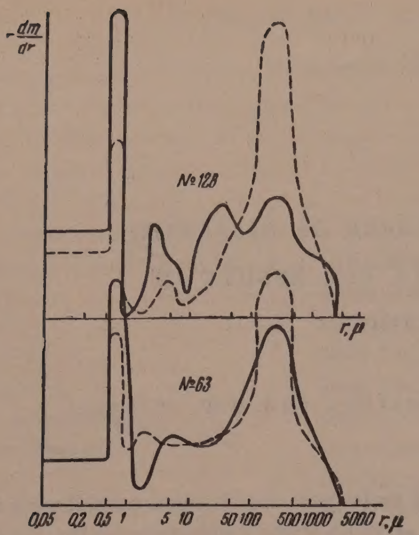

Fig. 3. Particle size distribution curves for peats: bottom No. 63 and upper No. 128. Continuous lines represent the original peats; broken lines represent peats after freezing.

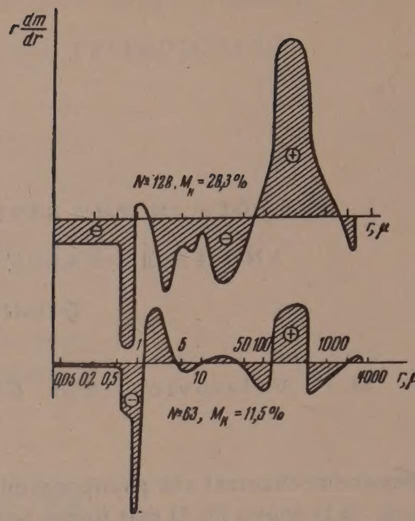

Fig. 4. Curves for dispersability ranges affected by coagulation on freezing, for peats Nos. 63 and 128.

the x-ray diagram in millimeters, and the ordinates represent the reciprocals of the intensities of the light beam passing through the x-ray diagram. The peats were subjected to low temperatures of the order of −15, −25° for several days. The moisture content of the peats was 86-88%. Figure 1 shows that all these peats in the original state give a fairly distinct diffraction maximum at $l = 30.5$ mm. The x-ray diagrams of these peats of a high degree of decomposition belong to the second type in our classification [6]. Such peats, in contrast to peats of a low degree of decomposition, do not show a cellulose structure in the x-ray diagrams. The diffraction maximum at $l = 30.5$ mm is caused by the presence of bitumens and waxes in peats [7], the structure of which is identical with that of normal petroleum paraffins. The interplane distance of the crystal lattice is 4.15-4.25 A. The lines in Figure 1 corresponding to frozen peats (the diagrams were taken after thawing and drying to an air-dry state) do not show diffraction maxima. Therefore, the structure of the peat bitumens and waxes is affected by freezing. Water is unlikely to be contained in the crystal lattice of peat bitumens and waxes. The structural change is probably the result of the fact that at these low temperatures the free water in the peat is frozen, and also the partially bound water, namely part of the physicochemically and physically bound water, in the Dumansky-Rebinder theory. As a result of the freezing large internal stresses arise in the peat, which deform the soft crystals of the peat bitumens and waxes, thus disturbing their crystal lattices.

The above results of laboratory experiments are confirmed by observations relating to peat frozen under natural conditions. Figure 2 shows microphotometric curves based on x-ray diagrams for samples of bottom sedge peat No. 63 (R = 55%) taken from various depths. It is seen that the sharp diffraction maximum at $l = 30.5$ mm is found only for the peat sample taken from a depth of 1.2 meters. The peat sample taken from a depth of 0.7 m has a diffuse maximum at $l = 30.5$ mm, which is almost imperceptible on the curve for the sample taken from 0.4 m. This maximum does not appear on the curve for peat taken from the surface layer (0.2 m). The explanation is that peat deposits usually freeze through down to a depth of 0.5-0.7 m in winter.

Dispersion analysis of the frozen peats was carried out by the method developed previously [8], fractions with equivalent radius greater than 125μ being subjected to wet sieve analysis, while fractions between 125 and 0.5μ were studied by means of the weight sedimentometer [9]. Figure 3 shows particle size distribution curves for bottom alder peat No. 63 (R = 55%) and for upper pinewood-cottongrass peat No. 128 (R = 50%). Electron micrographs were not taken, and therefore the highly disperse fraction ($r < 0.5\mu$) is shown in Figure 3 in the form of a rectangle. The peats were frozen for about three weeks, the minimum temperature reaching −30°.

It is clear from Figure 3 that when peats are frozen through and subsequently thawed out there are changes

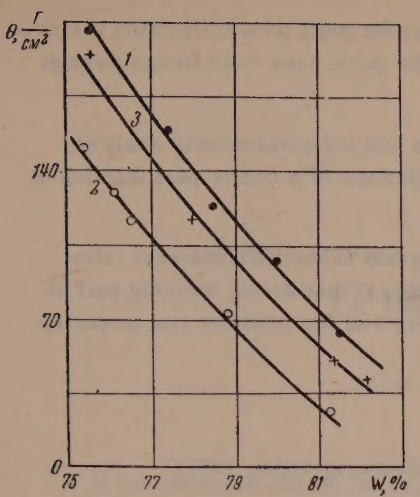

Fig. 5. Variation of yield value with moisture content of peat: 1) not frozen; 2) after thawing; 3) the same, but after two years of storage at positive temperatures.

in their degree of dispersion, caused by coagulation, the effect being most pronounced for peat No. 128. In particular, this peat underwent an abrupt transition from an initial plastic state into a loose coarsely granular system on freezing. An especially clear picture is obtained if coagulation dispersability range curves [8] are plotted, as shown in Figure 4, where the differences between the ordinates of the size distribution curves for each peat in the original and frozen states are shown. Here the finer fractions, which disappeared in course of coagulation, lie below the abscissa axis and are indicated by a minus sign, while the coarser fractions which appeared lie above the abscissa axis and are denoted by a plus sign. It was found that coagulation on freezing affected 11.5% of peat No. 63 and 28.3% of peat No. 128.

It is seen from Figures 3 and 4 that in peat No. 63 only the fraction with radius 0.5-1.5μ coagulated on freezing, while in peat No. 128 the coagulation process covered a wider range of fractions from hundredths of a micron to 60μ. Additional amounts of a coarse fraction, mainly between 100 and 500μ, appeared in both peats as the result of coagulation.

A comparison of the principal dispersion characteristics of the original and coagulated peats also reveals considerable changes in the degree of dispersion resulting from freezing. For upper peat No. 128, the specific surface (S), calculated by S.G. Solopov's method, of fractions with particle radius $r < 2\mu$ was $S_0 = 4520$ cm²/g for the original peat and $S_n = 3185$ cm²/g for the frozen peat, and the average weighted diameter (d) of the coarsely disperse fraction of the original peat was $d_0 = 495\mu$, and of the frozen peat $d_n = 600\mu$. The inhomogeneity coefficient (f), often used in relation to soils, which represents the ratio of the radii between which 50% of the mass of the particles of the solid phase is included ($f = r_{10}/r_{60}$), underwent an especially pronounced change; for the original peat $f_0 = 275$, and for the frozen peat $f_n = 10$. Bottom peat No. 63 was less coagulated as the result of freezing, as is indicated by the principal dispersion characteristics: the specific surface of the original peat was $S_0 = 3700$ cm²/g, and of the frozen peat $S_n = 3060$ cm²/g, while the average weighted diameter was almost unchanged, being $d_0 = 500\mu$ for the original and $d_n = 520\mu$ for the frozen peat. The inhomogeneity coefficient also changed little; for the original peat $f_0 = 58.8$, and for the frozen peat $f_n = 30.6$.

Part of the bound water in peat becomes free in the freezing process. Therefore after thawing the rheological properties of peat are different from those of the original peat. We determined the limiting shearing stress (yield value) of previously frozen peat by means of a cone plastometer [10] by Rebinder's method [11]. The constant for the cone (with a riffled surface) with an angle of 45° was taken as 0.416, in accordance with the theory developed by Agranat, Volarovich and Shirokov [12].

Figure 5 shows curves for the yield value θ as a function of the moisture content of wood-sedge peat No. 4 of degree of decomposition R = 45%, in the original state (Curve 1) and after freezing (Curve 2). The peat, taken out of the deposits, was subjected to low temperatures during winter. Its yield value was determined after thawing. It is seen that θ for peat decreases considerably (by 30-50%) after freezing. The explanation is that when peat is frozen at low enough temperatures some of the bound water freezes, while after thawing this water becomes free.

However, if peat is kept at positive temperatures for a prolonged time after thawing, its original rheological properties are to some extent restored. Curve 3 in Figure 5, which corresponds to peat kept for two years at positive temperatures after freezing, lies considerably nearer than Curve 2 to Curve 1 for peat which had not been frozen. It seems that after thawing part of the free water again becomes bound by the solid phase of the peat at positive temperatures, and the relative content of free water decreases. The yield value of the peat again increases as a result.

SUMMARY

1. The x-ray diagrams and the corresponding microphotometric curves for peats show diffraction maxima corresponding to peat bitumens and waxes; these maxima disappear after the peats have been frozen through at temperatures of −15 to −25°.

2. The particle size distribution curves for peats, determined by sieve and sedimentometric analysis, show that freezing causes coagulation in peat and considerable additional amounts of a coarse peat fraction of particle size 100-500μ are formed.

3. Experiments with the aid of the cone plastometer showed that the yield value of frozen peat (after thawing) is considerably lower than that of the original peat. The explanation is that during freezing part of the bound water in the peat becomes free, and this causes considerable changes in the structure and properties of the peat.

LITERATURE CITED

[1] V.G. Goryachkin, Fundamentals of Peat Production Technology (Gosenergoizdat, 1953).

[2] M.A. Veller et al., Technology of Hydropeat (Gosenergoizdat, 1956).

[3] M.P. Volarovich and K.F. Gusev, Trans. Moscow Peat Inst. No. 2, 97 (1954).

[4] K.F. Gusev, Factory Labs. No. 4, 477 (1953).

[5] M.P. Volarovich and K.F. Gusev, Trans. Moscow Peat Inst. No. 6, 38 (1957).

[6] M.P. Volarovich and K.F. Gusev, Trans. Moscow Peat Inst. No. 5, 31 (1957).

[7] M.P. Volarovich and K.F. Gusev, Colloid J. 18, 643 (1956) (T.p. 639).*

[8] M.P. Volarovich and N.V. Churaev, Colloid J. 17, 200 (1955) (T.p. 185)*; Trans. Moscow Peat Inst. No. 3, 33 (1955); Trans. 3rd All-Union Colloid Conference, Minsk 1953 (1956), p. 258.

[9] N.V. Churaev, Colloid J. 16, 220 (1954) (T.p. 221).*

[10] M.P. Volarovich and S.N. Markov, J. Peat Ind. No. 10, 23 (1951); Factory Labs. 17, No. 12, 1461 (1951).

[11] P.A. Rebinder and B.Ya. Yampolsky, Colloid J. 10, 466 (1948); P.A. Rebinder and N.N. Semenenko, Proc. Acad. Sci. USSR, 64, No. 6, 835 (1949).

[12] N.N. Agranat and M.P. Volarovich, Colloid J. 19, 3 (1957) (T.p. 1)*; N.N. Agranat and M.F. Shirokov, Colloid J. 19, 9 (1957)(T.p. 9).*

Received April 11, 1957

Moscow Peat Institute

---

*T.p. = C.B. Translation pagination.

INVESTIGATION OF ELECTROOSMOSIS IN CAPILLARY SYSTEMS OF DIFFERENT CHARGE AND STRUCTURE

O.N. Grigorov and K.P. Tikhomolova

It was shown in one of our papers [1] that a definite ratio of capillary length to cross section is required for electroosmotic flow to occur in systems of regular geometrical structure composed of capillaries of circular or square cross section. This ratio was not constant for capillaries of different cross section, but varied with the latter and with the potential gradient of the applied electric field. Increase of the capillary cross section resulted in an increase of this ratio, while increase of the potential gradient had the opposite effect.

It was desired to test the results of that investigation on powder capillary systems of various types, more similar in structure to natural materials. It also seemed likely that variation of the effective charge density on the particle surfaces of materials differing in their chemical nature should influence the ratio of capillary length to cross section at which electroosmotic flow can occur.

EXPERIMENTAL

The materials chosen for study were powders consisting of spherical polystyrene particles prepared by emulsion polymerization of styrene, and also quartz powders and powdered melts of polystyrene with MMG-1 anion exchange resin. The polymerization of styrene was carried out in presence of polyvinyl alcohol or polymethacrylic acid as emulsifier and benzoyl peroxide as catalyst, at 80-90°. To vary the charge on the polystyrene particles, a certain amount of dye was added to the styrene during polymerization until a saturated solution was formed. In this way, a series of specimens of polystyrene powders was obtained, with different ζ-potentials in KCl solution. Quartz powder, made by grinding quartz crystals in a steel ball mill, was treated with 10% H_2SO_4 solution with warming, and washed with distilled water to a negative reaction for SO_4 ions. Positively charged powders were made by taking finely powdered MMG-1 anion exchange resin which was melted together with polystyrene and ground in a mortar. The quartz and polystyrene powders were then fractionated by means of Tyler standard sieves. Powders with particle size < 44μ were fractionated by elutriation in an ascending current of water with cone apparatus. For dispersion analysis of the fractions, micrographs of individual samples of

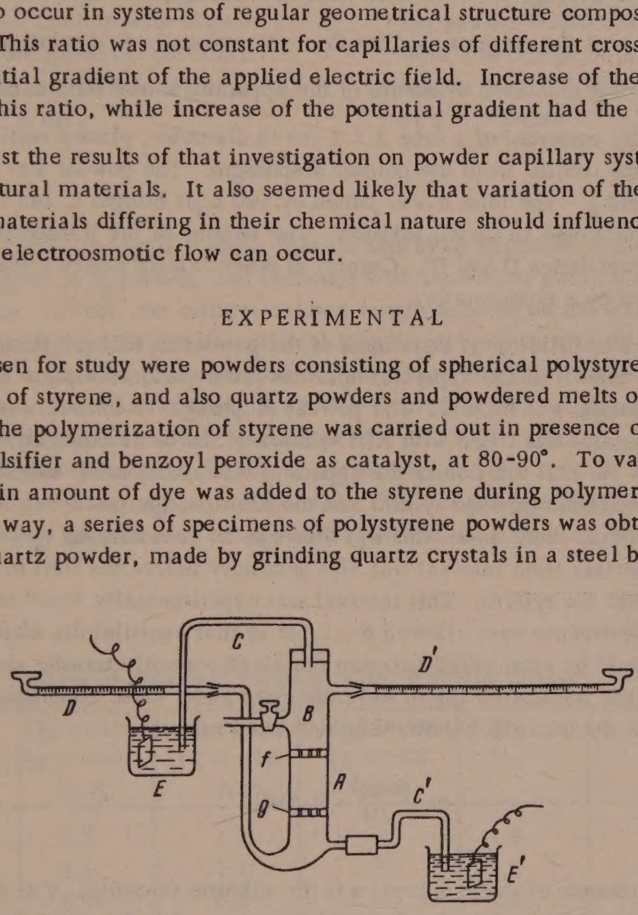

Fig. 1. Diagram of apparatus for measurement of electroosmotic transfer.

TABLE 1

ζ-Potentials of the Materials Used in the Experiments

Details of sample	Specific conductance of KCl solution $\times 10^4$ ohm^{-1} cm^{-1}	ζ in mv	Details of sample	Specific conductance of KCl solution $\times 10^4$ ohm^{-1} cm^{-1}	ζ in mv
Polystyrene (polymethacrylic acid emulsifier)	9.3	−15	Polystyrene with added Sudan III (saturated solution)	9.3	−33
Polystyrene (polyvinyl alcohol emulsifier)	9.3	−10	Quartz powder	3.5	−29
Polystyrene with addition of fat-soluble Brown K (saturated solution)	9.3	− 6	Quartz powder	9.4	−15
			Melt of polystyrene with MMG-1 resin	9.4	+21

the powders were taken and the average particle sizes were determined from these.

Data on the ζ-potentials of the samples used for the experiments in KCl solution are given in Table 1.

Electroosmotic transfer was measured by means of the apparatus shown schematically in Figure 1.

The apparatus essentially consisted of a tube A 1.1 cm in diameter, placed vertically for easier removal of air bubbles, which distort the results, from the powder diaphragm. The powder was pressed between two perforated "Plexiglas" plates f and g. The tube A was joined by two agar bridges C and C' to the beakers E and E', which contained copper electrodes in $CuSO_4$ solution. The volume of the transported liquid was read off by means of the two graduated capillaries D and D'. Current at potentials up to 410 v was supplied from a kenotron, its direction being varied by a commutator.

The apparatus was filled as follows. A suspension of the powder in KCl solution, of known concentration, was introduced into the main tube A of the apparatus onto the lower perforated plate and left to settle there until a column of the required length was formed. The powder diaphragm so formed was compressed between the two plates and the whole apparatus was filled with KCl solution of the same concentration. The constancy of the electrical conductance of the KCl solution in the apparatus was additionally checked after each experiment. To establish equilibrium between the disperse system and the solution, the powder to be studied was first kept in the given solution for not less than three days; this was shown to be necessary by special experiments. After the apparatus had been filled a certain time interval was also necessary before the start of the determinations, for equilibrium to be established in the system. This interval was experimentally found to be 10 to 12 hours. Intervals of 1 hour between experiments were allowed to elapse so that equilibrium, characteristic of the given system in the steady state, could be established between the electroosmotic transfer determinations, Definite and reproducible volumes of the transferred liquid were obtained under these conditions. The electrokinetic potential was calculated from the usual Helmholtz-Smoluchowski equation

$$\zeta = \frac{4\pi\kappa\eta V}{DI} 9\cdot 10^4, \quad (1)$$

where κ is the specific conductance of the solution; η is the solution viscosity; V is the volume of liquid transferred in cubic centimeters per second; D is the dielectric constant; I is the current strength in amperes, and $9\cdot 10^4$ is the conversion factor to give the ζ-potential in volts.

To find the minimum ratio of the length of the powder column (in other words, the thickness of the diaphragm) to the cross section, at which a definite constant value for the electroosmotic transfer of the liquid becomes established, which we term the "critical ratio," a series of parallel experiments with different lengths of column was carried out.* The results of experiments with powders consisting of spherical particles are shown

---

*In these experiments in a number of cases it was clearly seen that the liquid did not move in the graduated capillary when the length of the powder column was insufficient. With increasing column length a certain region was found in which the liquid was seen to move but the results were inconsistent, and this was followed by a region of constant values corresponding to steady electroosmotic flow. Values corresponding to the critical length (l_{cr}) were determined to an accuracy of 1-2 mm.

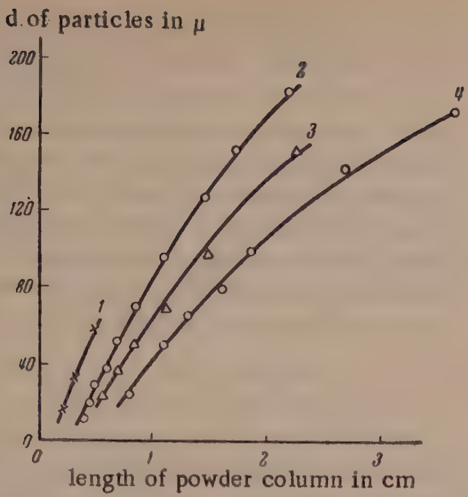

Fig. 2. Variation of the critical length of the powder diaphragm column with dimensions and charge of the spherical particles: 1) $\zeta = -30$ mv; 2) $\zeta = -15$ mv; 3) $\zeta = -10$ mv; 4) $\zeta = -6$ mv.

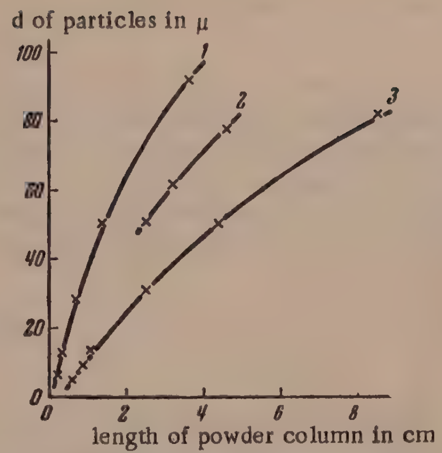

Fig. 3. Variation of the critical length of the powder diaphragm column with dimensions and charge of particles of irregular shape: 1) $\zeta = -29$ mv; 2) $\zeta = +21$ mv; 3) $\zeta = -15$ mv.

in Figure 2.

Examination of the curves in Figure 2 shows that, as was to be expected, the critical length of the powder column depends on the degree of dispersion, and increases with increasing particle size, which is equivalent to increase of capillary radius. Further, the critical column length depends on the surface charge, decreasing with increase of the latter. The differences between critical lengths for systems with different ζ-potentials are fairly large for a given degree of dispersion. For example, for particles 150μ in diameter, the critical length of a column of polystyrene powder with added fat Brown K ($\zeta = -6$ mv) is 3 cm, for polystyrene with ζ-potential -10 mv, $l_{cr} = 2.3$ cm, and for polystyrene with ζ-potential -15 mv, $l_{cr} = 1.9$ cm. A comparison of any two systems shows that, with variation of the particle size in a given system, the ratio of the critical lengths remains approximately constant for the same degree of dispersion. Table 2 gives comparative values of the critical length (l_{cr}) ratios for different diameters of the spherical particles in powders with different electrokinetic potentials.

TABLE 2

Critical Length Ratios for Systems of Spherical Particles with Different Charges

Particle diameter, in μ	l'_{cr} in cm ($\zeta = -6$ mv)	l''_{cr} in cm ($\zeta = -10$ mv)	l'''_{cr} in cm ($\zeta = -15$ mv)	l''''_{cr} in cm ($\zeta = -33$ mv)	$\frac{l'_{cr}}{l''_{cr}}$	$\frac{l'_{cr}}{l'''_{cr}}$	$\frac{l'_{cr}}{l''''_{cr}}$
150	3.0	2.3	1.3	–	1.3	1.6	–
100	1.8	1.5	1.1	–	1.2	1.6	–
50	0.9	0.75	0.6	0.5	1.2	1.5	1.8
20	0.65	0.55	0.45	0.3	1.2	1.4	2.2

Results of experiments with powders with particles of irregular shape are shown in Figure 3.

The results in Figure 3 show that the length of the powder column necessary for steady laminar flow of liquid to be established also increases in these experiments with increasing particle size in a given system, and decreases with increasing ζ-potential for the same degree of dispersion of the powders.

Thus, the results of our experiments for powder capillary systems fully confirm earlier data [1] for glass and polystyrene capillaries of regular geometrical form, Further, the influence of the effective charge density on the occurrence of electroosmotic flow has been established; this had not been studied previously. The results are of interest in relation to electroosmotic dehydration of dispersoids rich in water, and also, from the methodological aspect, in relation to experiments for determination of ζ-potentials of systems of complex structure. It seemed likely that the value of l_{cr} for capillary systems differing in structure should depend on their specific surface.

The dependence of l_{cr} on the specific surface of the system can be demonstrated, for any given substance, by the magnitude of the maximum electroosmotic rise. This question is of independent interest. Very few experiments have been carried out on determination of the maximum electroosmotic rise, and these were performed either in single capillaries in very narrow limits (Quincke [2]) or in heteroporous systems with pores of indeterminate structure, as in Manegold and Solf's experiments [3] with collodion membranes.

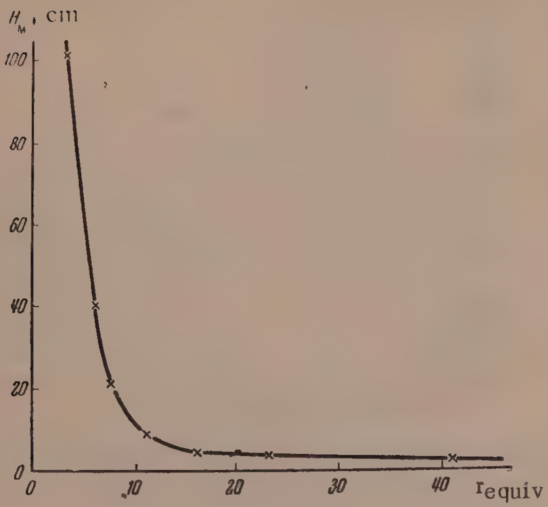

Fig. 4. Variation of the maximum electroosmotic rise with the equivalent capillary radius in a powder diaphragm consisting of spherical particles.

Theoretically, the maximum rise (H_M) is defined by the expression:

$$H_M = \frac{2\zeta ED}{\pi r^2}, \tag{2}$$

where E is the potential gradient at the membrane; D is the dielectric constant; ζ is the electrokinetic potential, and r is the capillary radius. The maximum rise is therefore inversely proportional to the square of the radius.

TABLE 3

Maximum Electroosmotic Rise in Powders of Spherical Polystyrene Particles

Average particle diameter (d) in μ	Equivalent pore radius (r_{equiv}) in μ	Maximum electroosmotic rise (H_M) in cm	$\frac{(H_M)_1}{(H_M)_i}$	$\left[\frac{(r_{equiv})_i}{(r_{equiv})_1}\right]^2$	Current strength in ma
10.15	2.8	105	1.0	1.0	2.9
16.5	4.4	41	2.6	2.5	2.9
26.9	7.4	12	8.7	7.0	2.8
41.5	11.5	3.5	28.5	17.0	2.9
62.6	17.4	2.1	50.0	38.0	2.8
86.5	23.9	1.4	78.0	73.0	2.7
108.5	29.3	1.0	105	109	2.7
152.5	42.0	0.5	210	224	3.0

In Quincke's experiments the maximum rise was found to be inversely proportional to the first power of the radius. In Manegold and Solf's experiments the results for some membranes were close to those required by the above formula, but in many cases there were considerable deviations, probably because of the uncertainty of the structure of the materials used. Their results cannot therefore be regarded as providing complete confirmation of the theory. Experiments for verification of this equation must be carried out for systems of constant structure with variations of capillary radius. Systems of spherical particles, in which the structure depends only on the nature of the packing and is not related to the particle size, are quite suitable for this purpose. Many structural parameters of a system of monodisperse spherical particles can be calculated by analogy with the "fictitious soil," a concept used in hydraulics and soil science in analysis of filtration processes of liquids through porous bodies [4, 5].

We calculated the average equivalent radius r_{equiv} of the capillaries, i.e., the radius of a circle equal in area to the average cross section of the capillary space between the equatorial planes of the spheres. If the packing of the spherical particles is considered as a combination of the most dense and the most free packings, i.e., packing of the eighth order, then the average free capillary cross section per 1 cm^2 will be 0.395 cm^2. The cross section of our apparatus is 0.95 cm^2. On the assumption that all positions of a plane cutting across these packings at right angles to the direction of liquid flow are equivalent, we find the value for the free cross section of one capillary (f)

$$f = \frac{0{,}95 \cdot 0{,}395}{(n_1 + n_2) \cdot {}^1/_2},$$

where n_1 and n_2 are the numbers of capillaries in the section with the most dense and the most free packings. The values of n_1 and n_2 were calculated by dividing the total cross section of the tube by the cross section of a unit gap in the given type of packing. The maximum electroosmotic rise was determined by the Manegold and Solf method [3].

The experiments to determine the maximum electroosmotic rise were performed on a powder of spherical polystyrene particles with ζ-potential of -10 mv. The experimental results are given in Table 3.

It follows from Equation (2) for the electroosmotic rise that the ratio $(H_M)_1/(H_M)_i$, i.e., the ratio of the maximum electroosmotic rises, varies in proportion to the square of the inverse ratio of the radii. The data in Table 3 show that the ratio of the electroosmotic rises is approximately equal to the square of the inverse ratio of the radii. This variation of H_M with capillary radius should be represented by a parabola; this is illustrated in Figure 4.

Thus, the maximum electroosmotic rise depends on the capillary radius in the system, variation of which leads, in its turn, to variation of the specific surface. Differences of the critical lengths of the capillaries (in relation to their radii) for a given substance are determined by differences of the motive electroosmotic forces, which depend on the specific surface of the capillary system and which may be characterized by the electroosmotic rise. Therefore variation of the critical capillary length is ultimately determined by variation of the specific surface of the system.

SUMMARY

1. Steady electroosmotic flow of liquid becomes established in a powder diaphragm at a definite ratio of the length of the powder column to the capillary cross section. This ratio increases with increasing particle size in the powder and decreases with increasing surface charge, which is characterized by the magnitude of the electrokinetic potential.

2. The ratio of the maximum electroosmotic rises for diaphragms with particles of different sizes varies in direct proportion to the inverse ratio of the capillary radii, in agreement with the classical formula.

LITERATURE CITED

[1] O.N. Grigorov and M.G. Leibovich, Colloid J. 12, 175 (1950).

[2] G. Quincke, Pogg. Ann. 107, 1 (1859).

[3] E. Manegold and K. Solf, Koll.-Z. 55, 3, 273 (1931).

[4] V. Zigel, Filtration (GONTI, 1939).

[5] L.S. Leibenzon, Movement of Natural Liquids and Gases in Porous Media (State United Press, 1947).

Received July 6, 1956

The A.A. Zhdanov State University
Leningrad

INVESTIGATION OF ADHESION EFFECTS IN BONDING RUBBER TO METAL BY LEUKONAT ADHESIVE

A.M. Medvedeva, B.V. Deryagin and S.K. Zherebkov

Adhesives based on isocyanates for bonding rubber to metals were first developed and used in Germany during the Second World War [1]. Adhesives, based on isocyanates, for rubber-metal bonding are used in a number of countries under various trade names (HDI, Vulcabond TX, Xylen M, Desmodur R, MD-1). In the USSR, "Leukonat" isocyanate adhesive is widely used. The reasons for the wide use of isocyanate adhesives are that the bonds obtained are the most suitable for general purposes and have a number of valuable properties: heat resistance, frost resistance, resistance to solvents, oils, and water, and good stability to repeated deformation.

There have been numerous investigations [2-5] of the properties of bonds formed by isocyanate adhesives. However, there is still no definite theory concerning the causes of bond formation at the adhesive-rubber and adhesive-metal boundaries. The various viewpoints advanced in the literature are often unsupported by experimental data. For example, in Bayer's paper [1] it is suggested that isocyanates react with the hydroxide layer on the metal surface during bonding of rubber to metal. Bayer also states that isocyanates can polymerize into compounds of high molecular weight under the action of metals or basic compounds.

Proske [6] also states that in rubber-metal bonding by means of isocyanates chemical reactions with the oxygen-containing groups of the rubber may occur.* The suggestion is made in the same paper that the $-N=C=O$ group is of decisive importance in adhesion of the adhesive film to metal; the rest of the isocyanate molecule, i.e., the hydrocarbon portion, forms a bond with rubber. On the whole it may be said that adhesion phenomena, which include rubber-metal bonding, are not sufficiently well understood. The electrical theory of adhesion put forward by Deryagin and Krotkova [7] is the most fully developed theory of the adhesive bond. The above examples cover all the existing views on the mechanism of rubber-metal adhesion by means of isocyanates.

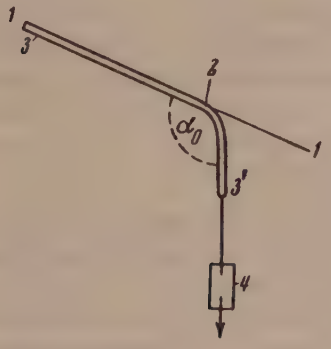

Fig. 1. Deryagin's rotating plate instrument: 1-1') plate; 2) axis; 3-3') film; 4) load.

An attempt is made in the present paper to approach the problem of rubber-metal bonding by means of Leukonat isocyanate adhesive. The isocyanates, as a chemical class, have a number of characteristic properties, such as polyfunctionality (mono-, di-, and triisocyanates exist), and exceptional chemical activity. The formation of isocyanate polymers is based on the fact that the isocyanate group $-N=C=O$ contains a double bond between N and C, at which active hydrogen can be added extremely readily. Bayer [1] arranged compounds containing active hydrogen in the following series by their order of reactivity toward isocyanates: amines > water > alcohols > > acids > urea derivatives > phenols > compounds with active methylene groups.

The present paper gives a description of an investigation of adhesion of rubber to metal by means of Leukonat, which is a 20% solution of triphenylmethane triisocyanate in dichloroethane.

Methods. The strength of the rubber-metal bond was measured in terms of the specific work of peeling the rubber from the metal. Several methods and instruments for this purpose have been described previously [7]. The principle of one of these is illustrated in Figure 1. The specific work of peeling was calculated by the equation:

---

*Proske does not exclude the possibility of electrical forces arising at the adhesive-rubber boundary.

$$A = \frac{P}{b}(1 - \cos\alpha), \tag{1}$$

where P is the weight of the load; l is the length of the plate; b is the width of the plate; α is the peeling angle; A is the specific work of peeling. If the plate is horizontal, then

$$A = P/b. \tag{2}$$

Deryagin and Krotova [7] showed that the work of peeling depends on the rate at which the polymer film is peeled from the support.

In the present paper the test results are also shown in the form of adhesion diagrams showing the work of peeling as a function of the rate at which the rubber is peeled from the metal. The peeling rate of the rubber from the metal was varied between 0.001 and 1 cm/second, approximately a 1000-fold range, and the peeling angle was 90°; for this, a special self-regulating device was designed.

The experimental procedure was as follows. The surfaces of steel plates (110 x 25 x 3) were cleaned with No. 100 fine grain emery paper or sandblasted, according to the experimental conditions, and washed with ligroine; the plates were then coated with a thin layer of Leukonat by dipping.* Prepared samples of raw rubber mixes were freshened by solvent, after which the coated plates and rubber samples were placed in a mold and vulcanized in a press under the optimum vulcanization conditions for the particular rubber. The projecting edges of the treated rubber-metal specimens were cleaned off and the specimens were tested as described above.

EXPERIMENTAL

The subject of this paper is a study of the influence of fillers in the rubber on the bonding of rubber to metal by Leukonat adhesive in vulcanization. As is known, fillers play an important part in vulcanized natural and especially synthetic rubbers. The physicomechanical properties of rubbers can be varied over wide limits by addition of various fillers. Fillers may be divided into two groups according to their effects on the physicomechanical properties of the vulcanized products: reinforcing and inert fillers. The commonest fillers used in the rubber industry are various carbon blacks. No single existing theory accounts for all the variety of effects associated with filler reinforcement. It has been shown however, that reinforcement is influenced by such factors as the degree of dispersion and the shape of the filler particles, the nature of the secondary structures formed by them, and the surface properties of the filler particles [9].

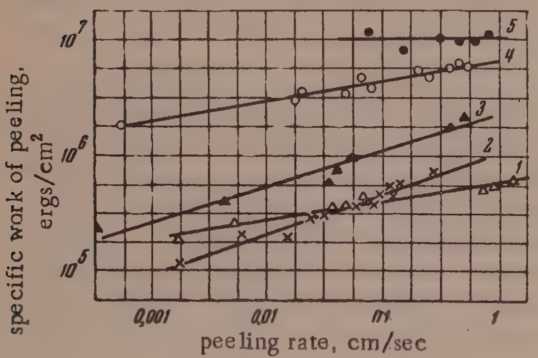

Fig. 2. Work of peeling of rubbers containing different carbon blacks, from steel: 1) gas channel black, adhesive on rubber after peeling; 2) lamp black, adhesive on rubber; 3) jet black, most of the adhesive on rubber; 4) without carbon, most of the adhesive on metal; 5) thermal black, adhesive on metal.

It is now known that the surface of a channel black particle is not chemically inert. Chemical groups containing hydrogen and oxygen are present on this surface. The oxygen is usually present in the carbon black structure entirely in the form of oxygen-containing groups. Several papers have appeared in the literature [10] on the chemical nature of the channel black surface, in which it is stated that the following groups may be present in the surface of channel black

---

*A special device was designed for applying a thin uniform film of adhesive to the metal.

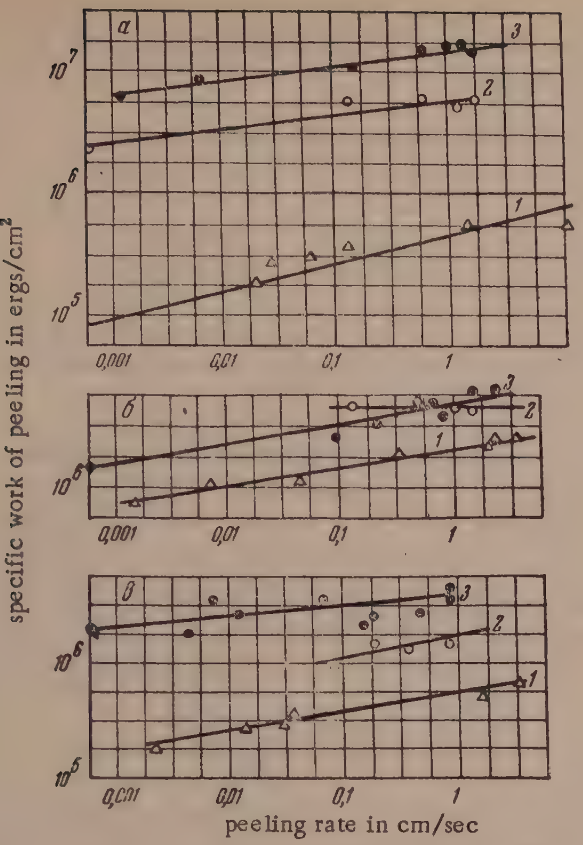

Fig. 3. Work of peeling of different rubbers, containing different fillers, from steel:
a) SKN-26: 1) gas channel black, adhesive on rubber after peeling; 2) without carbon, most of the adhesive on the metal; 3) thermal black, peeling along the rubber, adhesive on the metal;
b) NR: 1) gas channel black, adhesive on the rubber; 2) without carbon, peeling along the rubber, adhesive on the metal; 3) thermal black, rubber torn out in places, adhesive on the metal;
c) SKS-30: 1) gas channel black, adhesive on the rubber; 2) without carbon, rubber torn, adhesive on the metal; 3) thermal black, rubber torn, adhesive on the metal.

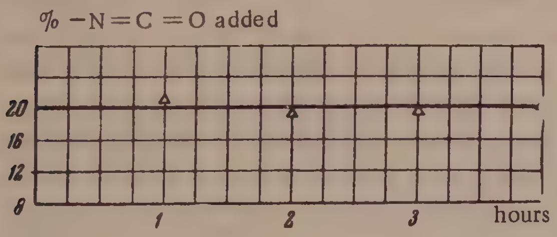

Fig. 4. Effect of heating Leukonat adhesive at 120° on its isocyanate group content.

particles: phenolic, carboxylic, quinone, ketone, aldehyde, peroxide, hydroperoxide, ester, alcoholic, etc. The complex nature of the chemical behavior of the carbon surface is a consequence of this diversity of the chemical groups present.

As is known, the carbon black surface adsorbs rubber and certain ingredients of rubber mixes. The adsorbed ingredients and those dissolved in the rubber participate in different ways in vulcanization, oxidation, or aging. Moreover, catalytic processes should occur at the carbon black surface, activated by condensation of the substances in adsorbed layers and orientation of their molecules [11]. On the other hand, a part of the ingredients adsorbed on the carbon reacts chemically with the carbon surface and is thereby deactivated [12]. There is no doubt that the nature of the carbon surface must play an important role in rubber-metal bonding.

A paper was published in 1952 [13], describing the use of an adhesive containing carbon black (of the channel black type) as an intermediate layer between the material causing adhesion to the metal (brass, and to chlorinated rubber) and the rubber. The adhesive containing the carbon black was made in a mixer from a mix made on rolls and in a ball mill into which the raw rubber and the other ingredients were introduced directly. The greatest bond strength was obtained with the use of the adhesive made in the ball mill. The investigation showed that the adhesive made in the ball mill contained the carbon black particles in the form of floccules, while the flocculation was considerably less in the adhesive made in the mixer. The authors consider that the carbon black particles in the floccules are incompletely wetted by the adhesive and are therefore able to react directly with adjacent surfaces. The effect of the pH of the carbon black added to the adhesive on the rubber-metal bond strength was also studied. It was found that the rubber-metal bond strength increases with decreasing pH of the carbon black. The diversity of the functional groups present on the carbon black surface is, in the opinion of the authors, an adequate explanation of this increase of adhesion.

It was mentioned earlier that isocyanates react very readily with substances containing groups with active hydrogen. In view of this property of isocyanates it was of interest to see how introduction of different kinds of carbon black into the rubber would influence its adhesion to a Leukonat film. The following blacks were tested: gas channel, furnace, jet, lamp and thermal.

The material to which various fillers were added was "Nairit" rubber, as it has fairly high strength both with and without fillers, so that adhesive peeling of the rubber from metal can be obtained in most cases.

Composition of Nairit Mix

Nairit B	100 parts by weight
Zinc oxide	5.0 "
Magnesium oxide	7.0 "
Stearic acid	1.0 "
	113.0 parts by weight

Fifty parts by weight of the different carbon blacks was added to this mix. The rubbers were bonded to steel plates cleaned with No. 100 emery paper. The metal surfaces were sandblasted only in special cases, which will be mentioned.

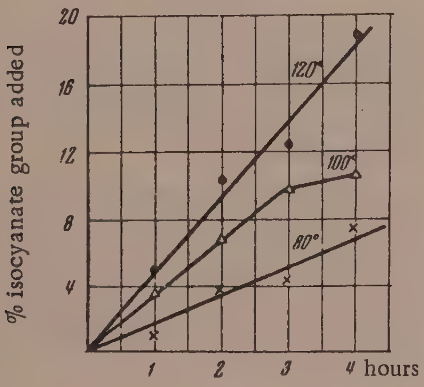

Fig. 5. Variation of the isocyanate group content of Leukonat on heating with channel black at 80, 100 and 120°.

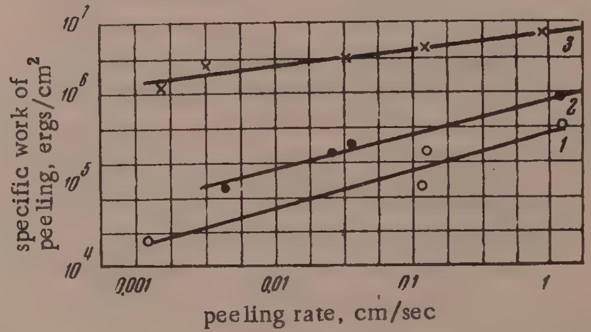

Fig. 6. Effect of type of filler on the bonding of butyl rubber to steel by means of Leukonat adhesive: 1) without carbon, adhesive on metal after peeling; 2) with thermal black, adhesive on metal; 3) with gas channel black, adhesive on metal, carbon particles on adhesive.

Figure 2 shows a series of adhesion diagrams for rubbers containing different carbon blacks. It is seen from Figure 2 that some blacks have a significant influence on the adhesion of rubber to metal with the use of Leukonat. Unfilled Nairit rubber has high adhesion to Leukonat film, but when it is peeled away most of the adhesive remains on the metal, so that the adhesion of the Leukonat film to metal is still higher. When active fillers of the channel black type are added to the rubber, the strength of the rubber-metal bond decreases, and the nature of the peeling changes: the adhesive film is attached to the rubber. Addition of thermal black (a filler of low activity) to the rubber produces some increase of the rubber-metal bond strength, the adhesive remaining on the metal and the peeling being mainly cohesive in character.

It was next decided to test how the same carbon blacks influence the bond strength between metal and other rubbers with Leukonat as adhesive. Two most characteristic types of carbon black — gas channel and thermal — were used for these experiments. Three rubbers were tested: butadiene-acrylonitrile (SKN-26), natural (NR) and butadiene-styrene (SKS-30). The compounding formulas are given in the table.

Figure 3 shows adhesion diagrams for the bond strengths between metal and rubbers based on SKN-26 (Figure 3a) NR (Figure 3b) and SKS-30 (Figure 3c) containing different carbon blacks.

The results given in Figure 3 show that in all cases, irrespective of the type of rubber, the presence of channel black in the rubber results in decreased rubber-metal bond strength, with the adhesive film attached to the rubber, while in presence of thermal black high adhesion of rubber to metal is obtained, and the peeling remains of the same character as with unfilled rubbers, i.e., the adhesive remains on the metal. Therefore the carbon added to the rubber is involved in the mechanism of rubber-metal bonding by means of Leukonat adhesive. To confirm this, in the following series of experiments the interaction of carbon blacks directly with the Leukonat adhesive was studied. The experimental procedure was as follows: 0.16 g of carbon black and 0.6 g

Compounding Formulas for the Rubber Mixes in Parts by Weight

Rubber and ingredients	Mix No.					
	121^K	121^T	122^K	122^T	123^K	123^T
Natural rubber	100.0	100.0	—	—	—	—
SKN-26	—	—	100.0	100.0	—	—
SKS-30	—	—	—	—	100.0	100.0
Stearic acid	0.5	0.5	0.5	0.5	2.0	2.0
Zinc oxide	5.0	5.0	5.0	5.0	5.0	5.0
Captax	0.7	0.7	0.8	0.8	0.6	0.6
Thiuram	—	—	—	—	0.1	0.1
Gas channel black	50.0	—	50.0	—	50.0	—
Thermal black	—	50.0	—	50.0	—	50.0
Sulfur	3.0	3.0	1.5	1.5	2.0	2.0
Total	159.2	159.2	157.8	157.8	159.7	159.7

of Leukonat adhesive was put into a glass tube. The tube was sealed and heated in a thermostat; it was then opened, the carbon was filtered off from the adhesive and repeatedly washed on the filter with dichloroethane until traces of isocyanate could no longer be detected in the washings. The isocyanate content of the solution was determined by titration.

As has already been stated, isocyanates are chemically very active and have a tendency to cyclization in certain conditions, resulting in a decrease of the isocyanate group content. It was therefore necessary to determine whether high temperature may itself produce the changes which occur in isocyanates on heating. Experiments were carried out in which Leukonat was heated by itself (without carbon black) for 1, 2, 3 and 4 hours at 120° (the most severe conditions used in the present investigation). The results of these tests, given in Figure 4, show that when Leukonat is heated at 120° for 4 hours its isocyanate group content is practically unchanged. The results obtained in heating of channel black with Leukonat adhesive at 80, 100 and 120° are given in Figure 5. From these results it was possible to calculate the apparent activation energy of the reaction of channel black with triphenylmethane triisocyanate by means of the Arrhenius equation. The apparent activation energy was found to be 8900 cal/mole.

Experiments in which thermal black was heated in sealed tubes with Leukonat showed that in these conditions thermal black does not react with triphenylmethane triisocyanate, and the isocyanate group content of the adhesive remains practically unchanged. These experiments showed that the nature of the filler present in the rubber influences the bonding of the rubber to metal by means of Leukonat. A comparison of the data on rubber-metal bonding with the results of experiments on the influence of the filler on the properties of the adhesive itself gives rise to the following picture.

Unfilled rubbers of the types studied are firmly bonded to metal by means of Leukonat adhesive. This means that the film of adhesive is bonded equally well to the rubber and to the metal during vulcanization. However, when the rubber is peeled away from the metal most or all of the adhesive (depending on the type of the rubber) remains on the metal, and therefore the adhesion of the Leukonat film is somewhat greater to metal than to rubber.

On addition of an active filler of the gas channel black type to the rubber, the interaction of one of the surfaces (the rubber) with the adhesive film is greatly intensified. The bonding at the adhesive-rubber boundary is now effected not only by interaction between isocyanate and rubber, but also by interaction of the adhesive with groups containing active hydrogen, present on the carbon black surface. The number of active centers with which the isocyanate can interact is increased. The interaction between the metal and the adhesive film remains the same as before. Therefore during the bonding process the isocyanate groups react sooner with the more active rubber surface (the adhesive film is attached to the rubber) and the adhesion to the metal is decreased. Inactive fillers of the thermal black type introduced into the rubber have little influence on the processes occurring at the adhesive-rubber boundary. The peeling in this case remains of the same character as with unfilled rubbers (the adhesive remains on the metal after peeling).

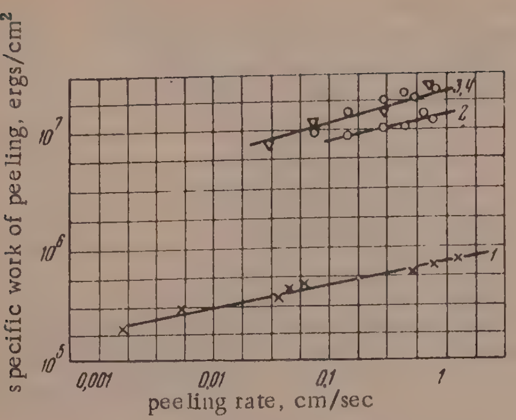

Fig. 7. Effect of treatment of the metal surface on its bond strength with Nairit rubber: 1) with channel black, metal cleaned with emery paper, adhesive on rubber after peeling; 2) with thermal black, metal cleaned with emery paper, large pieces of rubber torn out; 3) with channel black, metal sandblasted, peeling along the rubber; 4) with thermal black, metal sandblasted, peeling along the rubber.

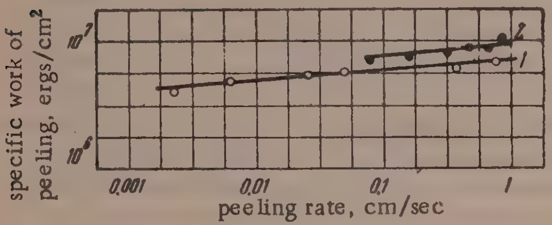

Fig. 8. Effect of treatment of the metal surface on its bond strength with butyl rubber containing gas channel black: 1) metal cleaned with emery paper, adhesive on metal after peeling; 2) metal sandblasted, adhesive on metal.

Experimental data providing further confirmation of these views are presented below. Most of the rubbers studied have fairly good adhesion to Leukonat films, without added fillers. The adhesion of butyl rubber to the Leukonat film is very low (Figure 6). The results of the experiments lead to the following empirical rule: if the rubber-metal bond strength produced by Leukonat is high, this means that both surfaces in contact with the Leukonat film interact with it with approximately the same intensity. This corresponds to the bonding of most unfilled rubbers.

If an active filler is added to such a rubber, one of the surfaces becomes more active, the adhesive becomes attached to it first, and the total bond strength produced is low. When unfilled butyl rubber is bonded to metal, the rubber surface has the lower intensity of interaction with the adhesive film; in this case addition of a filler of the gas channel black type may increase the intensity of interaction between the rubber and the adhesive film, thereby increasing the bond strength between the butyl rubber and the metal. Addition of a filler of the thermal black type to such a rubber should not greatly increase the adhesion of the rubber to the adhesive film. The experimental data in Figure 6 confirm this view. Thus, it is demonstrated once again that carbon black present in rubber is directly involved in bond formation at the adhesive-rubber boundary when rubber is bonded to metal by means of Leukonat.

It is well known from experience in the use of Leukonat adhesive that the metal should be sandblasted to obtain a sufficiently high bond strength between metal and rubber with the aid of this adhesive. It is reported in a number of papers that Leukonat adhesive softens during vulcanization and leaks out of the mold. It was assumed that sandblasting of the metal prevents leakage of the adhesive, thus increasing bond strength. However, as has been shown in the present investigation, good bond strength can be obtained also with smooth metal surfaces if the rubber formulation is suitably chosen (unfilled rubbers of a number of types, rubbers with thermal black). Therefore this is not the sole cause of poor bonding with smooth metal surfaces. It was also believed that sandblasting increases the contact area between the metal and the adhesive film, with greater bond strength as a result. Several experiments were performed to test this; it was found that sandblasting increases the true surface area of the metal by a factor of 1.5-2, while the bond strength becomes 20-100 times as great. Therefore increase of the contact area is also not the main cause of increased bond strength. The probable reason is that a sandblasted metal surface differs qualitatively from a surface which has not been so treated. The interaction intensity of adhesive films with such surfaces increases (Figure 7).

By sandblasting the metal surface we tend to equalize the degree of interaction of the Leukonat film with the metal and the rubber. The test results in Figure 7 show that rubber containing an active filler is bonded fairly firmly to a sandblasted metal surface; the peeling is cohesive in character. Sandblasting is quite ineffective for bonding rubber containing thermal black. As has already been stated, when butyl rubber (with or without fillers) is bonded to metal by means of Leukonat adhesive, the adhesive remains on the metal in all cases. Therefore in this instance it is necessary to seek methods of increasing the activity of the rubber, for improving the bond strength. Sandblasting of the metal does not result in any considerable increase of bond strength.

The slight increase of bond strength is evidently the result of an increase of the contact area of the sandblasted metal (Figure 8).

SUMMARY

1. In bonding of rubber to metal by Leukonat adhesive, the type of filler present in the rubber has a very great influence on the rubber-metal bond strength.

2. Active fillers of the gas channel black type in the rubber mixture increase the interaction of the rubber with the adhesive film.

3. Inactive fillers of the thermal black type have little influence on the interaction of the rubber with the adhesive film.

4. The results of the experiments suggest that Leukonat interacts chemically with active fillers present in the rubber during the bonding process.

5. The following empirical rule is formulated: high rubber-metal bond strength is obtained if the interaction of the adhesive film with the rubber is approximately of the same degree as with the metal. This rule is supported by the experimental data.

6. Sandblasting of the metal surface increases the true contact area by a factor of 1.5-2, while the bond strength is increased 20 to 100 times; this indicates that qualitative changes occur in the surface on sandblasting and that the nature of the metal-adhesive interaction is greatly changed in the process.

It is difficult to explain this other than on the assumption that the charge of the double layer at the metal-adhesive boundary is increased, and in consequence the work of separation of this layer at the boundary is greater.

LITERATURE CITED

[1] O. Bayer, Modern Plastics 24, 10, 149 (1947).

[2] T.J. Meyrick and J.T. Watts, IRI Transactions 25, 3, 150 (1949).

[3] H. Barron, Rub. Plastics Age 35, 1, 40 (1954).

[4] T.J. Meyrick and J.T. Watts, Ind.Rub. J. 72, 13 (1952).

[5] K.S. Zherebkov, Bonding of Rubber to Metals (Goskhimizdat, 1956).

[6] G.E. Proske, Kautsch. u Gummi 10, 153 (1952).

[7] B.V. Deryagin and N.A. Krotova, Adhesion (Izd. AN SSSR, 1949).

[8] A.A. Blagonravova and G.A. Levkovich, Progr. Chem. 24, 1, 93 (1955).

[9] F.F. Koshelev, Rubber Technology (State Tech. Press, 1951).

[10] K.S. Stearns and B.L. Johnson, Ind. Eng. Chem. 43, 146 (1951); M.L. Studebaker, Rubber Age 77, No. 1, 69 (New York, 1955); W.R. Smith and W.D. Schaeffer, Ind. Eng. Chem. 33, 1303 (1941); M.L. Studebaker and J.R. Hultman, Rubber World 132, No. 1, 74 (1955).

[11] N.N. Lezhnev and A.S. Kuzminsky, Proc. Acad. Sci. USSR 110, 1, 108 (1956).

[12] B.A. Dogadkin, B.V. Lukin and Z.N. Tarasova, Colloid J. 18, No. 4, 413 (1956) (T.p. 407).*

[13] G.M. Sheehan, G. Kraus and A.B. Conciatori, Ind. Eng. Chem. 44, 3, 580 (1952).

Received April 26, 1957

Institute of the Rubber Industry, Institute of
Physical Chemistry, Acad. Sci. USSR
Laboratory of Surface Phenomena — Moscow

---

*T.p. = C.B. Translation pagination.

EFFECT OF MERCAPTOBENZOTHIAZOLE ON STRUCTURAL CHANGES IN RUBBER ON OXIDATION, HEATING AND PLASTICIZATION

B. Dogadkin, A. Dobromyslova, L. Sapozhkova* and I. Tutorsky

Mercaptobenzothiazole (MBT, Captax) belongs to a class of compounds which, owing to presence of SH groups, are vigorous activators of rubber plasticization.

The first report of the plasticizing action of mercaptans is contained in a paper by Williams and Neal [1]. Subsequently some of these compounds (β-naphthylmercaptan, xylylmercaptan, etc.) were used in technological practice, designated as RPA (Rubber Peptization Agents). This name shows that it was originally believed that the plasticizing action of these compounds consists of peptization of the structural formations in the rubber. However our investigations showed that the acceleration of the plasticization process caused by mercaptans is largely the result of their influence on the interaction between oxygen and the rubber. Other authors [2] reached a similar conclusion. Our principal experimental data on the influence of mercaptobenzothiazole on oxidation and plasticization of rubber are given below.**

Effect of mercaptobenzothiazole on oxidation of natural rubber. There were no direct experimental data in the literature on the influence of mercaptans on the oxidation of rubber. We therefore carried out experiments on the kinetics of rubber oxidation in an apparatus of the Kohman type [3], at atmospheric, approximately constant, oxygen pressure, by measurement of the volume of the gas absorbed. The rubber was placed in the absorption vessel in the form of films deposited from solution on glass plates. The films were 0.015-0.02 mm thick. Figure 1 shows that addition of MBT significantly influences the oxidation of rubber, shortening the induction period and increasing the oxidation rate during the principal steady period. The apparent activation energy of oxygen absorption, calculated from data on the principal temperature over the temperature range of 100 to 120°,

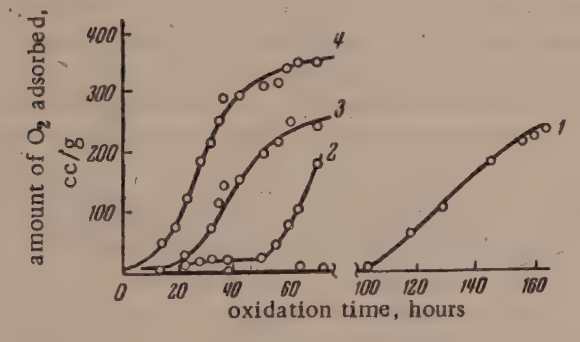

Fig. 1. Kinetics of oxidation of rubber at 100°: 1) without MBT; 2) with 0.31% MBT; 3) with 0.78% MBT; 4) with 1.55% MBT.

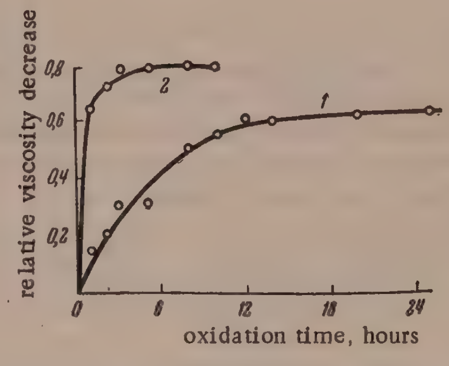

Fig. 2. Variation of the viscosity of rubber solutions as the result of oxidation: 1) without MBT; 2) with 1.55% MBT.

---

* Deceased

** These results were obtained in 1942-1944 and are given in the reports of the M.V. Lomonosov Institute of Fine Chemical Technology, Moscow, and in L. Sapozhkova's dissertation "Investigation of the Chemical Factors in the Plasticization of Rubber" (Moscow, 1947).

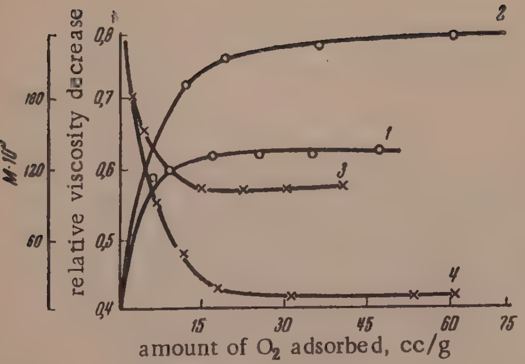

Fig. 3. Variation of the viscosity (1, 2) and molecular weight (3, 4) of rubber with the amount of oxygen absorbed: 1,3) rubber without MBT; 2,4) rubber with 1.55% MBT.

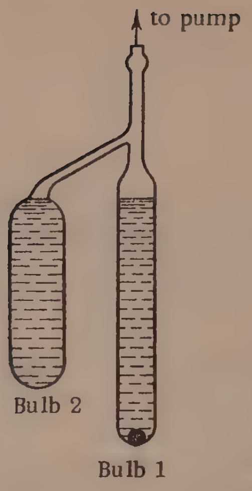

Fig. 4. Tube with ball for determining viscosity of rubber solutions.

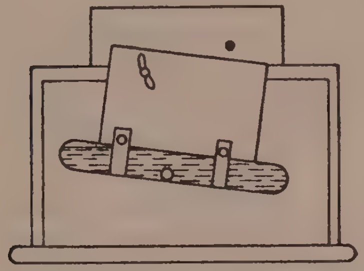

Fig. 5. Apparatus for determination of viscosity from the time of rolling of a ball in rubber solution.

is ~17 kcal/mole for pure rubber, and ~12 kcal//mole for rubber containing 1.55% MBT.

Oxidation of rubber in presence of MBT results in a greater decrease of solution viscosity than that found for rubber without MBT (Figure 2). This viscosity decrease is caused by scission of the molecular chains in the rubber, as is shown by data on the molecular weight of the rubber, determined by the osmotic method [4]. Degradation of the rubber occurs mainly during the initial (induction) period, and after 3 hours of oxidation the average molecular weight already falls from 200,000 to 54,000 (Table 1). A comparison of the molecular weight determined by the osmotic method (M_0) with the value calculated from viscosimetric data (M_v) indicates that the chain configuration remains practically unchanged during oxidation in presence of MBT. Therefore MBT not only accelerates the oxidation of rubber but favors preferential scission of the molecular chains without any appreciable secondary processes of structurization. This is seen particularly clearly in examination of curves showing the relative decreases of viscosity and molecular weight (Figure 3) as functions of the amount of oxygen absorbed.

The accelerating effect of mercaptans on oxidation of unsaturated compounds has not been adequately considered or studied experimentally. Ziegler's paper [5] merely mentions that oxidation of benzodimethylfulvene is accelerated in presence of thiophenol.

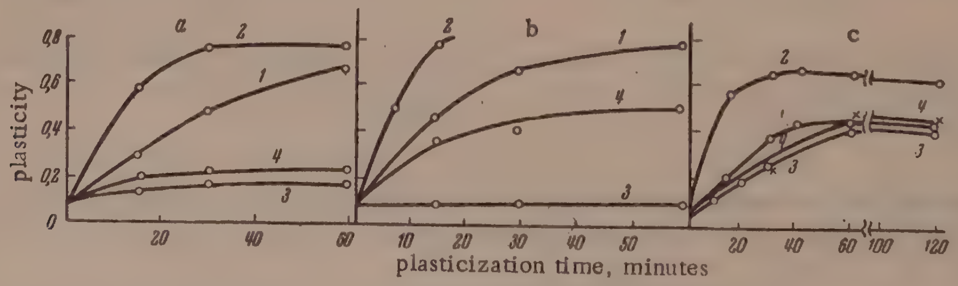

Fig. 6. Plasticization kinetics of natural rubber at 120° (a), at 150° (b) and at 100° (c): 1) in air without MBT; 2) in air with 1.55% MBT; 3) in nitrogen without MBT; 4) in nitrogen with 1.55% MBT.

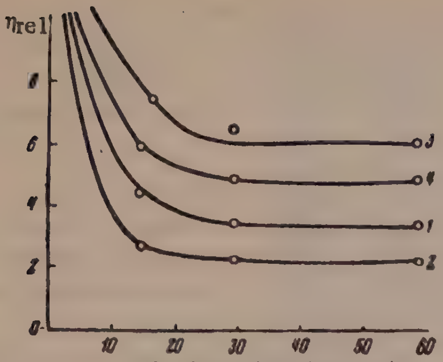

Fig. 7. Viscosity variations in plasticization of natural rubber at 100° (designations as in Figure 6).

In our opinion, MBT may act by the following mechanism. At high enough temperatures a reaction occurs with formation of HO_2* and RS* radicals:

$$RSH + O_2 \rightarrow RS^* + HO_2^*.$$

Interaction of RS* radicals with α-methylene groups in the rubber molecule (KaH) results in regeneration of the mercaptan and formation of a polymeric radical (Ka*) which initiates an oxidation chain:

$$RS^* + KaH \rightarrow RSH + Ka^*;$$
$$Ka^* + O_2 \rightarrow KaOO^*, \text{ etc.}$$

The HO_2* radical probably reacts with the double bond to form a hydroperoxide group, subsequent decomposition of which results in formation of an epoxide group and oxygen in active form.

TABLE 1

Change of Molecular Weight of Rubber on Oxidation

Rubber	M_v	M_O	M_O/M_v
Smoked sheet before oxidation	106,000	200,000	1.8
Ditto, after oxidation for 3 hours at 120°	33,000	54,000	1.6

The possibility is not excluded that the oxidation may be accelerated by an oxidation chain transfer mechanism as the result of direct interaction of peroxide radicals with MBT:

$$KaOO^* + RSH \rightarrow KaOOH + RS^*;\ RS^* + KaH \rightarrow RSH + Ka^*;\ Ka^* + O_2 \rightarrow KaOO^*.$$

Effect of mercaptobenzothiazole on thermal decomposition of rubber on heating in solution. The possibility of the thermal degradation of the molecular chains of natural rubber has been often discussed. Bolland [6] showed that no structural changes occur in solid purified rubber heated in a vacuum at temperatures up to 200°. We obtained similar results [7] in experiments with sodium butadiene rubber heated to 200°. Later, Watson [8], as the result of experiments in which natural rubber dissolved in chlorobenzene was heated at temperatures up to 120°, concluded that there is a possibility of purely thermal decomposition of the natural rubber molecules, containing a special type of weak bonds, the concentration of which is one bond per $1.3 \cdot 10^4$ monomer units.

The procedure used by Watson was similar to that used by us in earlier experiments,* in which we also found appreciable changes in the viscosity of rubber solutions heated to 100° in a nitrogen atmosphere. As we considered that the procedure used did not ensure complete removal of oxygen from the system,** we worked out a method whereby the action of oxygen was excluded to a greater extent when the rubber solutions were heated. The glass apparatus, shown diagrammatically in Figure 4, was repeatedly evacuated and filled with pure nitrogen in the heated state. A weighed quantity of MBT was then introduced into the bulb 2, followed by redistilled benzene saturated with nitrogen. The bulb 1, which contained a stainless steel ball 4 mm in diameter, was filled with 2% solution of purified rubber, all the purification stages of which (extraction, solution, reprecipitation and drying) were performed in a special apparatus in a nitrogen atmosphere. The apparatus was connected to a pump; after some of the benzene had been pumped out of bulb 2 the remaining benzene was frozen, while the benzene in bulb 1 was pumped out completely on heating to 35-45°. The residual pressure was 3-4 mm.

---

*See L.F. Sapozhkova's dissertation, the Lomonosov Institute of Fine Chemical Technology (Moscow, 1947).

**In Watson's experiments the rubber contained 0.25% of oxygen.

The apparatus was then again filled with pure nitrogen, the benzene in bulb 2 was poured over into bulb 1, and this bulb was then sealed off; the rubber in it was dissolved in the benzene, and the solution was heated to 100° in a thermostat. Structural changes in the rubber were characterized by the relative change of viscosity, calculated by the equation $(T_0 - T_1)/T_0$, where T_0 is the time for the ball to roll (between two marks on the bulb) before heating, and T_1, the time after heating. The bulb was fixed at a definite angle to the horizontal (Figure 5).

Table 2 shows that very little change of solution viscosity is produced by heating to 100°, and MBT does not increase thermal degradation of the rubber. These viscosity changes are reversible; if the solutions are kept in the dark at room temperature the viscosity gradually increases and in 100 hours already returns to practically its original value (Table 3). From this it may be concluded that the viscosity decrease in rubber solutions heated to 100° is to be explained by deaggregation of secondary structural formations in the rubber, which may be associated with the presence of oxygen-containing functional groups in the rubber molecules. Thermal dissociation of the rubber molecules into free radicals evidently does not occur on heating to 100°, since mercaptobenzothiazole and other free radical acceptors do not influence the course of the reversible thermal change of solution viscosity.

TABLE 2

Changes in the Viscosity of Rubber Solutions on Heating at 100° in a Nitrogen Atmosphere

Duration of heating, minutes	Solution without MBT		Solution with 1.55% MBT	
	T_1 sec	$\frac{T_0 - T_1}{T_0}$	T_1 sec	$\frac{T_0 - T_1}{T_0}$
0	67	0	63	0
15	55	0.18	51	0.19
30	–	–	52	0.18
45	56	0.16	–	–
60	–	–	49	0.23
100	50	0.22	–	–
120	–	–	50	0.20
160	53	0.21	51	0.19
180	–	–	51	0.19
300	53	0.21	–	–
360	53	0.21	–	–

TABLE 3

Restoration of Viscosity on Storage of Solutions in the Dark at Room Temperature

2% rubber solution	Initial viscosity in seconds	Viscosity after heating at 100°, in seconds	Viscosity after storage for	
			48 hours	100 hours
Without MBT	67	53	63	64
With MBT	63	50	59	60

Effect of mercaptobenzothiazole on plasticization of natural rubber. The experiments on plasticization of rubber were first performed in a specially constructed closed mixer with Z-shaped blades rotating at 24 and 30 revolutions per minute [9]. Two cocks fitted in the airtight lid were used for evacuation of the mixer and for admission of the required gas (nitrogen,air, nitrogen-oxygen mixture) after the rubber had been put in. The mixer was electrically heated; the temperature in the range of 50-175° was regulated to the nearest ± 2.5°.

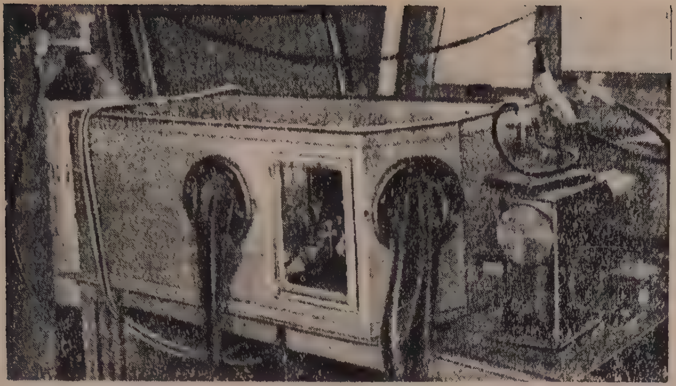

Fig. 8. Photograph of rolls in the "nitrogen" closet.

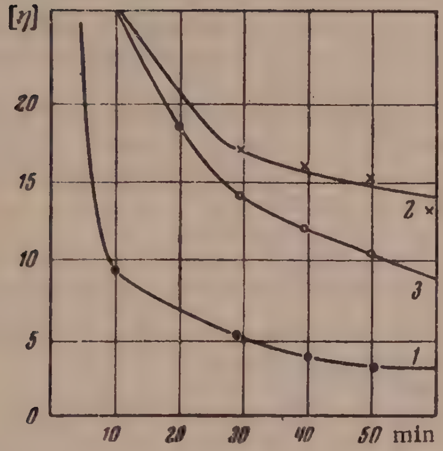

Fig. 9. Variation of the intrinsic viscosity of NR during mastication: 1) in air; 2) in nitrogen containing 0.5% O_2; 3) in nitrogen.

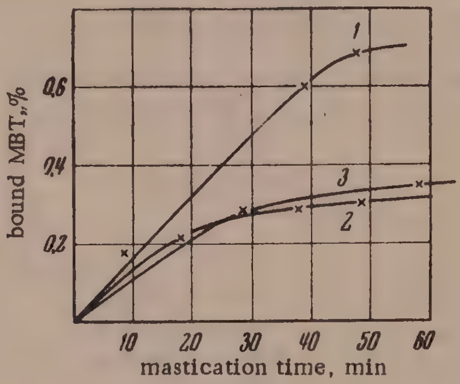

Fig. 10. Kinetics of MBT addition during mastication of NR: 1) in air; 2) in nitrogen containing 0.5% O_2; 3) in nitrogen.

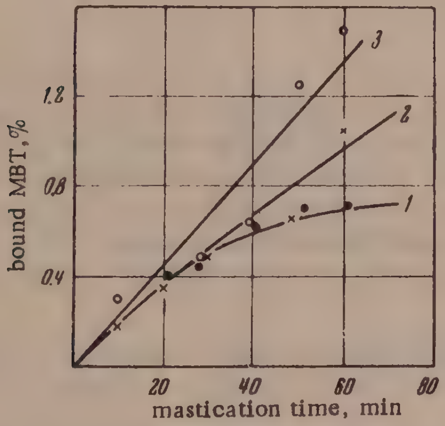

Fig. 11. Kinetics of MBT addition during mastication of NR in air. The numbers represent the amounts of MBT introduced (in %).

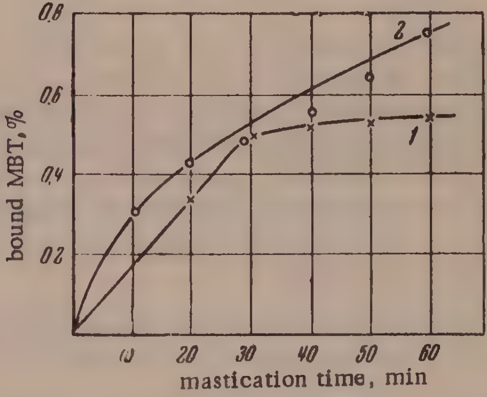

Fig. 12. Kinetics of MBT addition during plasticization of polyisobutylene: 1) in air; 2) in nitrogen.

Nitrogen was made free of oxygen by passing it over copper gauze at 475-525°.

Figure 6 represents the plasticization kinetics of natural rubber in nitrogen and in air at 120°. In both cases MBT increases the rate of the process, and is more effective in plasticization in air. Similar results were obtained in experiments at 100 and 150°. It is important to note that the temperature coefficient of plasticization of rubber in a nitrogen atmosphere (without MBT) is negative and at 150° practically no plasticization occurs. Structural changes in the rubber are characterized by the viscosity variation curves shown in Figure 7. It is seen in Figure 7 and also in Table 4 that mercaptobenzothiazole has a strong effect in decreasing the average molecular weight of the plasticized rubber. Thus MBT is involved both in thermooxidative and in mechanical processes of rubber degradation during mastication. In the latter case the mechanism of its action is probably in accordance with the views advanced by Pike and Watson [10] and other authors.

As has just been stated, mechanical degradation of the molecular chains during plasticization has a negative temperature coefficient. For a clearer determination of the role played by MBT in mechanical plasticization of rubber, experiments were performed at temperatures not exceeding 30°.* Specially designed micro-rolls fitted in a "nitrogen" closet (Figure 8) filled with the required gas (nitrogen, argon, air). The inert gas was passed through the closet until the exit gas was free from oxygen (cuprammonium solution was used as indicator). To prevent leakage of air into the closet, excess gas pressure was used. Cooling was effected by circulation of water through the hollow rolls. Natural rubber (smoked sheet), previously extracted with cold acetone in a nitrogen atmosphere, and several synthetic rubbers of different structures were used.

TABLE 4

Variation of the Molecular Weight of Rubber in Plasticization

Material studied	Plasticization time in minutes	Plasticity	Mol wt 10^{-3}
Original rubber	–	0.08	216
Rubber plasticized in air	30	0.65	57
Ditto, in nitrogen	60	0.10	107
Rubber plasticized with 1.55% MBT in air	15	0.67	35
Ditto, in nitrogen	60	0.44	72

Figure 9 shows that at 30° the plasticization of rubber, as measured by change of intrinsic viscosity, is more rapid in air. MBT is found to combine with the rubber (Figure 10), more rapidly in air than in nitrogen. This addition proceeds by a more complex mechanism than that of a simple bimolecular action, as shown by the consumption of MBT as a function of the concentration (Figure 11). The type of rubber has a significant influence both on the plasticization rate and on the addition of MBT. Table 5 shows that, for a given plasticization time, the amount of MBT added to the rubber increases with increasing contents of 1-4 structure in its molecular chains. Addition of MBT occurs also in plasticization of polyisobutylene, which does not contain double bonds in its molecules (Figure 12).

To elucidate the mechanism of the addition of MBT to rubber during mastication, a study was made of the distribution of the combined MBT between fractions of different molecular weight in the rubber.

Natural rubber, extracted with cold acetone in a nitrogen atmosphere, was masticated for 20 minutes on cold rolls with addition of 1 part by weight of MBT, tagged with radioactive S^{35} in the sulfhydryl group. The masticated product was fractionated by the method of A.S. Novikov and F.S. Tolstukhina. Methyl alcohol was added dropwise with stirring to 1% solution of rubber in benzene at 35° until the solution became turbid. The temperature of the solution was then raised by 2-3° until it became quite clear, and the solution was stirred for

---

*These experiments were performed in 1955.

1 hour at that temperature. The temperature was then again lowered to 35°; the solution was held at that temperature for 24 hours until the liquid above the precipitated fraction became quite clear. The liquid was decanted off, and the precipitated fraction was purified by threefold precipitation by methyl alcohol from benzene solution. Neozone (phenyl-β-napthylamine) was added each time to the solution. The isolated fraction was then dried under vacuum until the solvent was completely removed, dissolved in benzene, and analyzed for MBT by the radiometric method, the radioactivity of the film being determined. The intrinsic viscosities of benzene solutions of the fractions were determined.

TABLE 5

Binding of MBT by Rubbers of Different Structure During Mastication for 20 Minutes in Air

Type of rubber	Content of 1-4 bonds	$\frac{MBT_{bound}}{MBT_{total}}$
NR	100	0.48
SKBM	70	0.25
SKB	30	0.11

The results obtained are given in Table 6. Table 6 shows that the amount of combined MBT increases considerably (up to a certain limit) with decreasing molecular weight of the fractions. This shows that there is a direct connection between the reactions of mechanical degradation of the rubber molecules and of MBT addition. The lower MBT content of the last fraction can be attributed to the fact that this fraction contains the low molecular portion of the original rubber, which is less prone to mechanical degradation under shearing stresses.

TABLE 6

Contents of MBT in Different Fractions of Masticated Rubber

Fraction No.	Precipitation temperature, °C	Weight of fraction, in g	(η)	Average radiation activity with background correction	I_t/I_0	Amount of combined MBT in moles/liter x 10^3
Not fractionated	–	23	12.0	546	1	–
1	35.3	6	27	29	0.0531	3.21
2	26.7	7	24.5	50	0.0915	5.45
3	20.4	5	10.2	60	0.11	6.22
4	9.5	3	8.0	39	0.0715	4.28

From the results given in Table 6, and from the fact that during mastication MBT combines with saturated polyisobutylene, while in the case of unsaturated compounds the addition of MBT increases with increasing contents of diallyl bonds of 1-4 structure, the following mechanism can be postulated for the addition of MBT to rubber during mastication in an inert gas atmosphere. When the mechanical strains arising along the elastomer chains in a field of large shearing forces exceed the energy of the $=CH-CH_2 \underline{\downarrow} CH_2-CH=$ chemical bond, which is approximately 40 kcal/mole, these bonds are broken to give stable polymeric radicals of the allyl type:

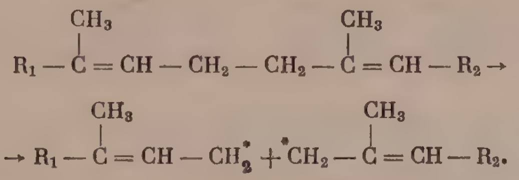

$$R_1-\overset{\overset{CH_3}{|}}{C}=CH-CH_2-CH_2-\overset{\overset{CH_3}{|}}{C}=CH-R_2\rightarrow$$

$$\rightarrow R_1-\overset{\overset{CH_3}{|}}{C}=CH-\overset{\bullet}{CH_2}+{}^{\bullet}CH_2-\overset{\overset{CH_3}{|}}{C}=CH-R_2.$$

These radicals react with MBT molecules, saturating their free valencies; this prevents their recombination and causes a sharp decrease of molecular weight:

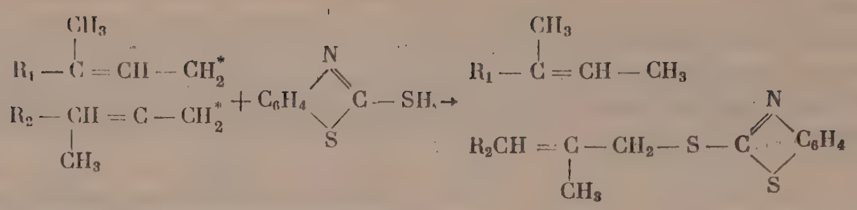

The benzothiazole radical 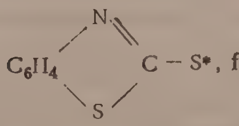, formed by removal of an H atom from the MBT molecule, does not initiate a new chain by addition at a double bond in the rubber molecule or removal of an H atom from an α-methylene group, as is the case when rubber is heated with dibenzothiazolyl disulfide [11]. Recombination of the benzothiazolyl and polymeric radicals is more advantageous from the energy standpoint. Moreover, the polymeric radicals formed by mechanical rupture of the macromolecules cannot be removed far apart owing to the high viscosity of the medium, so that the topochemical conditions also favor addition of MBT to two polymeric radicals.

SUMMARY

1. Mercaptobenzothiazole (MBT) accelerates the oxidation of natural rubber and considerably increases the rate of its oxidative degradation.

2. When benzene solutions of natural rubber are heated in an inert gas atmosphere at 100°, no irreversible changes occur in the rubber whether in presence or in absence of MBT.

3. Plasticization of natural rubber in air at 100-150° is intensified in presence of MBT, which is caused mainly by the accelerating action of the latter on the oxidative degradation of rubber.

4. Mercaptobenzothiazole assists plasticization of rubber at low temperatures in an inert gas atmosphere. MBT is consumed in the process, owing to its interaction with the polymeric radicals formed by mechanical rupture of the rubber molecules.

5. The amount of MBT reacting with the rubber increases with increasing contents of 1-4 structure in the rubber molecules.

6. It is shown that different fractions of the masticated product contain different amounts of MBT, indicating that MBT reacts preferentially with the end valencies of the radicals formed by cleavage of diallyl bonds.

7. Reaction schemes for the interaction of MBT with rubber in mechanical and oxidative processes are suggested.

LITERATURE CITED

[1] J. Williams and A.M. Neal, Ind. Eng. Chem. 22, 874 (1930).

[2] W.F. Busse and E.N. Cunningham, Proc. Rub. Techn. Conf (London, 1938), p. 288; D.F. Twiss, Ind. Rub. J. 108, 26 (1945).

[3] G.T. Kohman, J. Phys. Chem. 33, 226 (1929).

[4] B.A. Dogadkin, M.I. Arkhangelskaya and I.G. Soboleva, Investigations of High Molecular Compounds (Izd. AN SSSR, Moscow-Leningrad 1949), p. 253.

[5] K. Ziegler and K. Gänicke, Ann. 551, 213 (1942).

[6] J.L. Bolland and W.J. Orr, Trans. IRI 21, 2 (1945).

[7] B.A. Dogadkin and D.M. Pevzner, Trans. Sci. Res. Inst. Tire Ind. 47 (1950).

[8] W.F. Watson, Trans. IRI 29, 202 (1953).

[9] A.S. Novikov, Dissertation, Moscow Inst. Fine Chem. Technology (1945).

[10] M. Pike and W.F. Watson, J. Pol. Sci. 9, 229 (1952).

[11] B. Dogadkin, V. Selyukova, Z. Tarasova, A. Dobromyslova, M. Feldhstein and M. Kaplunov, Proc. Acad. Sci. USSR 92, 61 (1953); Colloid J. 17, 215 (1955) (T.p. 199).*

Received March 22, 1957

The M.V. Lomonosov Institute of
Fine Chemical Technology,
Moscow

---

*T.p. = C.B. Translation pagination.

~~THE~~ STRUCTURE OF GELS

10. GLOBULIZATION OF RUBBER UNDER THE ACTION OF NONSOLVENTS ADDED TO SOLUTIONS

P.I. Zubov, Z.N. Zhurkina and V.A. Kargin

It has been shown [1-4] that under certain conditions it is possible to obtain globular structures from ordinary linear polymers. Globulization of the molecules in these cases was induced by formation of intramolecular bonds between active groups which were either present in the molecular chains or were introduced into them in various ways. Globular structures of certain proteins, gelatin, casein and synthetic and natural rubbers were obtained. In a number of properties, namely: solubility, solution viscosity, mechanical properties of films and others, the polymers with "globular" molecular structure differed considerably from the original polymers, evidently because of the difference in the molecular form.

The degree of globulization was determined [1-4] mainly by measurement of solution viscosity. It is known, however, that changes in the composition of the medium also produce changes of solution viscosity in some instances. For example, alcohols are often used in the rubber industry for decreasing the viscosity of rubber adhesives. On the supposition that coiling of the molecules also takes place when nonsolvents are added to rubber solutions, we commenced an investigation of this effect. This study was also of interest because there is a significant difference between globulization of rubber caused by addition of active substances to solutions, and that caused by addition of nonsolvents. In the former case coiling of the molecules is largely the consequence of energy interaction, while in the latter globulization is determined by entropy effects.

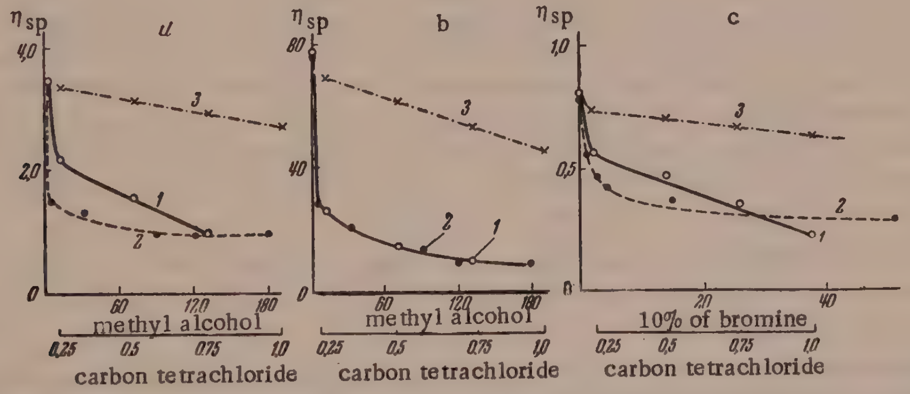

Fig. 1. Effects on the viscosity of 0.25% NR solution (a), 1% NR solution (b), and 0.25% SK-B solution (c), of additions of: 1) methyl alcohol; 2) 10% of bromine; 3) carbon tetrachloride.

The present communication contains data obtained in a study of the influence of added nonsolvents on the viscosity of solutions of different rubbers. The materials studied were natural smoked sheet rubber and synthetic rubbers, mainly of the sodium butadiene type. The solvent used was carbon tetrachloride, and the nonsolvent

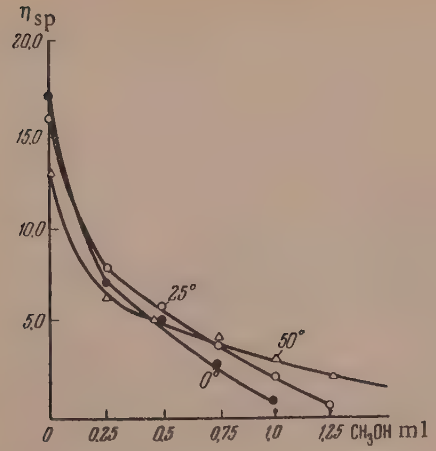

Fig. 2. Effect of additions of methyl alcohol on the viscosity of 0.5% NR solution in CCl_4 at various temperatures.

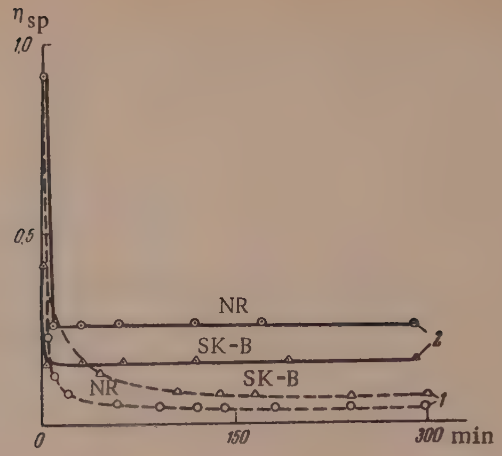

Fig. 3. Effect of additions of bromine (1) and methyl alcohol (2) on the viscosities of 0.16% solutions of NR and SK-B.

was methyl alcohol. The degree of globulization of the molecules was determined, as previously, by measurements of solution viscosity. Rubber solutions of different concentrations were used in the experiments.

The experimental results are shown in Figure 1, where the amounts of methyl alcohol or CCl_4 in milliliters added to 5 ml of the solution (Curves 1 and 3) and the time, Curve 2 (the time is taken from the moment of addition of bromine to the solution; the amount of bromine taken corresponded to 10% of the unsaturated bond content in the rubber) are taken along the abscissa axis and the specific viscosity along the ordinate axis; it is seen that the viscosity decrease of the rubber solutions is proportional to the amount of nonsolvent (methyl alcohol) added, right up to precipitation of the rubber. The limiting value of the viscosity of rubber solutions in presence of the nonsolvent differs little from the viscosity of globular rubber solutions produced by bromination.

Experiments were carried out to determine the effects of rubber solution concentration and temperature on the amount of methyl alcohol required to produce turbidity of the solution. The results show that the amount of methyl alcohol depends to some extent on the solution concentration (Table 1) and to a large extent on the temperature (Figure 2). Figure 2 gives curves for the viscosity variations of 0.5% solution of natural rubber (of a low degree of milling) in carbon tetrachloride on addition of methyl alcohol. The curves in Figure 2 correspond to experimental temperatures of 0, 25 and 50°. The amounts of methyl alcohol in milliliters added to 5 ml of rubber solution are taken along the abscissa axis, and the specific viscosity of the solution along the ordinate axis. Arrows indicate precipitation of the rubber. Figure 2 shows that one and a half times more methyl alcohol is needed at 50° than at 0° to precipitate the rubber.

In dilute solutions (0.16%) of a number of rubbers precipitation of rubber occurs at practically the same contents of methyl alcohol. The only exception is polyisobutylene, which is precipitated at a lower alcohol content than the other rubbers (Table 2).

It may be concluded from these results that globulization of rubbers by addition to the solutions of active substances which react with the rubber molecules (S_2Cl_2 and halogens) and the coiling of rubber molecules by the action of added nonsolvents have the common feature that in both cases the macromolecules assume a globular configuration. Experiments carried out in order to study the kinetics of globulization of the molecules caused by additions of nonsolvents to the rubber solutions showed that on addition of methyl alcohol the viscosity of the rubber solutions falls almost instantaneously and remains constant for a considerable time. In contrast to this, globulization of rubber effected by the action of 20% of bromine (calculated on the unsaturated bonds) is clearly seen to be a function of time (Figure 3).

The following experiments were carried out to investigate the reversability of the globulization of rubber

TABLE 1

Variation of the Amount of CH_3OH in Milliliters Required to Produce Turbidity, with the Concentration of the Rubber Solution

Concentration of NR solution in %	0.1	0.16	0.25	0.4
Specific viscosity of solution	0.68	0.77	2.73	6.77
Amount of CH_3OH in ml to produce turbidity in 5 ml of solution	1.14	1.07	0.52	0.39

TABLE 2

Amounts of CH_3OH in ml Causing Turbidity in 5 ml of 0.16% Rubber Solutions

Type of rubber	Amount of CH_3OH in ml	Type of rubber	Amount of CH_3OH in ml
Butyl rubber	1.25	Low-temperature No. 3	1.20
Low-temperature No. 1	1.25	SKS-30A	1.20
SK-B	1.30	Polyisobutylene	0.75
Isoprene	1.25	Neoprene	1.10
SK-B No. 1, low-temperature	1.30	NR, low mastication	1.10
SK-B No. 3, high-temperature	1.25		

TABLE 3

Effect of Additions of CH_3OH and CCl_4 on the Specific Viscosity of Rubber Solutions

Concentration of original NR solution in %	Specific viscosity			
	of original solution	after addition to 10 ml of the original solution, of 15 ml of		after evaporation of mixture and solution of rubber in CCl_4
		CH_3OH	CCl_4	
0.4	6.95	1.9	–	5.2
0.4	6.95	–	5.3	5.0
1	70.6	9.0	–	32.3
1	70.6	–	42.0	38.0

molecules caused by addition of nonsolvents to solutions. Methyl alcohol was added to a rubber solution the viscosity of which had been determined previously, and after thorough stirring the viscosity was measured again. The solvent was then removed from the mixture at room temperature by means of a vacuum pump. The residual rubber was dissolved in the pure solvent (CCl_4) and the viscosity of the solution was again measured. A comparison of the viscosity of this solution with the viscosity of the original rubber solution before addition of the methyl alcohol gave an indication of the reversibility of the globulization of the rubber molecules caused by addition of the nonsolvent. To allow for the influence of other factors (oxidation, etc.) on the viscosity of the rubber solution, a control experiment was carried out, which differed from the main experiment only by the addition of the same amount of pure solvent (CCl_4) instead of methyl alcohol to the rubber solution. The results of these experiments showed that even on incomplete evaporation of the rubber solution containing methyl alcohol, followed by dilution of the resultant concentrated solution with pure solvent (CCl_4) to the original concentration, the viscosity of the solution increases. Complete removal of the solvent followed by solution of the rubber in CCl_4 results in a greater viscosity increase (Table 3).

It seemed possible that in consequence of the globulizing action of methyl alcohol on the rubber molecules the solubility of rubber in a mixture of CCl_4 and CH_3OH should differ from the solubility in pure CCl_4. Experiments showed that different rubbers dissolve much more rapidly in a mixture of CCl_4 and CH_3OH than in pure CCl_4. The viscosities of solutions of rubbers in the mixture are much lower than the viscosities of solutions in the pure solvent. For example, a 2.5% solution of NR (of a low degree of mastication) in CCl_4 is a nonfluid gelatinous mass, while a 2.5% solution of the same rubber in a mixture of CCl_4 and CH_3OH in 6.7 : 1 ratio is quite fluid, although viscous. An interesting feature is that, in contrast to solution in the pure solvent, solution of rubber in the solvent-nonsolvent mixture proceeds almost without swelling, which, naturally, is associated with globulization of the molecules.

If a low-viscosity solution of rubber containing methyl alcohol is evaporated and the rubber residue is then dissolved in pure CCl_4, the viscosity of the solution so formed differs little from the viscosity of a rubber solution of the same concentration, prepared without the use of methyl alcohol (Table 4).

TABLE 4

Reversibility of the Globulization of Rubber Molecules

Composition of solvent	Specific viscosities of rubber solutions					
	1% NR		1% SKB		2.5% SKB	
	before evaporation	after evaporation and solution in CCl_4	before evaporation	after evaporation and solution in CCl_4	before evaporation	after evaporation and solution in CCl_4
CCl_4	52.3	68.3	4.1	4.0	20.4	16.8
$CCl_4 : CH_3OH = 20 : 1$	31.7	66.1	–	–	–	–
$CCl_4 : CH_3OH = 10 : 1$	25.2	63.7	–	–	–	–
$CCl_4 : CH_3OH = 6.7 : 1$	18.1	60.3	2.1	3.5	9.1	16.1

SUMMARY

1. Addition of nonsolvents to rubber solutions causes globulization of the macromolecules, similar to that occurring on addition of active substances (sulfur monochloride, halogens, etc.) to rubber solutions.

2. The difference between these processes lies in the fact that the coiling of the rubber molecules under the action of methyl alcohol is very rapid.

3. The globular structures in rubbers, produced by addition of nonsolvents to the solutions, in contrast to the stable globules formed in halogenation and vulcanization of rubber solution, are easily broken down and the molecules assume the linear form characteristic of the original rubber.

LITERATURE CITED

[1] P.I. Zubov, Z.N. Zhurkina and V.A. Kargin, Proc. Acad. Sci. USSR 67, 659 (1949).

[2] P.I. Zubov, Z.N. Zhurkina and V.A. Kargin, Colloid J. 16, 179 (1954) (T.p. 185).*

[3] P.I. Zubov, Z.N. Zhurkina and V.A. Kargin, Colloid J. 16, 345 (1954) (T.p. 337).*

[4] P.I. Zubov, Z.N. Zhurkina and V.A. Kargin, Colloid J. 17, 31 (1955) (T.p. 27).*

Received August 7, 1956

The L.Ya. Karpov Physicochemical
Scientific Research Institute

---

*T.p. = C.B. Translation pagination.

SEDIMENTATION VOLUMES OF POLYDISPERSE SUSPENSIONS OF $Ca_3(PO_4)_2$ IN ELECTROLYTE SOLUTIONS

G.G. Kandilarov

Earlier communications dealt with variations of the sedimentation volumes of polydisperse kaolin suspensions in relation to the concentrations of various electrolyte solutions [1, 2]. It was of interest to determine the extent to which the results are applicable to other suspensions, and to study the influence of the electric charge on the particles of a suspension on its sedimentation volume. A study has been made of polydisperse suspensions of calcium orthophosphate in basic and acidic electrolytes with ions of different valencies (sodium hydroxide, normal sodium carbonate, sodium phosphate, aluminum chloride, and hydrochloric acid). Pure normal calcium orthophosphate (analytical reagent grade), previously ground in a mortar, was used for the investigation. It was found by means of electrophoresis that its aqueous suspensions are positively charged. 2 g samples of $Ca_3(PO_4)_2$ were mixed with 10 ml of the given electrolyte solution and shaken during two periods of 2 minutes, with or without the use of a glass rod. The suspensions so formed were left to settle in a thermostat for 24 hours at 25°. The deposit formed generally had a curved surface, which made exact determination of its volume difficult. Despite this, the dependence of the volume of the $Ca_3(PO_4)_2$ sediment on the concentrations of the various electrolytes was fairly well defined.

The results of the observations are shown in Figures 1-4.

Results for $Ca_3(PO_4)_2$ suspensions in NaOH solutions are given in Figure 1a. It is seen that with increasing NaOH concentration in the solution the volume of the $Ca_3(PO_4)_2$ suspensions at first remains approximately constant; at a concentration of ~200 millimoles/liter a minimum is formed, after which the curve begins to ascend. Under the same conditions the sedimentation volume and internal friction curves for kaolin suspensions rise steeply.

Figure 1b shows the results of experiments with $Ca_3(PO_4)_2$ suspensions in solutions of Na_2CO_3. It is seen that with increasing concentration of Na_2CO_3 the volume of the $Ca_3(PO_4)_2$ deposits tends to decrease. In this case also there is a minimum (at a concentration of 500 millimoles/liter), but this is situated somewhat to the right of the corresponding minimum for suspensions containing NaOH. For suspensions in sodium phosphate solutions (Figure 1c) the same tendency to a volume decrease is seen, but the minimum is shifted still further to the right (1000 millimoles/liter).

Finally, the results of experiments with $Ca(OH)_2$ solutions (Figure 2) show the same tendency, although weak, to a decrease of the sedimentation volume of $Ca_3(PO_4)_2$. In this case, however, the curve ends at a low concentration of $Ca(OH)_2$ owing to its low solubility.

A comparison of the curves for the variation of the sedimentation volume of positively charged $Ca_3(PO_4)_2$ suspensions in solutions of these electrolytes [NaOH, Na_2CO_3, sodium orthophosphate, $Ca(OH)_2$] reveals a tendency for the sedimentation volume to decrease with formation of a minimum in all cases. It was shown in earlier investigations [1] that negatively charged suspensions of kaolin in NaOH solutions give steeply ascending sedimentation volume and internal friction curves.

The opposite character of the variations of the sedimentation volumes of $Ca_3(PO_4)_2$ and of kaolin suspensions is probably related to the opposite electric charges of these suspensions. Since the $Ca_3(PO_4)_2$ particles are positively charged, changes of its sedimentation volume in solutions of basic electrolytes must be associated with their anions, i.e., hydroxyl ions. The latter probably neutralize the positive charge of the suspensions,

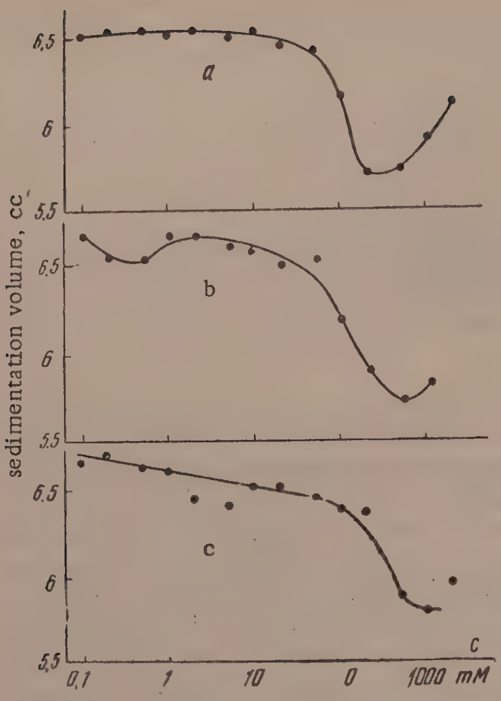

Fig. 1. Variation of the sedimentation volume of $Ca_3(PO_4)_2$ with electrolyte concentration: a) NaOH; b) Na_2CO_3; c) sodium orthophosphate.

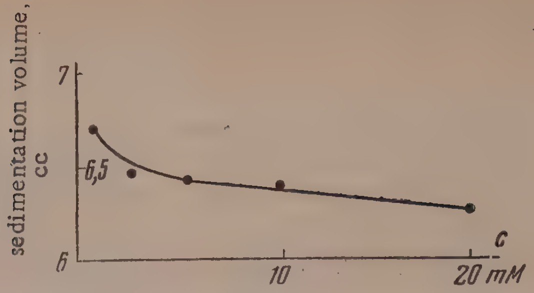

Fig. 2. Variation of the sedimentation volume of $Ca_3(PO_4)_2$ with $Ca(OH)_2$ concentration.

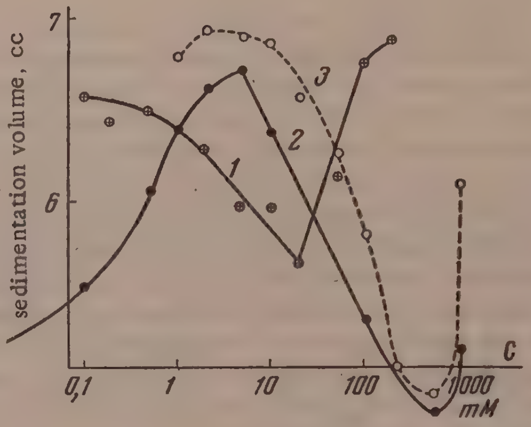

Fig. 3. Variation of the sedimentation volumes of: 1) $Ca_3(PO_4)_2$; 2) Schering kaolin; 3) Senovo kaolin, with $AlCl_3$ concentration.

thereby decreasing their hydration. In consequence the sedimentation volume of $Ca_3(PO_4)_2$ also tends to decrease. In kaolin suspensions, however, irrespective of hydration, hydroxyl ions repel the negatively charged particles (of the suspensions), resulting in a loose packing of the latter, so that the sedimentation volume of kaolin in sodium hydroxide solutions increases.

The charge of the anions also has an influence, seen in the fact that the minimum on the sedimentation volume curve for $Ca_3(PO_4)_2$ suspensions shifts, from a concentration of 200 millimoles/liter for sodium hydroxide, in the direction of higher concentrations for carbonate and phosphate ions, which have double and triple charges respectively.

It is seen in Figure 3 that with increasing concentration of aluminum chloride (which in this case can be regarded as a weak tribasic acid) the sedimentation volume of $Ca_3(PO_4)_2$ suspensions (Curve 1) decreases at first as the concentration changes to about 20 millimoles/liter, and then increases rapidly. At a concentration of 200 millimoles/liter the suspension becomes a mass with thixotropic properties, and the concentration-sedimentation volume curve is interrupted. It is highly probable that the increase of the sedimentation volume at high concentrations is the consequence of considerable hydration of the $Ca_3(PO_4)_2$ suspensions. At a concentration of 200 millimoles/liter the suspension becomes so thick that it resembles a gel, but strong agitation again converts it into a fairly mobile suspension.

At high concentrations of $AlCl_3$ the solubility of $Ca_3(PO_4)_2$ increases. With an $AlCl_3$ concentration of 500 millimoles/liter a turbid suspension is formed, with a deposit 2.25-2.40 cc in volume at the bottom of the vessel. At 1000 millimoles of $AlCl_3$ per liter the suspension becomes more transparent, and the volume of the sediment at the bottom of the vessel decreases to 0.70-0.75 cc.

Comparison of the curve for the variation of the sedimentation volume of $Ca_3(PO_4)_2$ suspensions in alumi-

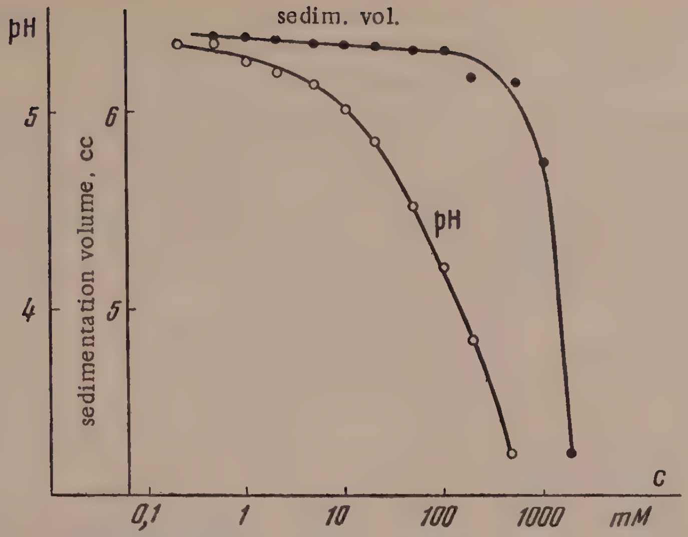

Fig. 4. Variation of the sedimentation volume of $Ca_3(PO_4)_2$ with HCl concentration.

num chloride solutions with the analogous curve for kaolin suspensions [1] (Figure 3, Curves 2 and 3) shows that the curves are opposite in character: with increasing aluminum chloride concentration the sedimentation volume (and the internal friction) of kaolin increases to a maximum at ~5 millimoles/liter, and then decreases rapidly. The sedimentation volume of $Ca_3(PO_4)_2$ suspensions, on the other hand, shows a minimum at a concentration of 20 millimoles/liter. This relative position of the curves is probably connected with the opposite electric charges of the two suspensions.

Figure 4 shows the variations of the pH of $Ca_3(PO_4)_2$ suspensions after exposure to hydrochloric acid for twenty four hours at 25°. The pH values were determined potentiometrically with quinhydrone and calomel electrodes. It is seen from Figure 4 that with increasing HCl concentration the sedimentation volume of $Ca_3(PO_4)_2$ suspensions remains at one relatively constant level up to an HCl concentration of 100 millimoles/liter. However, past this relatively high threshold value, at which the suspension reaches pH 4.2 in twenty-four hours, $Ca_3(PO_4)_2$ begins to be dissolved more rapidly, and the sedimentation volume quickly falls to zero. The relatively high threshold value beyond which rapid solution of $Ca_3(PO_4)_2$ in the acid begins is noteworthy. The concentration-pH curve also shown in Figure 4 indicates that in reality $Ca_3(PO_4)_2$ also dissolves at lower concentrations of hydrochloric acid, but because of its low content in the solution the acid is rapidly consumed in dissolving the salt, and the pH assumes higher values as a result.

In view of the fact that $Ca_3(PO_4)_2$ is present in soils or is added to soil as a phosphate fertilizer, and that it is present in urine (the pH of human urine is 5-7), these findings may shed some light both on the problem of phosphorus retention in the soil, and on the question of the formation of deposits of this salt in the human organism.

SUMMARY

1. The sedimentation volume of positively charged $Ca_3(PO_4)_2$ suspensions tends to decrease with increasing concentrations of NaOH, Na_2CO_3, sodium orthophosphate, and $Ca(OH)_2$, while the sedimentation volume and internal friction of negatively charged kaolin suspensions in sodium hydroxide increase sharply with increasing sodium hydroxide concentration. It may be assumed that this opposite course of the variation of sedimentation volume is associated with the opposite electric charges of the suspensions.

The curves for $Ca_3(PO_4)_2$ suspensions have a minimum which is shifted in the direction of higher concentrations with increase of the anionic charge. For NaOH solutions this minimum lies at ~200, for Na_2CO_3 at ~500, and for Na_2HPO_4 at ~1000 millimoles/liter.

2. With increasing $AlCl_3$ concentration the sedimentation volume of $Ca_3(PO_4)_2$ first decreases ($AlCl_3$ concentration 20 millimoles/liter) and then increases rapidly. At $AlCl_3$ concentration of ~200 millimoles/liter the suspension forms a viscous liquid with thixotropic properties. This course of the variation is opposite to the variation of the sedimentation volume and internal friction of kaolin suspensions in solutions of the same salt, which may be attributed to the opposite electric charges of the two suspensions.

3. With increasing hydrochloric acid concentration the sedimentation volume of $Ca_3(PO_4)_2$ suspensions remains constant up to an HCl concentration of 100 millimoles/liter. After this relatively high threshold value, at which the suspension attains a pH value of 4.2 in twenty-four hours, $Ca_3(PO_4)_2$ is dissolved more rapidly, and the sedimentation volume rapidly falls to zero. This may to some extent explain the fixation of phosphorus in soils and also deposition of $Ca_3(PO_4)_2$ in the human organism.

LITERATURE CITED

[1] G.G. Kandilarow, Koll. Z. 90, 321 (1940); 91, 56 (1940).

[2] G.G. Kandilarov, Colloid J. 13, 357 (1951); Sci. Trans. "V. Kolarov" VSI 1, 1 (1954); Colloid J. 18, 293 (1956) (T.p. 283).*

Received July 19, 1956

Chair of Inorganic, Analytical, Colloid and
Physical Chemistry at VIKhVPROM
Plovdiv, Bulgaria

---

*T.p. = C.B. Translation pagination.

GELATINIZED EMULSIONS

14. ETHYLCELLULOSE AS A STABILIZER OF EMULSIONS OF THE W/O ~~TYPE~~

L.Ya. Kremnev and G.A. Shadrin

Ethylcellulose is known to be a stabilizer for water-in-oil ("reverse") emulsions. However, no quantitative data are available on its emulsifying action, and the structure of the protective films which stabilize the droplets of the disperse phase in the emulsions is not known. The present investigation deals with these questions. Seven industrial ethylcellulose samples, differing in molecular weight and degree of ethylation, were used for studies of the emulsifying properties. The samples were previously fractionated. Four fractions were isolated by means of ligroine (b.p. 80-90°) from a solution of each sample in toluene; the molecular weights and ethoxyl group contents of the fractions were then determined. The molecular weights were calculated by the equation

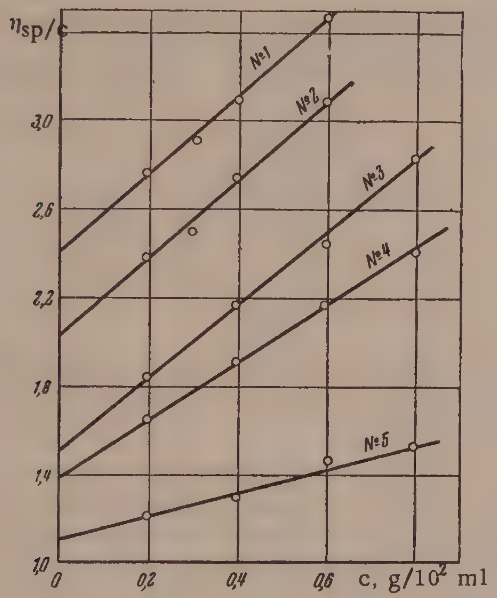

Fig. 1. Variation of reduced viscosity η_{sp}/c with concentration c of ethylcellulose fractions. The numbers correspond to the sample numbers in Table 1.

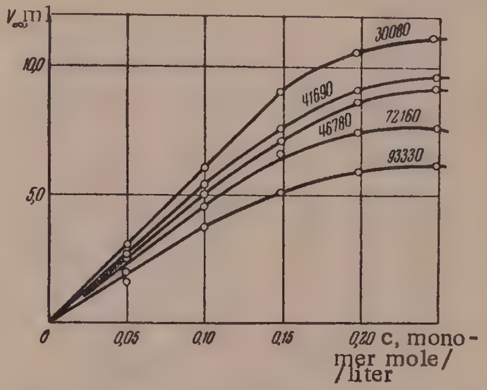

Fig. 2. Isotherm for emulsification as a function of concentration of ethylcellulose of different molecular weights (indicated on the curves).

$$[\eta] = KM^a,$$

where $[\eta]$ is the intrinsic viscosity; M is the molecular weight of the polymer; K and a are constants. The values of these constants for ethylcellulose were determined by Nikurashina and Glikman [1], and are:

For the high molecular fractions,	$K = 11.8 \cdot 10^{-4}$; $a = 0.666$;
For the low molecular fractions,	$K = 6.9 \cdot 10^{-4}$; $a = 0.715$.

As in the investigation cited [1], we determined the viscosity of alcohol-benzene solutions of the fractions in a capillary viscosimeter at 20 ± 0.05°. The values of the reduced viscosity η_{sp}/c were used to plot graphs for

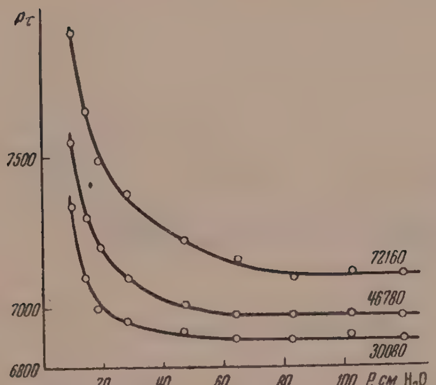

Fig. 3. Viscosities of ethylcellulose solutions of different molecular weights (shown on curves).

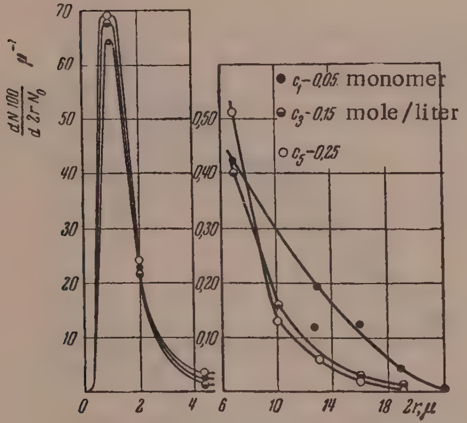

Fig. 5. Differential droplet size distribution curves for inverse emulsions stabilized by ethylcellulose of M = 72,160.

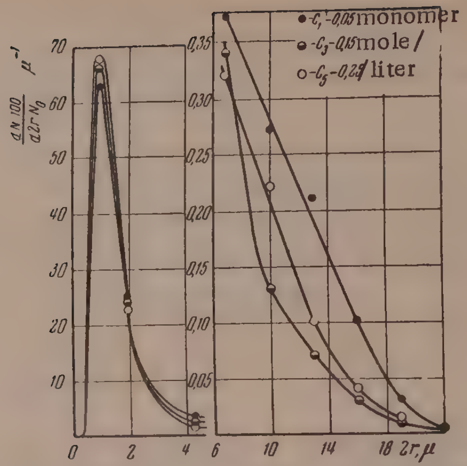

Fig. 4. Differential droplet size distribution curves for inverse emulsions stabilized by ethylcellulose of M = 93,330.

TABLE 1

Molecular Weights of Ethylcellulose Samples

Sample No.	Molecular weight	Ethoxyl number, %
1	93,330	48.66
2	72,160	48.90
3	46,780	48.79
4	41,690	48.86
5	30,080	48.73

$\eta_{sp}/c = f(c)$. Figure 1 shows that the lines cut off intercepts along the ordinate axis, corresponding to $[\eta]$ for each sample.

As the result of a preliminary investigation, five samples of different molecular weight but with similar ethoxyl numbers were selected (see Table 1). These samples were used for studying the effect of molecular weight of the polymer on emulsification.

Emulsions of water in toluene, of maximum concentration ("maximum emulsions") were prepared for the investigation, by our method with the use of a flexible spiral moving in a cylinder [2]. As usual, the end of emulsification was indicated when a successive addition of a small portion of water was no longer absorbed by the highly concentrated emulsion. The emulsions were diluted with xylene and subjected to microscopical dispersion analysis by the usual procedure adopted in our laboratory [3]. The results of this analysis were used to plot differential droplet size distribution curves, and the following were calculated: the thickness δ_{cr} of the protective films on the droplets, the surface S_{∞} developed by 1 ml of the dispersion medium in maximum emulsions, and the surface area S_0 per molecule of the polymer in the interphase.

Figure 2 shows emulsification isotherms, representing the maximum volume V_{∞} of the disperse phase in 1 ml of the dispersion medium as a function of the concentration $\underline{c}$ of ethylcellulose of different molecular weights. It is seen from Figure 2 that V_{∞} increases with $\underline{c}$, the curves being concave toward the abscissa axis; this, as in the other cases studied by us, is in agreement with the emulsification mechanism. The deviations from linearity, which increase with increasing $\underline{c}$, are explained by the fact that when each successive portion of the dis-

TABLE 2

Reverse Maximum Emulsions Stabilized by Ethylcellulose of High Molecular Weight

Ethylcellulose concentration		δ_{cr} in μ	S_∞ in m^2	S_0 in Å^2	S in Å^2
monomer mole/liter	mole/liter $\times 10^4$				
Sample No. 1; M = 93,330					
0.05	1.24	0.71	1.4	1860	15 200
0.10	2.49	0.25	4.0	2660	
0.15	3.73	0.17	5.9	2610	
0.20	4.97	0.16	6.2	2060	
0.25	6.21	0.15	6.5	1750	
Sample No. 2; M = 72,160					
0.05	1.61	0.56	1.8	1840	11 770
0.10	3.22	0.20	5.0	2560	
0.15	4.82	0.14	7.1	2430	
0.20	6.43	0.11	9.1	2330	
0.25	8.04	0.10	10.0	2050	

TABLE 3

Reverse Maximum Emulsions Stabilized by Ethylcellulose of Molecular Weight 30,080-46,780

Ethylcellulose concentration		δ_{cr} in μ	S_∞ in m^2	S_0 in Å^2	S in Å^2
monomer mole/liter	g mole/liter				
Sample No. 3; M = 46,780					
0.05	2,5	0,39	2,5	1660	7650
0.10	5,0	0,14	7,1	2360	
0.15	7,4	0,10	10,0	2220	
0.20	9,9	0,07	14,3	2380	
0.25	12,4	0,06	16,7	2220	
Sample No. 5; *M* = 30,080					
0.05	3.9	0.29	3.4	1440	4920
0.10	7.7	0.12	8.3	1780	
0.15	11.6	0.07	14.3	2030	
0.20	15.5	0.05	20.0	2130	
0.25	19.4	0.04	25.0	2130	

perse phase is introduced into the system, its emulsification is accompanied by further dispersion of all the emulsion droplets. Thus, the degree of dispersion of the highly concentrated emulsion increases continuously (homogenization occurs) during emulsification, up to the limiting value. Part of the stabilizer is expended in homogenization of the emulsion. Figure 2 shows that V_∞ decreases with increasing molecular weight of ethylcellulose. This influence of the molecular weight of the polymer is associated with the structural features of the protective films in emulsions, which will be discussed later. Another characteristic feature is that, at the limit, ethylcellulose emulsifies much smaller volumes of the disperse phase than typical stabilizers such as alkali soaps. This is also associated with the structure and properties of the protective films.

Table 2 gives details of the protective films in reverse maximum emulsions stabilized by ethylcellulose of relatively high molecular weight. The protective film thickness δ_{cr} decreases with increasing stabilizer concentration, tending to a constant value at high values of c. In this respect, polymeric emulsifiers are similar to the soaps studied previously. The significant difference is, however, that in the case of ethylcellulose stabilization of maximum emulsions is effected by much thicker protective films. It may be noted that in the case of sodium oleate δ_{cr} in direct and reverse emulsions is between 0.006 and 0.01μ at high soap concentrations.

The emulsifying power, quantitatively represented by the magnitude of the film surface S_{∞}, changes in the reverse emulsions. The emulsifying power of ethylcellulose is not high, and is appreciably lower than that of alkali soaps, as shown by the values of S_{∞}.

For an indication of the structure of the protective films it is useful to calculate the surface S_0 per molecule of ethylcellulose in the interphase, and to compare it with the surface S which the stabilizer molecule would occupy if it was situated completely at the liquid interface in the emulsion. On the assumption that all the polymer present in the maximum emulsion is adsorbed at the droplet surfaces, we find that the surface S_0 per molecule of No. 1 or No. 2 ethylcellulose is 2000-2500 A^2 (see Table 2).

Further, for an ethoxyl number of ~48.8 the degree of substitution of OH groups in the cellulose molecule is 2.5. In this case the "molecular weight" of the monomer is 232 and its degree of polymerization $n = 402$. Then, from x-ray data on the dimensions of the cellobiose molecule [4], we find that the area S of a molecule of ethylcellulose No. 1 is 15,220 A^2. Similarly, S for ethylcellulose No. 2 is 11,770 A^2. Comparison of the values of S_0 and S leads to the highly important conclusion that the protective films of ethylcellulose, in contrast to alkali soaps, are not monomolecular but consist of several layers of polymer molecules.

To determine the principal factors influencing the stability of the emulsions studied, the viscosities of solutions of ethylcellulose of different molecular weights in toluene were measured by means of a capillary viscosimeter at 20 ± 0.05°. Figure 3 shows curves for the viscosities of solutions of three ethylcellulose fractions, at a concentration of 0.1 monomer-mole/liter (0.1 base-molar), for different efflux pressures P. The measure of viscosity is the value of $P\tau$ (τ is the efflux time). It is seen that ethylcellulose solutions have structural viscosity even at relatively low concentrations. The effective viscosity increases with increasing ethylcellulose concentration. Increase of the molecular weight of the polymer acts in the same direction. There is therefore no doubt that the dispersion medium in the emulsions is structurized. The mechanical properties of ethylcellulose solutions can be characterized by the yield value. Moreover, the solutions are thixotropic, and the spatial networks in them which are broken down at high pressures are restored during rest, as shown by the results of repeated viscosity determinations at initial low pressures.

The results indicate that, in full agreement with Rebinder's theory [5], protective films in emulsions consist of two-dimensional gels, greatly solvated by the dispersion medium and having considerable mechanical strength. Such high polymer gel films have a strong stabilizing effect on highly concentrated emulsions and, having peculiar structuro-mechanical properties, they are able to withstand considerable destructive forces for long periods.

The degree of dispersion of the emulsions studied is high; this is illustrated by the differential droplet size distribution curves in Figures 4 and 5.* An interesting feature is that despite the above structural peculiarities of the polymeric stabilizer films, the maximum on the distribution curves always corresponds to a droplet size of the order of 1μ. This is in full agreement with kinetic data on the emulsification process [6]. It should be remembered that stabilization of droplets of such limitingly small size is favored by rapid thixotropic build-up of the structures broken down in emulsification.

Table 3 gives the characteristics of the protective films in maximum emulsions stabilized by two ethylcellulose samples** of lower molecular weight than those described above.

The relationships found for the samples of higher molecular weight are also found for these samples. However the thickness δ_{cr} of the protective films decreases with decreasing molecular weight of the polymer, while the emulsifying power, represented by S_{∞}, increases (compare the data in Tables 2 and 3). The degree of dispersion of the maximum emulsions stabilized by ethylcellulose of lower molecular weight is also high. Comparison of the values of S and S_0 (Table 3) shows that, as for the polymers of high molecular weight, stabilization of maximum emulsions by ethylcellulose samples Nos. 3 and 4 is effected by means of gel films.

SUMMARY

1. Emulsions of water in toluene, of maximum concentration, have been prepared with ethylcellulose as

---

*For convenience the right hand regions of the distribution curves are shown separately in the diagrams.

**The emulsifying properties of sample No. 4 with M = 41,690 (see Table 1) are very similar to those of No. 3 with M = 46,780, and are therefore not given in the table.

stabilizer.

2. The emulsifying power of ethylcellulose increases and the thickness of the protective films which stabilize the droplets decreases with decreasing molecular weight of the ethylcellulose.

3. Maximum emulsions stabilized by ethylcellulose, like those with other stabilizers, are highly disperse, the maximum on the size distribution curves corresponding to droplets of the order of 1μ.

4. The main factor determining the stability of the emulsions studied is the mechanically strong multimolecular stabilizer gel film at the droplet surfaces.

LITERATURE CITED

[1] I.I. Nikurashina and S.A. Glikman, Sci. Mem. Saratov State Univ. 30, 66 (1952).

[2] L.Ya. Kremnev, Proc. Acad. Sci. USSR 79, 655 (1951); Colloid J. 13, 394 (1951).

[3] L.Ya. Kremnev and S.A. Soskin, Colloid J. 9, 269 (1947).

[4] Meyer and Misch, Helv. Chim. Acta 20, 232 (1937).

[5] P.A. Rebinder, Colloid J. 8, 157 (1946); P.A. Rebinder and K.A. Pospelova, introductory chapter to W. Clayton, Emulsions, translation edited by P.A. Rebinder (IL 1950).

[6] L.Ya. Kremnev and A.A. Ravdel, Colloid J. 16, 17 (1954) (T.p. 19).*

Received July 12, 1956

The Lensoviet Technological Institute

---

*T.p. = C.B. Translation pagination.

COLLOIDOCHEMICAL PROCESSES IN REACTIONS OF TETRAALKOXYSILANES WITH AQUEOUS ALUMINATE SOLUTIONS

A.P. Kreshkov, L.V. Myshlyaeva and L.M. Khananashvili

During the last decade there has been a considerable increase of interest in the organosilicon compounds. This is the consequence of the extension of their uses in industry and modern technology [1].

Particular theoretical and practical importance attaches to studies of reactions of orthosilicic acid esters (tetraalkoxysilanes) with various organic and inorganic compounds [2-7].

The present paper deals with a study of the reactions of tetraalkoxysilanes with aqueous sodium aluminate solutions.

Esters of orthosilicic acid are hydrolyzed by water, with condensation of the hydrolysis products

$$Si(OR)_4 + HOH \rightarrow (RO)_3SiOH + ROH;$$

$$(RO)_3SiO\boxed{H + HO}Si(OR)_3 \rightarrow (RO)_3SiOSi(OR)_3 + H_2O$$

etc., up to formation of polymeric compounds corresponding to the formula $(RO)_3SiO[Si(OR)_2O]_nSi(OR)_3$. With excess water, further alkoxy groups are split off.

Alkalies accelerate the hydrolysis of alkoxyl groups, and give rise to silanolates: $NaOSi(OR)_3$, $NaOSi(OR)_2OSi(OR)_3$, etc.

Subsequent hydrolysis produces polydisperse systems containing small amounts of silicic acid in true solution, colloidally dissolved silicic acids, and alkoxypolysiloxanes. Hydrolysis of tetraalkoxysilanes ultimately leads, as has been shown by Grimaux [8], to formation of colloidally soluble silicic acid.

The polydisperse system: true aluminate solution – aluminum hydroxide sol in alkali, is in a state of equilibrium. Decrease of the alkalinity of the medium, change of temperature, and other factors may result in a shift of the equilibrium and coagulation of the $Al(OH)_3$ sol to a gel. The presence of alcohols in high concentrations also leads to coagulation owing to desolvation of the disperse phase micelles. The rate of each of these reactions depends on various conditions. For example, in highly alkaline media coagulation of $Al(OH)_3$ is retarded, and ester hydrolysis is accelerated.

The products of hydrolysis and dissociation of tetraalkoxysilanes and aqueous alkaline aluminate solutions interact:

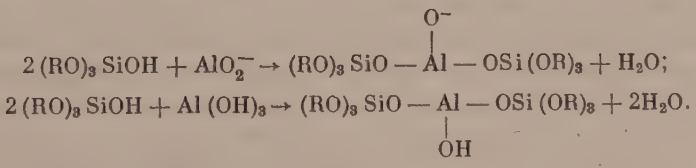

$$2(RO)_3SiOH + AlO_2^- \rightarrow (RO)_3SiO-\overset{O^-}{\overset{|}{Al}}-OSi(OR)_3 + H_2O;$$

$$2(RO)_3SiOH + Al(OH)_3 \rightarrow (RO)_3SiO-\underset{OH}{\underset{|}{Al}}-OSi(OR)_3 + 2H_2O.$$

In addition to purely chemical processes, coagulation of sols of $Al(OH)_3$ and $mSiO_2 \cdot nH_2O$ present in the reaction mixture also occurs.

Loewenstein's investigations [9] have shown that aluminosilicate crystal lattice, in accordance with the

Pauling rule, cannot contain more than 50% of aluminum. This has been confirmed experimentally by Iskoldsky [10] for the interaction of aqueous solutions of silicates with aluminates. The ratio of SiO_2 to Al_2O_3 in the reaction products varies between 2 and 3.

Nevertheless, we obtained precipitates which, on the basis of the foregoing considerations, cannot be regarded as individual substances, as their contents of aluminum were considerably higher than 50%. Their formation can be explained quite satisfactorily on the basis of colloidochemical concepts. In view of the complex nature of the processes involved, the laws governing them could be determined only by wide variations of the ratios of the reactants, their concentrations, reaction temperature, and other factors. It may be regarded as established that total mutual coagulation of the hydrolysis and condensation products of tetraalkoxysilanes and aqueous alkaline aluminate solutions occurs over a fairly wide range, but is nevertheless restricted by the proportions and concentrations of the reactants. No coagulation occurs at very high or very low molar Al: Si ratios. The reactions were in most cases accompanied by exothermic effects, which may be largely attributed to heat of hydrolysis of orthosilicic acid esters and heat of silicate formation.

The latent and visible coagulation periods were largely determined by the reaction conditions. During the reaction, coagulation apparently began to be accompanied by chemical reactions between the principal components of the system: $Na_2O-Al_2O_3-SiO_2-H_2O$, which were contained in the precipitates formed. Because of the considerable duration of the coagulation, it was possible to establish the sequence of the processes occurring in the reaction mixture by analysis of consecutive samples. It may be regarded as established that the primary process in most instances was coagulation of $Al(OH)_3$ sol. This was followed by deposition of precipitates containing increasing amounts of silicon. In strongly alkaline media at low aluminum concentrations, gelation of the reaction mixture usually took place, probably owing to coagulation of the hydrolysis and condensation products of tetraalkoxysilanes.

The reactions with tetramethoxysilane were very violent, even on considerable cooling, and it was therefore not possible to determine the consecutive stages of the process. On the other hand, the reactions with tetrapropoxy- and tetrabutoxysilane were so slow that it was possible to establish the formation of $Al(OH)_3$ precipitate at room temperature. Precipitation of $Al(OH)_3$ at the interface between aqueous aluminate solution and tetraalkoxysilane may be regarded as an instance of the adsorptive instability of $Al(OH)_3$ sol with respect to tetraalkoxysilanes.

Partial hydrolysis of tetrapropoxy- and tetrabutoxysilanes in strongly alkaline media proceeds with formation of silanolate groups, which results in removal to the stabilizing OH^- ions and coagulation of $Al(OH)_3$ [11]. The reaction with tetraethoxysilane continues for a considerable time in some cases. This is fully explained by the fact that the tendency of orthosilicic acid esters to hydrolysis decreases with increasing size of the organic radical.

Chemical analysis of the liquid phase separated from the precipitate showed that it consisted of an aqueous alcoholic solution of alkali. The solid reaction products contained only very small amounts of alkoxy groups, while the molar Al: Si ratios were the same as the original. The products were optically inhomogeneous. They were purified by repeated extraction in a Soxhlet apparatus, first with absolute ethyl alcohol and then with benzene. This purification considerably decreased the alkalinity and the aluminum contents of the products, probably owing to peptization of $Al(OH)_3$. Analysis of the purified products showed that they were of constant composition. In addition, a crystalline product identified as sodium hydroaluminosilicate was isolated.

To determine whether the solid reaction products are mixtures of gels of alkoxypolysiloxanes and silicic acid with aluminum hydroxide gel, or whether the coagulation processes are accompanied by chemical reactions with formation of alkoxyaluminosilicates or aluminosilicates, the reaction products were studied by physical methods of analysis (spectroscopic, x-ray structure, and optical crystallography). Usually structures are determined from chemical and physical analytical data by analogy with compounds described in the literature. No data are available in the literature on compounds similar to those prepared by us. However, certain structural groups characteristic of these compounds are also characteristic of compounds which have been studied and described in the literature. Calculations of interplane distances on the basis of x-ray data for most of our products showed that their basic structure is that of orthosilicates. On the other hand, samples containing aluminum showed characteristic features of aluminosilicates. It was shown by means of infrared absorption spectroscopy (powder method) that all the products gave absorption maxima characteristic of Si—O and Na—O bonds. The reaction products of tetraethoxysilane and aqueous sodium aluminate solution gave an absorption maximum at

10.2μ (981 cm^{-1}), characteristic of aluminosilicates of the albite and anorthoclase type.

EXPERIMENTAL

Sodium aluminates were prepared by dissolving chemically pure $Al(OH)_3$ in concentrated NaOH [12]. Details of the sodium aluminate solutions are given in Table 1.

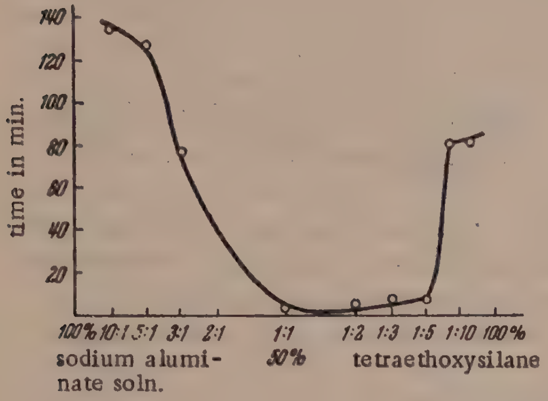

Fig. 1. Coagulation rates with different proportions of the reactants (in moles).

TABLE 1

Composition of Sodium Aluminate Solutions

Aluminate solutions	Na_2O in %	Al_2O_3 in %	Caustic ratio in moles
Sodium aluminate I	30.20	18.00	2.76
Sodium aluminate II	21.05	19.40	1.78

Orthosilicic acid esters were synthesized by methods described in the literature [1]. The reactions between tetraalkoxysilanes and alkaline aluminate solutions were carried out in a three-necked flask fitted with a stirrer and thermometer. Experiments in which it was required to determine the times for visible coagulation were performed in test tubes or cylinders with stirring by hand.

Tetraalkoxysilanes behave differently in their reactions with aluminate solutions. Tetramethoxysilane reacted practically completely within 1-2 minutes, with a high exothermic effect, in experiments with Al : Si ratios from 1 : 10 to 10 : 1, in which the aluminate solution was diluted with water to give aluminate : water ratios of 1 : 0, 1 : 1, etc., up to 1 : 20. The reaction products were gels of various consistencies, from which a liquid phase separated by syneresis; this was found to contain methyl alcohol and alkali in addition to water. With tetrapropoxy- and tetrabutoxysilanes no large amounts of precipitate were formed even after many hours of stirring at room temperature or at 65-70°. Analysis of the precipitate formed with tetrapropoxysilane (ratio of Al : Si = 1 : 1) at room temperature with continuous stirring for 10 hours gave the following results: Na_2O – 2-3%; SiO_2 – traces; Al_2O_3 – 10.15%; with tetrabutoxysilane at the same ratios and under the same conditions the small amount of precipitate contained: Na_2O – 1.96%; SiO_2 – traces; Al_2O_3 – 9.87% (analytical data not recalculated on the dry substance). Consequently, the precipitate consists of aluminum hydroxide with adsorbed alkali.

TABLE 2

Chemical Composition of Reaction Products

Molar Al : Si ratio	Nature of products	Na_2O in %	SiO_2 in %	Al_2O_3 in %	C_2H_5O in %	Molar ratios of Na_2O : SiO_2 : Al_2O_3 : C_2H_5O
1 : 6	Liquid	1.21	26.06	6.53	66.20	0.05 : 1 : 0.15 : 3.4
1 : 6	Solid	28.60	17.42	51.68	2.30	1.59 : 1 : 1.74 : 0.2
1 : 9	Liquid	0.73	23.50	4.33	71.44	0.03 : 1 : 0.1 : 4.15
1 : 10	Solid product, extracted twice	14.52	42.46	40.03	2.99	0.33 : 1 : 0.55 : 0.1

To study the influence of the proportions of the reactants, the original aluminate I solution was reacted with tetraethoxysilane with continuous stirring at room temperature, at different molar Al : Si ratios. The variation of the time for visible coagulation (i.e., turbidity and formation of a precipitate) with the ratio used is shown in Figure 1. It is seen in Figure 1 that coagulation in the system tetraethoxysilane-sodium aluminate solution proceeds at the maximum rate at moderate concentrations of AlO_2 ions. The end of the reaction is easily seen by homogenization of the whole mass, and by subsequent coagulation if it occurs. At Al : Si ratios of

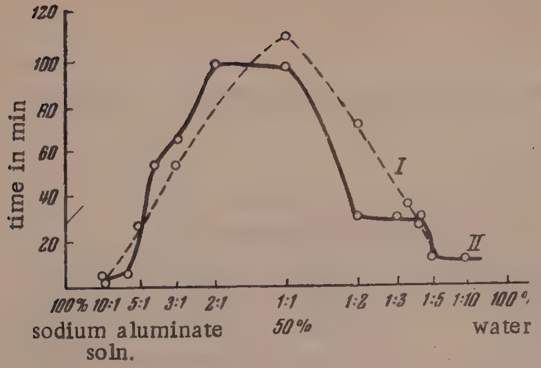

Fig. 2. Coagulation rates at a constant ratio of the reactants (Al: Si = 1: 1 molar) at different dilutions of aluminate solutions I and II with water.

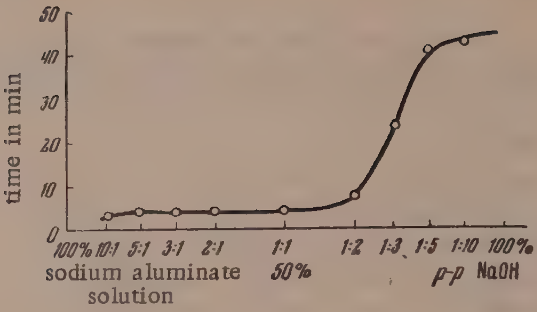

Fig. 3. Coagulation rate at a constant ratio of the reactants (Al: Si = 1: 3 molar) for different dilutions of aluminate II solution by alkali.

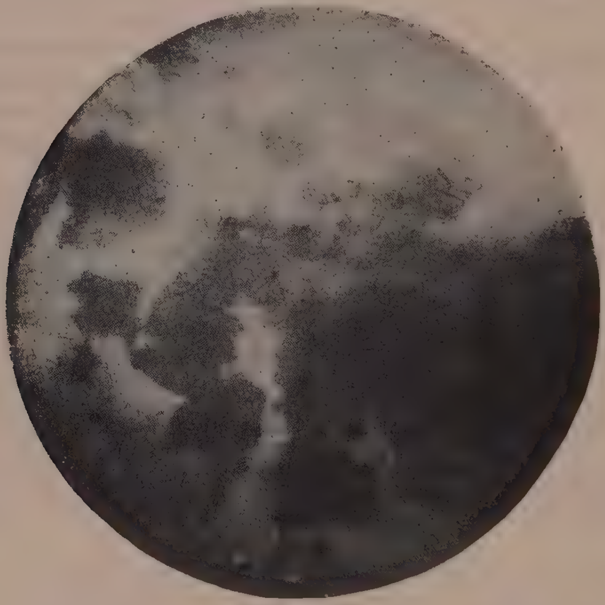

Fig. 4. Micrograph of reaction product of tetraethoxysilane with sodium aluminate solution (Al: Si = 1: 3 molar, and aluminate solution:NaOH = 1: 10).

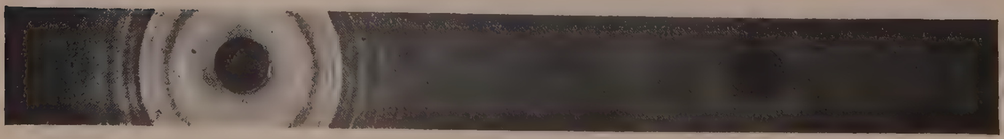

Fig. 5. X-ray diagram of reaction product of tetraethoxysilane with sodium aluminate solution (Al: Si = 1: 3 molar and aluminate solution: NaOH = 1: 10).

8: 1 and over coagulation did not take place.

At Al: Si ratios from 1: 6 to 1: 10 slight precipitates were formed some time after the mixture became homogeneous. Some of the reaction products were analyzed. Silicon [13] and aluminum [14] were determined gravimetrically. Alkalinity was determined by titration with standard hydrochloric acid against phenolphthalein [14], and alkoxyl groups by Nessonova's modification [15] of Pregl's semimicro method. Analytical data for products with high Al: Si ratios (recalculated on the dry substance) are given in Table 2.

The analytical results showed that the precipitates (after washing with benzene) were practically free of ethoxyl groups; the Al: Si ratio changed in the direction of an increase of the relative amount of aluminum in comparison with the original ratio. The liquid products contained, in addition to small amounts of alkali, alkoxyl groups, silicon, and aluminum. The Al: Si ratio remained almost unchanged, apart from a slight decrease of the aluminum content. Qualitative analysis of the liquid separated out by syneresis in cases in which the reaction mixture solidified completely showed that the liquid consisted of an aqueous alcoholic solution of alkali.

To study the effect of dilution of aluminate solutions with water, aluminate solutions I and II diluted with water to aluminate solution: water ratios of 1:1, 1:2, etc., up to 1:50, were reacted with tetraethoxysilane at constant ratios of Al: Si = 2:1; 1:1; 1:2; 1:3 and 1:4 at room temperature. The results obtained for these ratios are shown in Figure 2, where it is seen that for both aluminates the reaction rate decreases with increasing dilution, up to a certain limit, and then begins to increase again.

Chemical analysis of the unpurified product formed at a ratio of Al: Si = 2:1 with 1:3 dilution of the aluminate solution with water gave the following results (recalculated on the dry substance): $Na_2O = 41.70\%$; $SiO_2 = 18.64\%$; $Al_2O_3 = 35.46\%$; $C_2H_5O = 4.20\%$, corresponding to molar proportions of $Na_2O : SiO_2 : Al_2O_3 : C_2H_5O = 2.18 : 1 : 1.1 : 0.3$. The same product, purified by repeated extraction first with absolute ethyl alcohol and then with benzene, contained: $Na_2O - 25.14\%$; $SiO_2 - 63.25\%$; $Al_2O_3 - 10.03\%$; $C_2H_5O - 1.58\%$, corresponding to molar proportions of $Na_2O : SiO_2 : Al_2O_3 : C_2H_5O = 0.38 : 1 : 0.1 : 0.034$.

TABLE 3

Analytical Data for Consecutively Precipitated Reaction Products

Na_2O in %	Al_2O_3 in %	SiO_2 in %	Al : Si in g-molar	Na_2O in %	Al_2O_3 in %	SiO_2 in %	Al : Si in g-molar
Aluminate solution $H_2O = 1:2$				Aluminate solution $H_2O = 1:3$			
7.82	1.89	9.48	5.88	6.68	2.07	5.90	3.35
8.49	1.46	6.46	5.50	6.58	1.84	5.75	3.70
8.31	1.84	8.01	5.10	5.40	2.14	6.14	3.37
7.24	4.16	18.40	5.20	6.14	1.74	5.44	3.67
7.24	2.07	7.50	4.26	5.92	2.14	6.03	3.32
7.82	3.67	13.15	4.22	5.46	2.68	6.42	2.82
5.34	2.07	7.49	4.26	6.00	1.95	3.32	2.00
10.00	1.97	7.82	4.66	6.68	2.16	4.58	2.50
6.93	1.78	5.06	3.34	4.84	1.62	Traces	—

Comparison of the molar proportions of the purified and unpurified products shows that the Al: Si ratio in the purified product was considerably lower. The alkalinity of the purified product was also lower. Similar results were obtained by purification of other solid products. Precipitation extended over a considerable period made it possible to carry out fractional analysis of consecutively precipitated reaction products. Aluminate I was used for the reactions. The analysis was performed for the ratio Al: Si = 1:1 and aluminate solution: water = = 1:2 and 1:3. The analytical results are given in Table 3.

The analytical results show that the precipitates have higher aluminum contents than the original mixture, i.e., that the coagulation of $Al(OH)_3$ sol must be regarded as the predominant process. For the ratio of aluminate solution: $H_2O = 1:3$ the relative content of aluminum in the precipitates is less than for aluminate solution: $H_2O = 1:2$.

To study the effect of amount of alkali in the reaction mixture, a series of experiments was carried out, in which the aluminate was diluted with alkali, so calculated that its concentration in the solution remained constant (i.e., with increasing caustic ratio). Increase of the caustic ratio had the following effects: first the time for the start of visible coagulation decreased in comparison with corresponding experiments on dilution with water; this may be attributed to acceleration of ester hydrolysis (Figure 3). The end of visible coagulation was somewhat retarded.

In a reaction mixture with ratios of Al : Si = 1 : 3 and aluminate solution: NaOH = 1 : 10, the amorphous precipitate initially formed crystallized after prolonged standing in the form of needles and branched crystals (Figure 4). The crystals had the following composition: $Na_2O - 44.62\%$; $Al_2O_3 - 7.63\%$; $SiO_2 - 46.45\%$; $C_2H_5O - 1.3\%$. This corresponds to molar proportions of: $Na_2O : SiO_2 : Al_2O_3 : C_2H_5O = 0.93 : 1 : 0.1 : 0.038$. The average refractive index of the crystals was 1.483 ± 0.003.

Experiments to determine the effect of temperature on the reaction rate showed that the reaction rate increases considerably with temperature. Table 4 gives the reaction rates, at different temperatures, of tetraethoxysilane with aluminate II at a ratio of Al : Si = 1 : 1 and with the aluminate solution diluted with water in the ratio aluminate solution: $H_2O = 2 : 1$. The reaction products of tetraethoxysilanes and aqueous sodium aluminate solutions were examined in transmitted polarized light; their average refractive indices were determined by the immersion method. Many of the products had a fine crystalline structure, while some were deposited in the form of large crystals. In some cases study of the crystals was difficult owing to their hygroscopic nature.

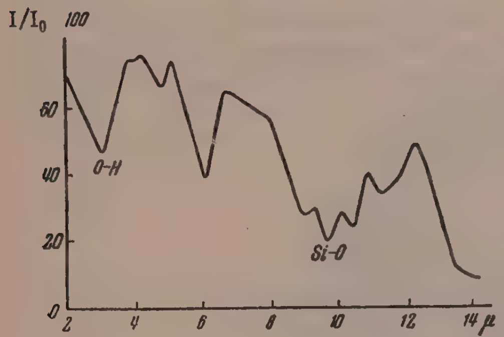

Fig. 6. IR-absorption spectrum of the interaction product of tetraethoxysilane with aqueous sodium aluminate solution (Al : Si = 1 : 2; aluminate solution: $H_2O = 1 : 4$).

TABLE 4

Coagulation Rates of Reaction Products at Various Temperatures

Temperature, °C	End of visible coagulation	Temperature, °C	End of visible coagulation
0	28 hours	50	25 minutes
10-12	12.5-13 hours	75	5 minutes
20	98 minutes	100	3 minutes

The crystalline product formed in the interaction of tetraethoxysilane with aqueous sodium aluminate solution (Al : Si = 1 : 3; aluminate solution: NaOH = 1 : 10) had the following characteristics. It crystallized in the form of needles and dendrites. The average refractive index $N_m = 1.483$. The crystals were not pleochroic. The micrograph (Figure 4) shows the crystals under a magnification of 800. The same product was examined by x-ray analysis. This was performed by the Debye method (with the RKD camera). Soft Cuα radiation was used. The interplane distances were calculated from the equation $d = \lambda / 2 \sin \theta$. The line intensities were evaluated on a five-point scale. The product had a well defined crystalline structure. A comparison of the calculated interplane distances with literature data for various modifications of SiO_2, sodium silicates, and aluminosilicates leads to the conclusion that the structure of the product contains elements characteristic of albite and kaolin [16]. It is impossible to identify any of the compounds described in the composition of the product. An x-ray diagram of the product is shown in Figure 5.

The product obtained in the interaction of tetraethoxysilane with sodium aluminate solution (Al : Si = = 1 : 2; aluminate solution: $H_2O = 1 : 4$) was studied by the infrared spectroscopic method. Absorption spectra were obtained by the powder method by means of the IKS-11 infrared spectrograph in the region between 2 and 15μ. The absorption spectra of the products were found to contain absorption bands characteristic of individual functional groups. The absorption spectrum (Figure 6) contained the following maxima: 3.00μ ($3333\ cm^{-1}$), characteristic of the O–H bond in aluminosilicates [17]; 9.6μ ($1042\ cm^{-1}$), for the Si–O bond [18]; 11.4μ ($878\ cm^{-1}$) for the Na–O bond [19], and 10.2μ ($982\ cm^{-1}$) for the albite and anorthoclase structure [20].

SUMMARY

1. Interaction of tetraalkoxysilanes with aqueous alkaline aluminate solutions results not only in chemical processes (hydrolysis of orthosilicic acid esters and formation of aluminoalkoxy- and aluminosilicates), but also in colloidochemical processes (coagulation of $Al(OH)_3$ and $mSiO_2 \cdot nH_2O$ sols and peptization of the corresponding gels).

2. In a number of cases the primary process in the interaction is coagulation of $Al(OH)_3$ sol caused by decrease in the concentration of the stabilizing OH^- ions. This may be regarded as an instance of the adsorptive instability of $Al(OH)_3$ sol with respect to tetraalkoxysilane.

3. It is shown that the nature of the processes taking place differs according to the conditions:

a) at high molar Al : Si or Si : Al ratios precipitates are not formed. The explanation is that the reaction products can form colloidal solutions in the reaction medium;

b) the times for visible coagulation to begin depend considerably on dilution, temperature and other factors.

4. Amorphous and crystalline products have been isolated; these have been shown by chemical and physical analysis to consist of sodium aluminosilicates of the albite and anorthoclase type.

LITERATURE CITED

[1] A.P. Kreshkov, Organosilicon Compounds in Technology, 2nd edition (Industrial Construction Press, Moscow 1956).

[2] A.P. Kreshkov, Proc. Acad. Sci. USSR 59, 723 (1948).

[3] A.P. Kreshkov, A.N. Chivikova, G.D. Nessonova, V.A. Matveev and M.L. Darashkevich, Trans. Mendeleev Inst. Chem. Technology Moscow 17, 15 (1952).

[4] A.P. Kreshkov and L.V. Myshlyaeva, Trans. Mendeleev Inst. Chem. Technology Moscow, 13, 38 (1948).

[5] A.P. Kreshkov, J. Appl. Chem. 23, 545 (1950).

[6] A.P. Kreshkov, J. Gen. Chem. 20, 1415 (1950).

[7] A.P. Kreshkov and G.S. Petrov, J. Chem. Ind. No. 8, 10 (1944).

[8] E. Grimaux, Comptes rendus 98, 1434 (1884).

[9] W. Loewenstein, Am. Mineral 39, 92 (1954).

[10] I.I. Iskoldsky, Chemistry of Solutions in the Aluminum Industry (ONTI, Moscow-Leningrad 1937).

[11] N.P. Peskov and E.M. Aleksandrova-Preis, Course of Colloid Chemistry (Goskhimizdat, Moscow-Leningrad 1948).

[12] Prascott, J. Am. Chem. Soc. 2, 27 (1880) (cited through [10]).

[13] P.N. Grigoryev, Water Glass (Industrial Construction Press, Moscow 1948), p. 185.

[14] W.G. Hillebrand and G.E. Lundell, Applied Inorganic Analysis (ONTI, Moscow 1937).

[15] A.P. Kreshkov, V.A. Bork, L.V. Myshlyaeva and G.D. Nessonova, Analysis of Organosilicon Compounds (Goskhimizdat, Moscow 1954).

[16] J.D. Hanawalt, H.W. Rinn and L.K. Frevel, Ind. Eng. Chem. 10, 469 (1938).

[17] A. Buswell and Dudenbostel, J. Am. Chem. Soc. 63, 2554 (1941).

[18] A.P. Kreshkov, Yu.Ya. Mikhailenko and G.F. Yakimovich, J. Phys. Chem. 28, 537 (1954).

[19] P.N. Ghosh and B.D. Catterjee, Z. Physic. 72, 542 (1931).

[20] G.S. Bachman, Glass Industry 29, 435 (1948).

Received December 1, 1956

The D.I. Mendeleev Institute of
Chemical Technology

~~STUDY~~ OF THE COLLOIDAL PROPERTIES OF SULFOSUCCINIC ACID ESTERS

1. ESTERS OF THE LOWER ALIPHATIC ALCOHOLS

R.V. Kucher,, A.A. Yavorsky* and M.A. Kovbuz

The colloidal properties of soaps and soaplike substances have great significance in relation to a number of important problems of modern chemistry. These include chemical reactions in emulsions (polymerization, hydrocarbon oxidation). Our earlier publications [1-3] described the colloidochemical properties (micellar weight, critical concentration, etc.) of various sulfonated soaps. Although the substances studied had been purified to remove electrolytes, they could still contain various impurities which might influence the behavior of colloidal electrolytes in aqueous solutions. It was therefore very desirable to investigate the colloidal properties of a number of pure colloidal electrolytes in which the influence of impurities would be excluded. From this standpoint the esters of the sodium salts of sulfosuccinic acid are particularly worthy of attention. Data on the colloidal properties of these substances, which were synthesized by us, will be presented in this and subsequent communications.

Sulfosuccinic acid esters are of considerable theoretical and practical interest. Under the names of Aerosols OT, MA and IB, some of them are widely used as very effective surface active agents. Nevertheless, the literature contains no data on systematic investigations of their colloidochemical properties or on methods for synthesizing these esters. Such investigations are essential for systematic selection of a particular representative of the series for a given purpose.

We have studied the colloidochemical characteristics of a series of completely substituted sulfosuccinic acid esters in aqueous solutions, with different, gradually increasing numbers of carbon atoms in the alkyl chain. The present communication deals with the four lowest representatives of the series – the dimethyl, diethyl, dibutyl, and diisoamyl esters. Very little information on the synthesis of such compounds is given in the literature. The first reports on sulfosuccinic acid esters as wetting agents appeared in 1936 [4]. Subsequently numerous other publications appeared on the subject [5-8]. However, methods of synthesis of individual members of the series are mentioned only very briefly.

The literature cited above contains reports of the production of sulfosuccinic acid esters from maleic acid esters. The preparation of sulfosuccinic acid from maleic acid by bisulfite addition has been described in considerable detail [9-11]. The sulfosuccinic acid esters and a number of other compounds studied in the present investigation were synthesized from the corresponding maleic acid esters by addition of sodium or potassium bisulfite. The conditions for the addition reaction, however, differ considerably for different representatives of the series. Therefore, questions relating to the syntheses will be described in greater detail in a separate communication.

The substances studied, in the form of the sodium salts, were thoroughly purified after synthesis. For this they were recrystallized 2-3 times from water, and then dried under vacuum at a residual pressure of 10 mm Hg over calcium chloride at 100-110° for 12-24 hours; they were then analyzed. The dimethyl and diethyl esters were also azeotropically distilled with toluene and held for 24 hours under vacuum at 40° over paraffin.

The analyses were carried out by the Korshun and Gelman combustion method, with the sulfur combined with metallic silver. The analytical results are given in Table 1.

The present communication describes the results of a study of the colloidochemical properties of aqueous

---

* Deceased.

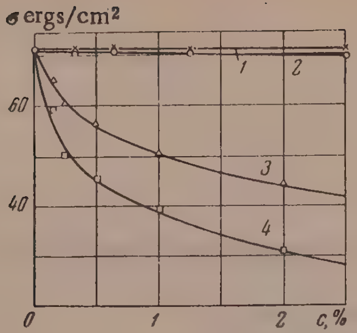

Fig. 1. Surface tension isotherms for aqueous solutions of sodium sulfosuccinate esters at 20°: 1) DME; 2) DEE; 3) DBE; 4) DIAE.

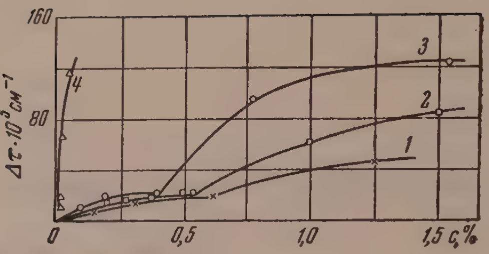

Fig. 2. Turbidity of dilute aqueous solutions of sodium sulfosuccinate esters: 1) DME; 2) DEE; 3) DBE; 4) DIAE.

TABLE 1

Analytical Data on the Dimethyl (DME), Diethyl (DEE), Dibutyl (DBE), and Diisoamyl (DIAE) Esters of Sodium Sulfosuccinate

Compound	Carbon content, %		Hydrogen content, %	
	found	calculated	found	calculated
DME	28.75	28.98	3.55	3.67
DEE	36.12	36.05	4.87	4.92
DBE	42.95	43.32	6.46	6.37
DIAE	44.63	44.66	6.66	6.69

TABLE 2

Colloidochemical Properties of Lower Esters of Sodium Sulfosuccinate in Aqueous Solutions at pH 9.9 (20°)

Compound	CCM moles/liter	W_m/kT	Micellar weight, M	Degree of micellization, N_0	$N - N_0$
DEM	$2.89 \cdot 10^{-2}$	10.6	2330	10.8	2.09
DEE	$2.19 \cdot 10^{-2}$	11.5	4350	17.8	2.49
DBE	$1.28 \cdot 10^{-2}$	13.1	5820	19.4	2.43
DIAE	$3.05 \cdot 10^{-5}$	30.8	71400	217.1	5.31
Aerosol MA	$1.29 \cdot 10^{-3}$	20.0	10000	25.8	2.56

solutions of the four compounds indicated in Table 1.

Figure 1 shows the surface tension isotherms (at 20°) of aqueous solutions of DME, DEE, DBE and DIAE, determined by the maximum bubble pressure method by means of P.A. Rebinder's apparatus. The results show that the first two members of the series (DME and DEE) have practically no surface activity in aqueous solutions. The dibutyl ester produces an appreciable decrease of surface tension in aqueous solution (to 44 ergs/cm² at $c = 2\%$). The diisoamyl ester has even greater surface activity; in this respect it approaches such well known sulfonates as Nekal [1]. Similar results are obtained both in acid (6% HNO_3) and alkaline media (0.1 N soda solution, pH 9.9).

We may conclude from these results that in the series of sodium sulfosuccinate esters surface activity at the water-air interface reaches appreciable values starting with the third member of the series, the dibutyl es-

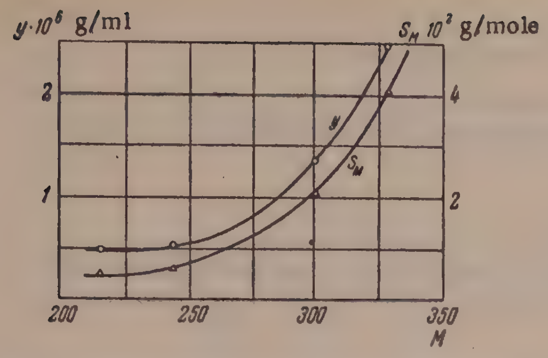

Fig. 3. Solubilization (y) and molar solubilization (S_M) of Sudan III in aqueous solutions of lower esters of sodium sulfosuccinate, in relation to the molecular weight (M) of the colloidal electrolytes.

ter. The hydrophobic radical of the molecule of this compound is large enough to cause considerable surface adsorption. In addition to surface activity, a very important property of colloidal electrolytes is micelle formation in aqueous solutions. This property plays an especially important role when colloidal electrolytes are used as emulsifiers for chemical reactions in emulsions (for example, polymerization or liquid phase oxidation of hydrocarbons). To determine the tendency to micelle formation in the lower esters of sodium sulfosuccinate, we studied their critical concentrations of micelle formation (CCM) and micellar weights. A 0.1 N soda solution was added to all the solutions to give pH 9.9, as it is colloidal behavior in alkaline media which is important in relation to chemical reactions in emulsions, when the aqueous medium usually has pH > > 7. It has recently been shown [12] that the micelle formation of soaps and soaplike substances increases considerably in presence of electrolytes. Micelle formation was studied by the light scattering method described previously [2].

Variations of turbidity with concentration of very dilute solutions of these colloidal electrolytes are shown in Figure 2. By means of these data it is possible to determine CCM from the point at which the turbidity begins to increase. Figure 2 shows that these points are fairly distinct. The values of the CCM for the substances studied are given in Table 2.

The micellar weights of the compounds were determined from the results of turbidity measurements for solutions of higher concentrations (up to 2.5%). The micellar weights given in Table 2 were found by extrapolation of $H(c/\Delta\tau) = f(c)$ to zero concentration, as described previously [2]. The first three members of the series have relatively high CCM and low micellar weights. Therefore, the degree of micellization N_0 (ratio of micellar to molecular weight), and the energy of association, calculated from the equation [13, 14]

$$w_m = -3\,kT \ln c_0$$

(where c_0 is the critical concentration of micelle formation (CCM) and w_m is the association energy of two molecules of the colloidal electrolyte) are also low. Thus, the colloidal nature of these two lowest members of the series under investigation is very weak. The diisoamyl ester, however, has low CCM and a fairly high micellar weight. It is interesting to note that the colloidal properties of Aerosol MA (an imported dihexyl ester of sulfosuccinic acid), data for which [14] are included in Table 2 for comparison, are weaker than those of DIAE, although the hydrophobic portion of its molecule contains two more CH_3 groups than that of the latter compound. It seems that the greater tendency to micelle formation of DIAE as compared with Aerosol MA is related to the iso-structure of the alkyl hydrocarbon chain in the DIAE molecule. It is intended to study this question in greater detail in a later investigation.

We may also note that the polydispersity of the micelle $(N - N_0)$, calculated by the Debye equation [13] is low for all the compounds studied. Finally, as was shown previously [3], the colloidal properties (micellar weight) are closely associated with solubilization of oleophilic substances in aqueous solutions of colloidal electrolytes. Thus, solubilization can also serve as a measure of the colloidal nature of a soaplike substance. Moreover, solubilization is an important factor in chemical reactions in emulsion systems.

We studied the solubilization of the oleophilic water-insoluble dye Sudan III in aqueous solutions of the esters; the solution pH was 9.9. The solubility of the dye was determined photometrically [3]. Figure 3 shows the variation of the solubilization of Sudan III in 2% solutions of the colloidal electrolytes studied with the molecular weight of the latter. The graphs show the solubilization[(y) in g/ml)]and the molar solubilization (S_M in grams of dye per mole of colloidal electrolyte). The solubility of Sudan III in aqueous solutions of the lowest two esters is almost the same. Solubilization is greatly increased in presence of the dibutyl and especially of the diisoamyl ester. This indicates that in this series of compounds colloidal properties first appear in DBE, which must be regarded as the first member of the series to have appreciable colloidal properties.

All this shows that in the series of aliphatic sodium sulfosuccinate esters the alkyl residue in the molecule must contain at least four carbon atoms (butyl and higher) for formation of colloidal solutions in an aqueous medium.

SUMMARY

1. Surface tension isotherms of aqueous solutions of dimethyl, diethyl, dibutyl, and diisoamyl sodium sulfosuccinate have been studied. It is shown that in this series appreciable surface activity begins within the dibutyl ester.

2. Micelle formation in aqueous solution in the first three members of this series of esters is slight, as confirmed by the values of the critical micelle concentration and micellar weight determined by the light scattering method. The diisoamyl ester has definite colloidal properties.

3. The solubilization of Sudan III in aqueous solutions of the lower sulfosuccinate esters begins to increase starting with the dibutyl ester, and is especially high with the diisoamyl ester.

LITERATURE CITED

[1] A.I. Yurzhenko and R.V. Kucher, Proc. Acad. Sci. USSR 85, 1337 (1952).

[2] A.I. Yurzhenko and R.V. Kucher, Colloid J. 13, 226 (1951); 14, 219 (1952) (T.p. 243).*

[3] A.I. Yurzhenko and R.V. Kucher, Colloid J. 14, 283 (1952) (T.p. 311).*

[4] A.O. Jaeger, U.S. Patent 2028091; C.A. 30, 1466 (1936).

[5] F.C. Ross, Amer. Dyestuff Reporter 26, 825 (1937).

[6] C. Caryl and W. Ericks, Ind. Eng. Chem. 31, 44 (1939).

[7] C. Caryl, Ind. Eng. Chem. 33, 731 (1941).

[8] A.O. Jaeger, U.S. Patent 2252401; C.A. 35, 7585 (1941).

[9] H.J. Backer and J.M. van der Zanden, Rec. trav. chim. 46, 473 (1927).

[10] E. Hägglünd and A. Ringbom, Z. anorg. Chem. 150, 231 (1926).

[11] J.M. van der Zanden, Rec. trav. Chim. 45, 242 (1926).

[12] A.N. Mankowich, J. Phys. Chem. 58, 1827 (1954).

[13] P.J. Debye, J. Phys. Colloid Chem. 53, 1 (1949).

[14] R.V. Kucher and M.A. Kovbuz, Colloid J. 18, 193 (1956) (T.p. 185).*

Received August 7, 1956

The I. Franko State University, Lvov
The Ukrainian Scientific Research
Institute for the Polygraph Industry

---

* T.p. = C.B. Translation pagination.

HEAT EVOLUTION IN THE INITIAL PERIOD OF HYDRATION OF CEMENT WITH PLASTICIZING ADDITIONS

O.I. Lukyanova, E.E. Segalova and P.A. Rebinder

The chemical interaction of water with cement clinker minerals includes exothermic reactions the heat effects of which are fairly high, and which may serve as a sensitive quantitative measure of the cement hydration process. Studies of the exothermal effects in cements are also of independent importance in relation to massive concreting problems, concreting in winter conditions, and to hydrothermal treatment of concrete.

Hydration of Portland cement in the form of paste, suspension, or concrete is a slow process. It has been shown [1-5] by several investigators that cement evolves heat for at least 6 months during hardening, but most of the heat, sometimes up to 80%, is liberated during the first few days after it is mixed with water. Heat evolution by cement is therefore studied by one of the following methods. The heats of hydration at different stages are determined as the differences between the heats of solution of the anhydrous and the hydrated cement. This method has been used to determine the heats of hydration of individual minerals in Portland cement clinker in the form of concentrated aqueous suspensions [1, 6]. The kinetics of heat evolution in the hydration of cement during the first few days can be studied by direct calorimetric [7, 8] or thermometric [9, 10] methods.

The results of such investigations show the existence of two stages in the initial hydration of Portland cement. The first stage, which lasts 1-2 hours after the cement is mixed with water, is characterized by an initially high but rapidly decreasing rate of heat evolution. This stage consists largely of hydration of tricalcium aluminate in the clinker. The rate of heat evolution increases again after 5-14 hours, depending on the mineralogical composition and the degree of dispersion of the cement, on the content of added gypsum, and a number of other factors. The kinetics of heat evolution in the hydration of cement, both in the initial and in the subsequent stages, may be changed considerably by addition of hydrophilic plasticizers.

In our previous investigations we studied the effect of the hydrophilic plasticizer SSB on the properties of concentrated cement suspensions during the initial stages of their interaction with water. The studies included investigation of changes in the kinetics of structure formation in cement paste as the result of additions of SSB resulting from adsorptive retardation of hydration and adsorptive dispersion of tricalcium aluminate in the clinker. Data on the influence of SSB lignosulfonates on the kinetics of the chemical interaction of cement with water were obtained either by an indirect method, or by determinations of the chemically bound water, which is an insensitive although in some cases convenient method.

In the present investigation the influence of the hydrophilic plasticizer SSB on the kinetics of the chemical interaction of cement with water in the initial stage was studied by the course of the evolution of heat in the process. Ground factory clinkers without added gypsum were used for the work. The contents of the principal minerals in the clinker, calculated from analytical data, and the degree of dispersion (by Tovarov's method) are given in the table.

The reasons for the choice of the calorimetric method were: the relatively low heat effect at the first stage of heat evolution, the desirability of carrying out the hydration in a concentrated aqueous suspension (cement paste), and the necessity of making such suspensions directly in the calorimeter. The diathermic method was used, at a variable heat exchange rate and at a low rate of cooling. The calorimetric vessel in which the cement was mixed with water was of the massive calorimeter type, contained an interior glass vessel for water or the solutions to be studied, and was fitted with a special stirrer for mixing the cement (Figure 1). A calorimeter of this type was used by Logginov [11].

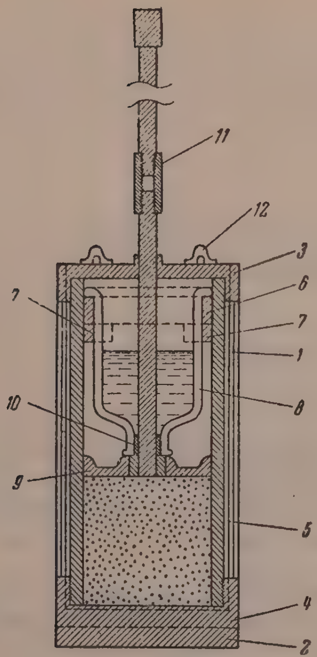

Fig. 1. Calorimetric vessel: 1) brass cylinder; 2) detachable cylinder base; 3) brass lid with gap for stirrer; 4 and 5) grooves for thermistor and leads; 6) seal ring; 7) half-ring supports; 8) inner brass or glass vessel for solutions; 9) stirrer for cement mixing; 10) rubber seal ring; 11) heat insulating collar.

The temperature was measured to the nearest 0.01° by means of a semiconductor resistance thermometer, the MMT-1 thermistor, connected in a Wheatstone bridge circuit. Thermistors are being more and more widely used as resistance thermometers in physicochemical research [12-15]. Our preliminary experiments showed that the MMT-1 thermistor mounted in the calorimeter is stable in operation and gives reproducible readings when standardized against a mercury thermometer (Figure 2, Curve R).

For calculation of the temperature from the thermistor resistance we used the approximate equation:

$$\Delta t = (\log R_2 - \log R_1)/C_{av}, \qquad (1)$$

valid for fairly narrow temperature ranges, derived from the general expression $1/R = C \cdot e^{B/T}$, (2), where C_{av}, C and B are constants determined from the calibration data. Over temperature ranges greater than 4-5°,C_{av} depends appreciably on the temperature (Figure 2, Curve C_{av}).

The cooling rate and the heat capacity of the calorimeter were determined by the usual calorimetric methods [16]. The average specific heat of the cements at room temperature was calculated by a method used for complex silicate systems [17], by summation of the specific heats of the constituent oxides in the cement; it was found to be 0.19 cal/g degree for the clinkers studied.

The kinetics of heat evolution in the interaction of cements (without gypsum) with water and with aqueous solutions of SSB sulfonates was studied in suspensions with water-cement ratio (w/c) of 0.4, so that it was possible to compare the results with data on structure formation in such suspensions. Figure 3 represents the kinetics of initial heat evolution by the high-alumina clinker N with additions of 0.10 to 1.00% SSB, calculated as the dry substance, on the weight of the cement. Curve 1 represents heat evolution during hydration of cement without added SSB; Curves 2-5 represent heat evolution in systems containing increasing amounts of SSB. Curve 3 shows that there is practically no induction period of heat liberation (hydration) in cement pastes without SSB and with small amounts of SSB (less than 0.25% for clinker N).

Mineral Contents and Degree of Dispersion of Clinkers

Factory	Mineralogical composition, in %*				S
	C_3S	C_2S	C_3A	C_4AF	m²/g
Komsomolets (K)	58	18	5	16	0.32
Novorossiisky (N)	56	22	8	13	0.18
Gigant (G)	53	20	9	14	0.28

---

*The clinker minerals are denoted by the usual symbols: $C_3S-3CaO \cdot SiO_2$; $C_2S-2CaO \cdot SiO_2$; $C_3A-3CaO \cdot Al_2O_3$; $C_4AF-4CaO \cdot Al_2O_3 \cdot Fe_2O_3$.

An increase of the amount of SSB to 0.5-1.0% results in the appearance of an induction period, the duration of which increases with the amount of SSB added. Heat evolution during the induction period is very small, thus

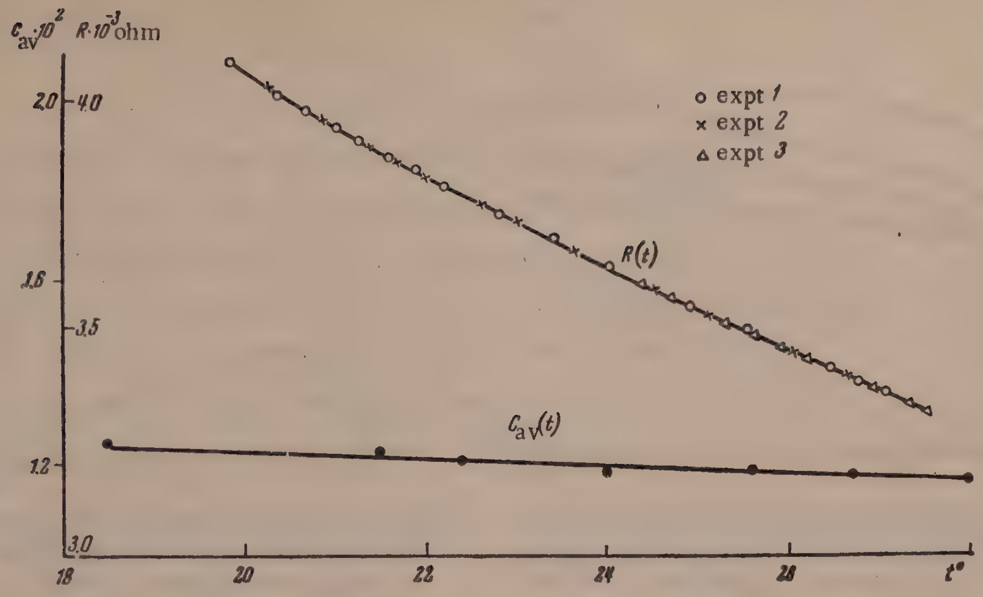

Fig. 2. Variation of the resistance (R) of thermistor MMT-1 with the calorimeter temperature (intervals of 1 month between experiments). Variation of the coefficient C_{av} in the approximate Equation (1) with temperature.

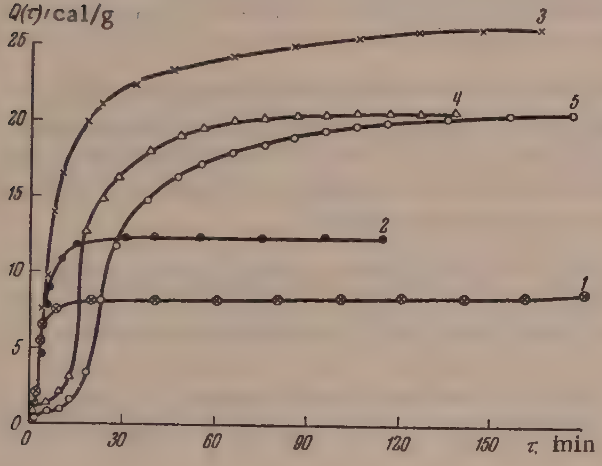

Fig. 3. Kinetics of heat evolution in hydration of cement from clinker N; w/c = 0.40: 1) without SSB; 2) 0.10% SSB; 3) 0.25% SSB; 4) 0.50% SSB; 5) 1.0% SSB.

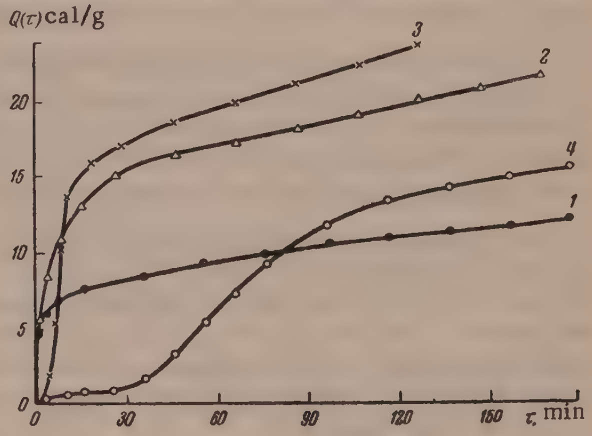

Fig. 4. Kinetics of heat evolution in hydration of cement from clinker G; w/c = 0.40: 1) without SSB; 2) 0.10% SSB; 3) 0.25% SSB; 4) 0.50% SSB.

confirming the previously reported [18, 19] retardation of the hydration of Portland cement by SSB lignosulfonates. The small initial jump on the heat evolution curves probably corresponds to heats of wetting and adsorption, which are small compared with the heat of subsequent hydration. The total heat evolved during the first stage is considerably greater in cement paste with added SSB than without additions.

Similar results were obtained for the other two clinkers, differing in tricalcium aluminate contents, but of similar specific surface (0.3 m²/g). A great increase of the initial heat evolution in presence of SSB is found for clinker G (Figure 4); the optimum addition of SSB in this respect is 0.25%. Addition of 0.5% SSB, despite the considerable adsorptive retardation of cement hydration which it produces (as shown by the appearance of a noticeable induction period), also produces a certain increase of the initial heat evolution after the end of the induction period. Clinker K, with a lower content of tricalcium aluminate, also shows a noticeable increase of

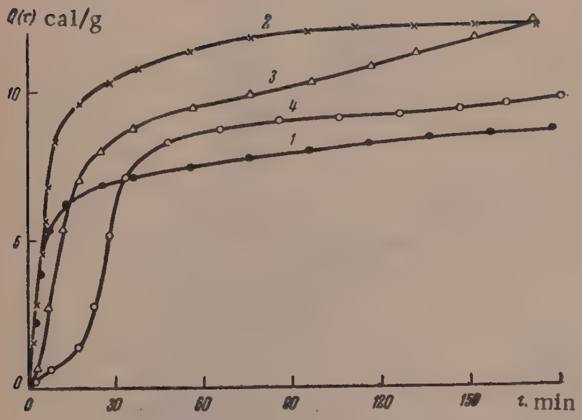

Fig. 5. Kinetics of heat evolution in hydration of cement from clinker K; w/c = 0.40: 1) without SSB; 2) 0.10% SSB; 3) 0.25% SSB; 4) 0.50% SSB.

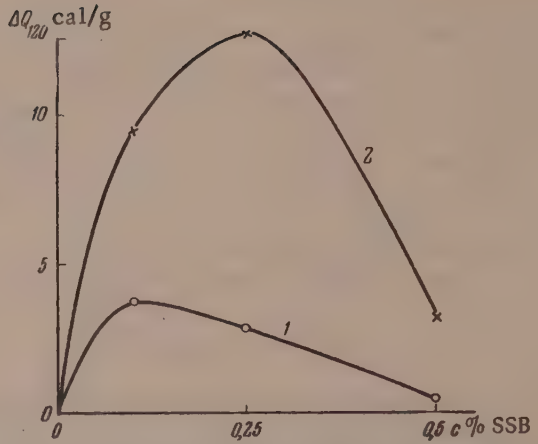

Fig. 6. Increase of the heat effect on addition of SSB in the first stage of heat evolution: 1) clinker K; 5% C_3A; 2) clinker G; 9% C_3A.

initial heat evolution in presence of SSB, the effect being greatest with 0.1% addition (Figure 5).

In comparing these results it is necessary to note that the increase of the initial heat evolution in presence of SSB is considerably greater in cements with high tricalcium aluminate contents, as can be clearly seen in Figure 6; this indicates that C_3A plays an important role in the process.

These results show that the chemical interaction of cement with water is intensified in presence of SSB. This can be attributed either to an increase of the particle surface of the cement as the result of additional adsorptive dispersion, primarily at the tricalcium aluminate inclusions, or to the fact that added SSB prevents crystallization of hydroaluminates directly on the cement particle surfaces, thus favoring more complete hydration of the aluminate minerals at the initial stages of the interaction of cement with water.

A comparison of the kinetics of heat evolution, studied in this investigation, and the kinetics of structure formation in cement paste as indicated by the plastic strength increase at the initial stage of hydration [18, 19], indicates a complete correlation between the two processes. Delay of the start of hydration by means of added SSB produces an induction period of structure formation, of the same duration. The increased heat evolution at the initial stage of hydration in presence of added SSB, which indicates accelerated hydration, produces an appreciable increase in the strength of the crystallization structure of the hydroaluminate at the corresponding stage of structure formation.

This coordination of the structure formation and hydration (heat evolution) processes in gypsumless cements at the initial stage of their interaction with water is found in all cases, if allowance is made for such important factors as the duration of mixing of the cement, which has a strong influence on the kinetics of structure formation, and also heat loss from the system studied, which often distorted earlier data on the heat evolution by cements.

SUMMARY

1. A method has been developed for quantitative study of the initial heat evolution in hydration of cement pastes mixed within the calorimeter.

2. A study has been made of the kinetics of heat evolution in the initial hydration stage of gypsumless cements with various contents of tricalcium aluminate, and of the effects of the hydrophilic plasticizer SSB, added in amounts from 0.1 to 1.0%,on the weight of the cement, on the kinetics of heat evolution.

3. It is shown that the induction period of cement hydration (as indicated by heat evolution) increases with increasing amounts of SSB added, resulting in an induction period of structure formation of the same duration.

4. It is shown that additions of SSB over a wide range result in an increase of the initial heat evolution in comparison with cement pastes without plasticizer; this increases the strength of the crystallization structure of the hydroaluminate at the corresponding stage of structure formation.

LITERATURE CITED

[1] V.A. Kind, S.D. Okorokov and S.L. Volfson, Cement No. 7 (1937).

[2] G. Verbeck and C. Foster, ASTM Proceedings 50, 1235 (1950).

[3] E.C. Newman and L. Wells, J.Res. N. Bur. Stand. 49, 55 (1950).

[4] S.A. Mironov, The Temperature Factor in Concrete Hardening (Stroiizdat, 1948).

[5] R.H. Bogue, The Chemistry of Portland Cement (1947), p. 434.

[6] W. Lerch and R.H. Bogue, J. Res. N. Bur. Stand. 12, 645 (1934).

[7] W. Lerch, ASTM Proceedings 46, 1252-97 (1946); W. Lerch and C.L. Ford, J. Am. Concr. Inst. 19, 745-95 (1948).

[8] W. Swietoslawski, Microcalorimetry (1946).

[9] A.A. Baikov, Collected Works, Vol. 5 (Izd. AN SSSR, 1948), p. 34.

[10] V.A. Tikhonov, Hydrotech. Constr. No. 7 (1953).

[11] G.I. Logginov, J. Acad. Sci. USSR No. 7 (1954).

[12] V.Ya. Mikhelson, J. Anal. Chem. 9, No. 1 (1954).

[13] A.A. Kampe-Nemm, Factory Labs. No. 6 (1954).

[14] A.C. Zettlemoyer and G.I. Young, J. Phys. Chem. 57, 649 (1953).

[15] M.J. Rand and L.P. Hammett, J. Am. Chem. Soc. 72, 287-93 (1950).

[16] M.M. Popov, Thermometry and Calorimetry (Izd. MGU, 1954).

[17] I.I. Kitaigorodsky, K.S. Evstropyev, et al., Glass Technology (State Light Ind. Press, 1939).

[18] E.E. Segalova and O.I. Lukyanova, Trans. 3rd All-Union Conf. Colloid Chem. (Izd. AN SSSR, 1956).

[19] E.E. Segalova, P.A. Rebinder and O.I. Lukyanova, Bull. Moscow State Univ. No. 2 (1954).

Received March 3, 1957

The M.V. Lomonosov State University,
Moscow, Faculty of Chemistry

EFFECT OF TEMPERATURE ON THE MAGNITUDE AND RATE OF SWELLING OF AGAR

V.P. Mishin and N.D. Verderevskaya

Data on the influence of temperature on the magnitude and rate of swelling are of interest not only in relation to the complex problem of the temperature coefficient of swelling of high polymers, but also in connection with the submicroscopic structure of the latter. However, the literature contains very few publications dealing with the influence of temperature on the magnitude and rate of swelling.* By using an improved technique for measurement of swelling, and various media in which the solubility of the swelling substance could be varied within certain limits, we set out to show that when the solubility of a swelling substance remains practically unchanged at different temperatures, the degree of swelling increases with increasing temperature, but otherwise it should pass through a maximum which shifts in the direction of lower temperatures in the transition to media in which the temperature coefficient of solubility progressively increases.

The substance used was finely divided domestic fibrous white agar purified by prolonged treatment with water containing ethyl ether in the cold. The washed agar was dried at 40°; particles 0.5-1 mm in diameter were sieved off for the experiments. The ash content of the agar after treatment was 1.87%, and the moisture content (at 110°) was 17.8%. The swelling media were redistilled water and aqueous solutions of potassium sulfate and thiocyanate (extreme members of the lyotropic series). The temperature in the experiments was varied between 0 and 50°. In addition to swelling, the solubility of agar was determined gravimetrically.

The increase in volume on swelling was taken as the measure of swelling. Most investigators use the weight increase as a measure of swelling. It must be pointed out that there is no direct proportionality between the weight and volume changes of a substance on swelling, and the functional relationship between the two has not been accurately established [2]. An automatic recording instrument of our design was used for measurements of the volume increase (Figure 1). The main part of the apparatus consists of a cylindrical glass vessel a with a perforated bottom. The substance to be studied is placed in the vessel, and on this is placed a light (7.75 g) hollow glass cylinder b 1.50 cm in diameter with a perforated bottom. The small vessel a is fixed in a vessel A, contained in a thermostat and filled at the right moment with the swelling liquid. The upper part of the movable cylinder b is connected to a long glass tube e, which is a lever with unequal arms, with one end slightly bent and drawn out into a capillary. The capillary and part of the tube are filled with ink and brought into contact with millimeter squared paper on a drum rotated uniformly by means of a Warren motor. By this apparatus it is possible to measure the swelling of small amounts of substance in large volumes of solution, so that the concentration of the latter remains practically constant throughout the experiment. In all the experiments the agar-liquid volume ratio was 1:200, the weight of agar was 0.2500 g, and the average volume of the loose material was 1.06 cc. After the pen had been put into position and the drum started, the zero reading line was drawn. The liquid was then introduced into the vessel a by displacement of the bottle B from position d' into position d". As the substance swells, the pen e is displaced and traces a curve. The experiment is continued until the pen follows its own trace. With the aid of a calibration curve, the experimental curves were used to determine the volume increments at various time intervals; the results were used to plot swelling-time curves.

The calibration curve was plotted by measurement of definite volumes of mercury introduced into the small vessel and of the corresponding displacements of the pen from the zero line. The average error was ~3%.

---

*A detailed critical analysis of the literature is given in [1].

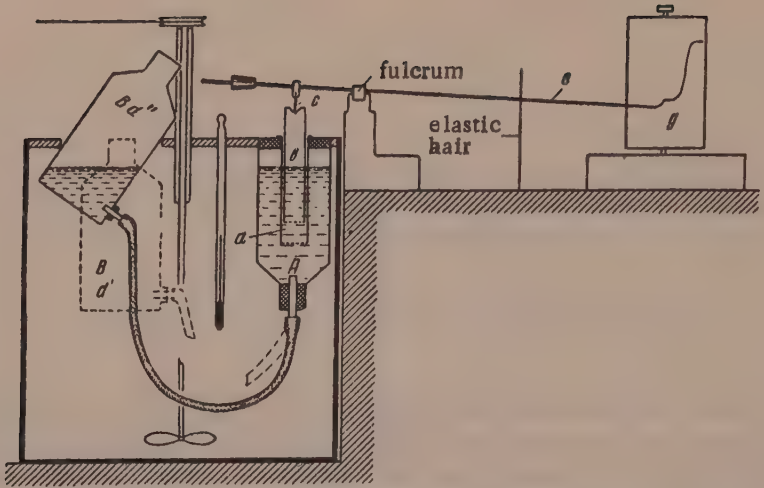

Fig. 1. Automatic recording apparatus for measurement of volume increase: A) glass vessel 300-400 ml in capacity; B) bottle with tube (d' — position before experiment; d" — position during experiment); a) small glass vessel with perforated bottom; b) hollow glass cylinder with perforated bottom and a depression at the top end; c) metal rod; e) pen; g) rotating drum.

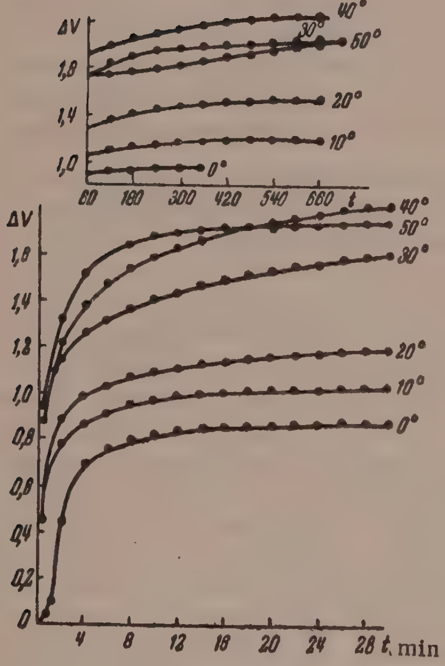

Fig. 2. Curves for the swelling of agar in water at various temperatures.

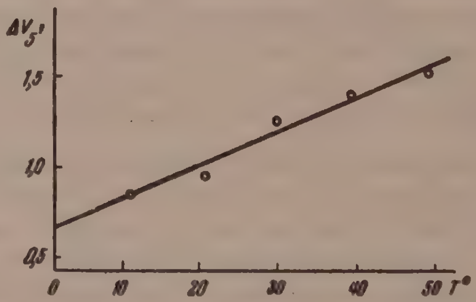

Fig. 3. Polytherm for the swelling of agar in water, in the rapid swelling region.

The advantages of this method over other methods for determination of volume swelling described previously [3] include the relative simplicity of the apparatus, the small amount of substance needed for the experiment, the relatively large volume of liquid in which the swelling occurs, automatic continuous recording of the volume increase, and the possibility of determining the swelling of any substance which can be obtained in finely divided form. It should be noted that the values measured by means of this apparatus are not the true changes in the volume of the swelling substance, as a certain volume of the "dead" space between the particles is added to the volume of the particles themselves. However, this presents no obstacle in comparative studies of the swelling of substances under different conditions, if the original degree of dispersion of the substance and the packing density of its particles under a small and

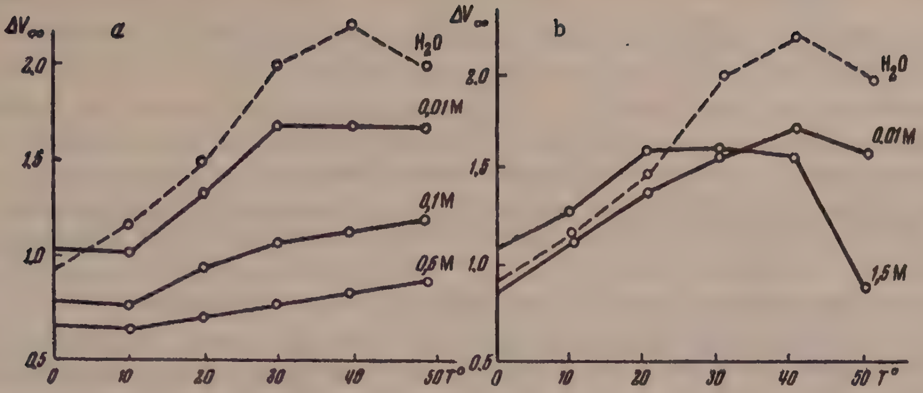

Fig. 4. Polytherms for the swelling of agar in water and: a) in 0.5 M; 0.1 M; 0.01 M solutions of K_2SO_4; b) in 1.5 M and 0.01 M solutions of KCNS.

constant pressure (0.004 atmos) exerted by a piston are the same in all the experiments. If necessary, the apparent volume increments can be converted into the true values with the aid of a calibration curve showing the relationship between the apparent and true volume increments. Such a curve can be found by determination of the true volume of a substance at different stages of swelling by the method of weighing in two liquids of different densities, proposed by one of us [4].

Each experimental curve (examples of such curves are given in Figure 2) has three characteristic regions: a region of rapid swelling, with a rapid rise of the curve, corresponding to the time interval of 0-10 minutes, irrespective of the temperature; a region of slow swelling with retarded ascent of the curve; and the region of maximum swelling, reached after prolonged times, different for different temperatures, in which the curve is practically parallel to the abscissa axis. At low temperatures the swelling rate during the time interval of about 0-0.5 minute is low. The probable explanation is that after the liquid comes into contact with the particles of the substance some time is required for their complete wetting. This time decreases with increase of temperature, and the region of the curve with a low swelling rate disappears. None of the equations for the kinetics of swelling known to us completely covers the whole $\Delta V = f(t)$ curve. The best of these equations are: the Rotinyan equation [5]

$$\frac{1}{t}\ln\frac{1}{1-i'} - \beta\frac{i'}{t} = M,$$

where $i' = i/i_\infty$; i is the swelling at time t; i_∞ is the maximum swelling; β and M are constants which satisfactorily fits the experimental data for the slow swelling region, and our proposed equation

$$\Delta V_t = \frac{\Delta V_\infty t}{K+t},$$

where ΔV_∞ is the maximum swelling; ΔV_t is the swelling at time t; K is a constant equal to the time at which

$$\Delta V_t = \frac{1}{2}\Delta V_\infty.$$

The last equation satisfactorily fits the region of rapid swelling, and partly the region of slow swelling.

As regards the effect of temperature on the swelling of agar, in all cases in which the swelling process was not complicated by solution the degree of swelling increased with increase of temperature. When the solubility of agar increased considerably with temperature, the $\Delta V_\infty = f(T)$ polytherms had maxima. A comparison of the values for the swelling of agar in water denoted by ΔV_5, found in the rapid swelling region in 5 minutes from the start of the process [6] shows, as illustrated in Figure 3, that the degree of swelling increases practically linearly with temperature, while the polytherm for the maximum swelling ΔV_∞ passes through a maximum, found at 40° in Figure 4 (broken lines). The decrease of ΔV_∞ after 40° is the result of a sharp increase of the solubility of agar, which is 20.7% at 50°, and only 2.6% at 20°. The solubility was measured for the time required to reach maximum swelling.

If the presence of a maximum on the $\Delta V_\infty = f(T)$ polytherm is indeed associated with a change of solubility, then experiments performed under conditions in which the solubility of agar is considerably decreased should give rise to polytherms without maxima, or with maxima shifted into the region of higher temperatures. Conversely, the maxima should be shifted into the region of lower temperatures for media in which the solubility of agar is higher than in water. To test this, experiments on the swelling of agar in solutions of K_2SO_4 and KCNS were carried out. As was to be expected, the $\Delta V_\infty = f(T)$ polytherms for K_2SO_4 solutions do not show maxima (Figure 4a). The solubility of agar in K_2SO_4 solutions is considerably lower than in water; it is 5% in 0.5 M solution at 50°, while it is 4 times as high in water at the same temperature. The polytherm for a very dilute KCNS solution (Figure 4b) differs little in its course from the polytherm for swelling of agar in water, but at high concentrations of KCNS, when its lyotropic effect is prominent, the $\Delta V_\infty = f(T)$ polytherm has a maximum at a lower temperature than for water. The solubility of agar in 1.5 M KCNS solution, even at 20°, is 13.5%, which is 5.2 times the solubility in water at the same temperature. It is interesting to note that the position of a salt in the lyotropic series, as is shown by the polytherms given, is determined not only by the nature of the salt but also by its concentration and the swelling temperature.

Temperature Coefficient of the Swelling Rate I

Temperature, °C	In H_2O	In solution of K_2SO_4			In solution of KCNS			
		0.01*M*	0,1*M*	0.5*M*	0,01*M*	0,1*M*	0,5*M*	1,5*M*
0—10	1.80	1.16	1,24	1,22	3.90	1,36	1.18	1,19
10—20	1,14	1,22	1.25	1,04	1.21	1.19	1.16	1.25
20—30	1.30	1,27	1.08	1,24	1.04	0.99	1,03	1.09
30—40	1,05	1,00	1,09	1,02	1,12	1,11	1,12	0.99
40—50	1,10	1.10	1,03	1,08	1.08	1.11	1.06	0,69

The authors [7-11] of a number of well-known books on colloid chemistry take into account the exothermic character of the swelling process and apply the Le Chatelier principle to it, reaching the conclusion that the degree of swelling should decrease with increasing temperature. Our data on the swelling of agar in various media, and also earlier data on the swelling of gelatin in water [12-14] and of rubbers in organic solvents [15-17], do not confirm this conclusion. In all instances when the swelling of agar is not appreciably complicated by solution we found that the maximum swelling increases with increasing temperature. The Le Chatelier principle cannot be applied in this way to the complicated process of swelling, since most of the liquid is absorbed osmotically by the swelling substance, and this absorption occurs without any appreciable heat effect.

In studies of the influence of temperature on the rate of swelling the rapid swelling region is of the most interest. The table contains data on the temperature coefficient I, which represents the change of the average rate of swelling during two minutes from the start of the process, when the temperature is changed by 10°.. It is seen that I is not constant, but depends on a number of factors, the most important of which are: the temperature range over which the swelling is studied, the nature and the concentration of the dissolved salt. In most cases the coefficient I is close to unity, which indicates a relatively small change of the swelling rate with temperature. The value of I becomes fairly large only for dilute solutions of KCNS and for water in the region of low temperatures, when the swelling process is not complicated by solution.

SUMMARY

1. An automatic recording instrument has been used to study the variations of the magnitude and rate of swelling of agar in water and in solutions of salts of the lyotropic series with the temperature.

2. It is shown that if the swelling of agar is not complicated by solution, the degree of swelling increases with temperature, while otherwise the $\Delta V_\infty = f(T)$ polytherm passes through a maximum which shifts in the di-

rection of lower temperatures for media in which the temperature coefficient of solubility of the swelling substance is greater.

3. It is shown that the swelling rate of agar increases slightly with increase of temperature and that the temperature coefficient of the swelling rate is close to unity and depends on the nature of the liquid and the temperature range.

LITERATURE CITED

[1] N.D. Verderevskaya, "Effect of Temperature on the Magnitude and Rate of Swelling" Dissertation (1 MOLMI, Moscow 1956).

[2] V.K. Tile, "Methods for Determination of the Degree of Swelling" (Dissertation, Moscow 1955).

[3] I.N. Ermolenko and M.I. Mazel, Sci. Mem. Lenin Belorussian State Univ. No. 20, Chem. Ser.-(Acad. Sci. Belorussian SSR Press, Monsk 1954).

[4] Ya.S. Przheborovsky and V.K. Tile, Colloid J. 16, 304 (1954) (T.p. 297).*

[5] A.L. Rotinyan, Colloid J. 11, 431 (1949).

[6] A.A. Tager, Solutions of High Polymers (Goskhimizdat, Moscow-Leningrad 1951).

[7] H. Freundlich, Kapillarchemie B. 2 (1932).

[8] V.A. Naumov, Colloid Chemistry (State Chem. Tech. Press, Leningrad 1932).

[9] D.L. Rubinshtein, Physical Chemistry (Izd. AN SSSR, Moscow-Leningrad 1940).

[10] I.A. Izgaryshev, Course of Colloid Chemistry (Art.Acad. Press, 1944).

[11] N.P. Peskov and E.M. Aleksandrova-Preis, Course of Colloid Chemistry (Goskhimizdat, Moscow-Leningrad 1948).

[12] D.J. Lloyd and B. Pleass, Biochem. J. 21, 135 (1927); 23, 358 (1929); 24, 1472 (1930); 25, 1943 (1931).

[13] S.M. Lipatov, Colloid J. 5, 615 (1939).

[14] A.A. Bromberg and S.A. Merikalov, J. Appl. Chem. 23, 1280 (1950).

[15] F. Kirchof, Kolloid. Beih. 6, 1 (1914).

[16] P. Powers and B. Billmeyer, Ind. Eng. Chem. 37, 64 (1945).

[17] V.E. Gul and A.G. Shvarts, Colloid J. 17, 24 (1955).(T.p. 21).*

Received July 15, 1956

The I.M. Sechenov First Medical
Institute, Moscow
Chair of General Chemistry

---

* T.p. = C.B. Translation pagination.

INVESTIGATION OF THE STRUCTURE AND PROPERTIES OF CARBON CHAIN POLYMERS IN DILUTE SOLUTIONS

3. MIXTURES OF POLYVINYL CHLORIDE AND POLYACRYLONITRILE

N.V. Mikhailov and S.G. Zelikman

For production of polymeric materials with a great variety of properties, the method of molecular mixing of polymers with the aid of common solvents or in melts is used, in addition to copolymerization reactions. Plasticizers of high molecular weight are becoming increasingly important [1]. Studies of the properties of polymer mixtures have therefore become necessary for the proper practical utilization of high polymers and for further development of our theoretical knowledge of the relationship between the structure and properties of polymers.

Some data on the properties of polymer mixtures have been obtained in the course of selection of materials for particular practical purposes. The thermodynamic, mechanical and optical properties of polymer mixtures have been described in a number of publications [1, 2]. The basic laws of the phase state of polymer mixtures have been noted in a number of papers [3-5], in which it is established that the compatibility of polymers depends on the molecular weight and relative proportions of the polymers, solution concentration, and a number of other factors. Some workers [6] use a simpler approach to polymer compatibility, and evaluate it from mechanical data. The view has been put forward [7] that mutual solubility of polymers is determined principally by enthalpy changes in the system, and on this basis the following criterion of polymer compatibility has been suggested: polymers are mutually soluble if the heat effect of mixing $\Delta H < 0$. This criterion was experimentally confirmed by Strumynsky [2], attention being drawn to the importance of volume contraction when certain polymers are mixed. It follows from these data that the energy factor plays a predominant role in the compatibility of polymers, especially polar polymers.

Morawetz and Gobran [8] studied the influence of intermolecular forces in solutions of polymer mixtures; they measured the osmotic pressure of solutions of mixtures containing acidic (copolymer of methyl methacrylate with methacrylic acid) and basic (copolymer of methyl methacrylate with dimethylaminomethyl methacrylate) copolymers. Fairly stable aggregates are present even in very dilute solutions of such mixtures. The maximum degree of association is found in mixtures consisting of 50% of acidic and 50% of basic copolymer; its value is 5.43 at 30° and 3.2 at 50°.

In our earlier publications [9] certain properties of solutions of polyvinyl chloride, polyacrylonitrile, and copolymers based on them were described. It seemed of considerable interest to compare such "chemical mixtures" as copolymers with model systems consisting of molecular mixtures of the polymers of the equivalent chemical composition, and to compare their behavior in solution with that of the pure polymers.

The present communication contains the results of an investigation of the viscosities and osmotic pressures of such molecular mixtures of polymers. Since it was necessary to examine simultaneously the corresponding data on pure polymers, their copolymers, and molecular mixtures, the components were chosen to be as close as possible to each other in molecular weight; this was achieved by careful fractionation of the starting materials. Three mixtures of polyvinyl chloride and polyacrylonitrile were prepared, in the following proportions: 13 : 87; 29 : 81 and 40 : 60 by weight. The reason for these proportions was the composition of the copolymers described previously. The methods used for viscosity and osmotic pressure determinations were described in the earlier communications [9].

EXPERIMENTAL

The variation of viscosity with concentration in the 0.25-0.85% range, and the variation of viscosity with temperature in the 20-60° range, was studied for all the mixtures. The osmotic pressure was determined at 20, 35 and 50°.

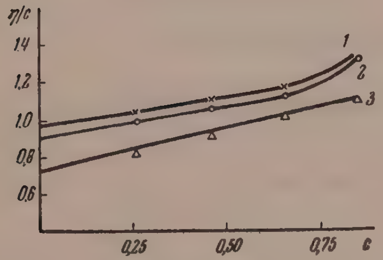

Fig. 1. Variation of reduced viscosity of polymer mixtures with concentration: 1) 40 : 60 mixture; 2) 29 : 71 mixture; 3) 13 : 87 mixture.

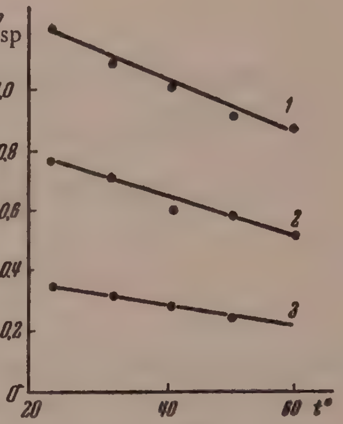

Fig. 2. Variation of viscosity with temperature for the 40 : 60 mixture; solution concentrations: 1) 0.85%; 2) 0.65%; 3) 0.45%.

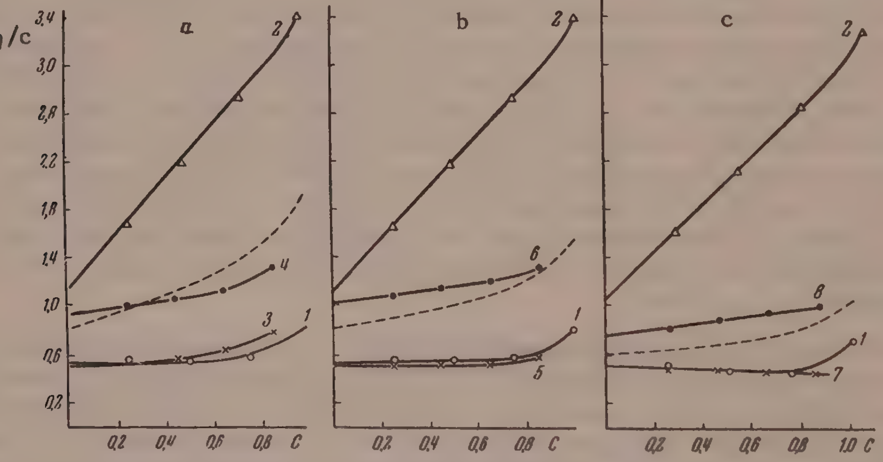

Fig. 3. Variation of reduced viscosity with solution concentrations: 1) PVC; 2) PAN; 3, 5, 7) copolymers; 4, 6, 8) mixtures. Ratios of PVC to PAN in the copolymers and mixtures: a) 40 : 60; b) 29 : 71; c) 13 : 87.

Variations of the reduced viscosity for the three mixtures are plotted in Figure 1, while variation of viscosity of the 40 : 60 mixture with temperature is shown in Figure 2. As for copolymers and pure polymers, the specific viscosity of polymer mixtures is a linear function of the temperature. For comparison, Figure 3 shows variations of the reduced viscosity with concentration for the copolymers, mixtures, and pure polymers. The broken lines represent the reduced viscosities calculated additively from the viscosities of the pure polymers. Figure 4 shows the variation of reduced osmotic pressure with solution concentration for all the polymer mixtures at 20, 35 and 50°. For comparison, Figure 5 shows the variation of the osmotic pressure of polyvinyl chloride, polyacrylonitrile and polymer mixtures at 20°.

A curious feature is that, in contrast to the pure polymers, the apparent molecular weight of the polymers in mixtures decreases with increase of temperature (Table 1).

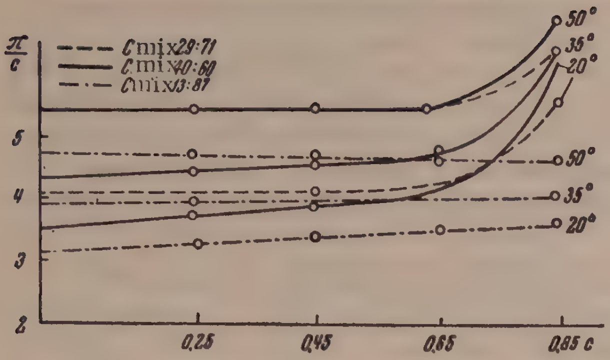

Fig. 4. Variation of reduced osmotic pressure of polymer mixtures with concentration.

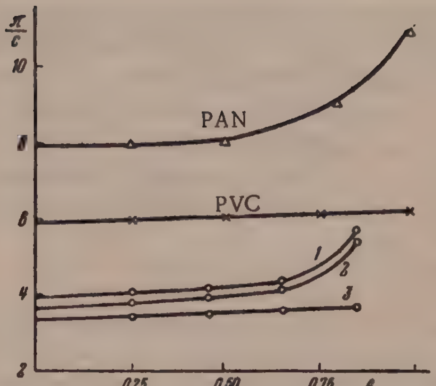

Fig. 5. Variation of osmotic pressure with concentration of PAN, PVC, and mixtures of the polymers at 20°; PVC : PAN ratios in mixtures: 1) 40 : 60; 2) 29 : 71; 3) 13 : 87.

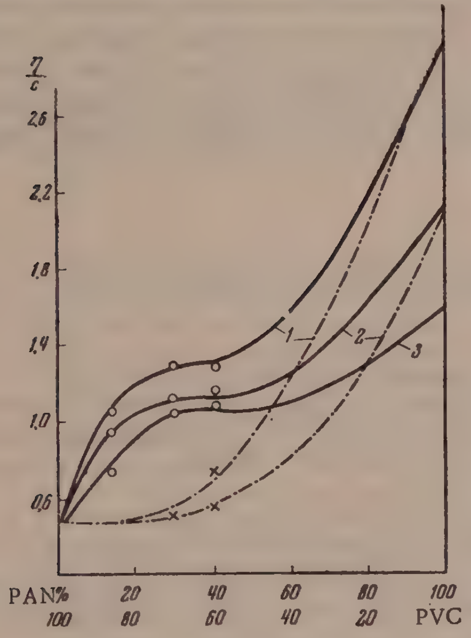

Fig. 6. Variation of viscosity with composition of mixtures (continuous lines) and copolymers (broken lines). Solution concentrations: 1) 0.85%; 2) 0.65%; 3) 0.25%.

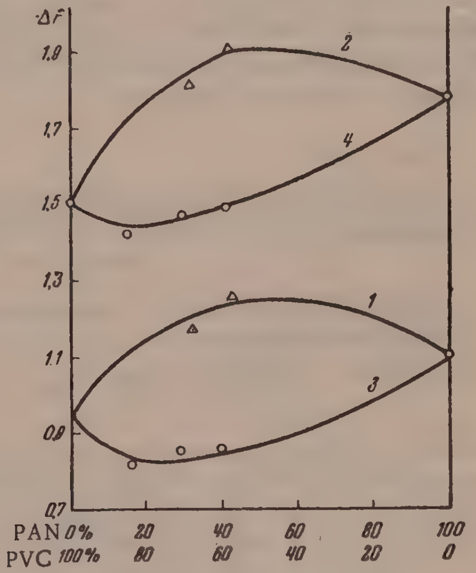

Fig. 7. Variation of free energy with composition. Copolymer solutions: 1) 0.45%; 2) 0.85%. Solutions of mixtures: 3) 0.45%; 4) 0.85%.

It must also be borne in mind that these apparent molecular weights of the polymers in the mixtures are considerably higher than the molecular weights of the pure polymers used for making the mixtures. This suggests that aggregates are formed as the result of intermolecular interaction in solutions of polymer mixtures. The degree of association calculated from the above data at 20° is in the range of 1.6-1.8. The intermolecular forces are weakened with increase of temperature, but even at 50° the degree of association is still 1.2-1.3, so that the aggregates are not completely destroyed. Molecular mixtures of the polymers also differ sharply from the corresponding copolymers in solution viscosity. With equal contents of functional groups in the mixtures and copolymers, and with almost equal molecular weights, the intrinsic viscosity of the mixtures is approximately double that of the corresponding copolymers, for all ratios.

TABLE 1

Variation of Molecular Weight with Temperature

PVC : PAN ratio in mixture	Molecular weight of polymer at 20°	35°	50°
40:60	73,000	63,000	54,000
29:71	66,000	58,000	54,000
13:87	82,000	71,000	62,000
Polyvinyl chloride	47,000	47,000	47,000
Polyacrylonitrile	39,000	38,800	37,700

TABLE 2

Temperature Coefficients of Viscosity for Mixtures and Copolymers with Different PVC : PAN Ratios

	Temperature coefficients of viscosity of PVC : PAN mixtures 40:60	29:71	13:87
Mixtures	0.100	0.125	0.083
Copolymers (mol wt 50,000)	0.076	0.063	0.043
Copolymers (mol wt 30,000)	0.041	0.043	0.043

Thus, the viscosity of the mixtures also shows that aggregation in solutions of polymer mixtures occurs even at low concentrations. It is very interesting to compare the viscosities of the mixtures with the calculated values based on additivity of the corresponding values for the pure polymers. As is to be expected from the osmotic pressure data, the observed interaction between unlike macromolecules in solutions of polymer mixtures should result in nonadditivity of the viscosity. Such deviations from additivity are demonstrated especially clearly by a plot of the viscosity against the composition. As Figure 6 shows, the viscosity curves for the mixtures are S-shaped, and even the 0.25% solution deviated from additivity. The aggregates in solutions of polymer mixtures are rigid formations, as is shown by the values of μ calculated from the osmotic pressure-concentration relationship. The value of μ is not less than 0.47-0.48 for any of the mixtures. For copolymers of the same composition, the molecular weight of which is considerably less than the apparent molecular weight of the mixtures, μ has values of 0.38-0.41.

TABLE 3

Variations of the Thermodynamic Functions of Mixtures of Different Composition with Temperature

Composition of PVC : PAN mixture	Concentration in g/100 g solution	$\Delta F_1 \cdot 10^4$ cal/mole 293°K	308°K	323°K	$\Delta H_1 \cdot 10^4$ cal/mole 300,5°K	315,5°K	$\Delta S_1 \cdot 10^5$ cal/mole 300,5°K	315,5°K	ΔS_{id} 10^6 cal/mole
40 : 60	0,25	0,163	0,197	0,240	0.48	0,70	2,2	3,0	0,50
	0,45	0,300	0,360	0.428	0.87	1,03	4.0	4.5	0,87
	0.65	0.437	0,525	0,608	1,29	1,20	5,9	5,6	1,29
	0,85	0,942	0,993	1.027	0.05	—0,29	3.4	2,3	1,70
29 : 71	0,25	0.171	0.205	0.240	0,48	0,51	2,2	2,3	0,55
	0.45	0.325	0.368	0.419	0,53	0.66	2,9	3,3	1.01
	0.65	0,470	0.531	0,599	0.72	0.87	4.1	4,5	1.47
	0.85	0.856	0,976	0,950	1,48	—	8.0	—	1,89
13 : 87	0.25	0.145	0,171	0.205	0,36	0.53	1.7	2.3	0.46
	0,45	0,274	0.317	0,368	0.56	0,73	2.8	3,4	0.78
	0.65	0,394	0,462	0,539	0,93	1,10	4,5	5,1	1.15
	0.85	0,531	0.616	0,702	1,11	1,15	5,6	5,8	1,52

As the specific viscosity is a linear function of the temperature, the temperature coefficient of viscosity remains constant over the whole temperature range of 20-60°.

The variations of viscosity when the temperature of 0.85% solution is raised by 10° are given in Table 2. Table 2 shows that the temperature coefficient of viscosity for the mixtures is nearly double the corresponding value for the copolymers. For comparison it may be noted that the temperature coefficient of viscosity of 0.85% polyvinyl chloride solution is 0.040, and of polyacrylonitrile solution, 0.170.

The results for the osmotic pressure-temperature relationship were used to calculate the thermodynamic functions (Table 3).

The change of free energy as a function of composition is shown graphically in Figure 7 for 0.45 and 0.85% solutions. It is seen in Figure 7 that copolymers have the minimum value of free energy ($-\Delta F$ is maximum). As the contents and nature of the polar groups in the mixtures and the corresponding copolymers are the same, it may be assumed that the differences between the values of ΔF represent differences in the flexibility of the molecules of the mixtures and of the copolymers in solution. This assumption is admissible if the solvation of the same polar groups is the same in the mixtures and in the copolymers. From this it follows that the flexibility is greatest in the 40 : 60 copolymer and least in the 13 : 87 mixture. This is in good agreement with other results. In fact, the greatest degree of association is found in the 13 : 87 mixture, and the minimum value of μ is found for the 40 : 60 copolymer.

The considerable differences of behavior between the molecules of copolymers and of polymer mixtures can be explained by the relative positions of the polar groups and their influence on molecular structure and interaction. The polarity of CN and Cl bonds and their polarizability in an external field are probably the decisive influences with regard to the flexibility of the polymer molecules. In considering the properties of the copolymers, the mutual influence of the polymer groups in the copolymer chain itself must be primarily taken into account. This influence leads to mutual intramolecular saturation of the polar groups, probably resulting in some globulization of the molecules, owing to which the intermolecular interaction is weakened. In consequence, the copolymers are more readily soluble, have lower solution viscosity, etc. In mixtures, interaction occurs between polar groups in different chains; this leads to formation of relatively rigid aggregates of unlike polymer molecules in solution, with an increase of solution viscosity.

Thus, because of intramolecular interaction and disturbance of the regular structure, the copolymer molecules become more flexible, while intermolecular interaction between the same functional groups in polymer mixtures leads to decreased flexibility.

SUMMARY

1. The osmotic pressure and viscosity of dilute solutions of molecular mixtures of polyacrylonitrile and polyvinyl chloride in different proportions have been measured and compared with the corresponding values for copolymers of the same chemical composition, and for the pure polymers.

2. It is shown that the viscosity and osmotic pressure of solutions of polymer mixtures deviate from the additivity rule over the whole range of component ratios studied: the viscosity, in the direction of an increase, and the osmotic pressure in the direction of a decrease. These results are attributed to the formation of stable aggregates by molecules of the different polymers.

3. It is shown that the viscosity and osmotic pressure of polymer mixtures vary with the temperature. The decrease of the apparent molecular weight with temperature, and also the existence of an appreciable temperature coefficient of viscosity for polymer mixtures, in contrast to solutions of the corresponding pure polymers and copolymers, confirm the presence of aggregates of unlike molecules in solutions of polymer mixtures.

4. A comparison of data on molecular mixtures and on copolymers shows that they differ sharply in their behavior; this is attributed to intramolecular interaction between the polar CN and Cl groups in copolymers, and intermolecular interaction in polymer mixtures.

LITERATURE CITED

[1] R.A. Reznikova, A.D. Zaionchkovsky and S.S. Voyutsky, Colloid J. 15, 108 (1953) (T.p. 111)*; S.E. Bolam, Rubb. Age Synth. 34, No. 10, 436 (1953); V.I. Alekseenko and I.U. Mishustin, Colloid J. 18, No. 3, 257 (1956)(T.p. 247).*

[2] G.V. Struminsky, Dissertation (Moscow, 1953); R.A. Reznikova, Dissertation (Moscow, 1952).

[3] A. Dobry and F. Boyer Kawenoki, J. Pol. Sci. 2, 90 (1947).

[4] H. Tompa, Trans. Faraday Soc. 45, 1142 (1949).

---

*T.p. = C.B. Translation pagination.

[5] N.V. Mikhailov, Z.V. Ukhanova, V.S. Klimenkov and E.A. Kurilchikov, Text. Ind. 14, No. 9, 11 (1954).

[6] V.I. Alekseenko, I.U. Mishustin and S.S. Voyutsky, Proc. Acad. Sci. USSR 95, No. 1, 93 (1954).

[7] M.F. Komskaya, Dissertation (Moscow, 1952).

[8] H. Morawetz and R.H. Gobran, J. Pol. Sci. 12, No. 1, 133 (1954).

[9] N.V. Mikhailov and S.G. Zelikman, Colloid J. 18, No. 6, 717 (1956) (T.p. 715)*; S.G. Zelikman and N.V. Mikhailov, Colloid J. 19, No. 1, 35 (1957) (T.p. 37).*

Received September 7, 1956

All-Union Scientific Research Institute
for Artificial Fibers, Mytishchi

---

* T.p. = C.B. Translation pagination.

ALTERATION OF THE INTERMOLECULAR STRUCTURE OF CAPRON FIBERS AS THE RESULT OF HEAT-TREATMENT*

L.I. Pokrovsky and A.B. Pakshver

Capron fibers are subjected to various kinds of heat treatment in the course of production and during subsequent processing, in order to improve the performance characteristics of the articles made from them. Heat treatment of the fibers in the free state, known as heat shrinking, results in a considerable increase of the extensibility without appreciable decrease of tenacity, and an improvement of the elastic properties. Heat treatment of the fibers or articles on rigid forms, in the stretched state, known as heat setting, fixes the geometrical dimensions and stabilizes them against subsequent heat treatment. Despite the extensive use of a great variety of heat treatments, the literature contains no reports of systematic investigations of the mechanism of this process or of the structural changes which occur as the result of heat setting and heat relaxation.

Mikhailov and Fainberg [1], who studied the sorption of water vapor and determined the heats of wetting and solution of undrawn and drawn capron fibers, showed that drawing of capron fibers causes only slight changes in the energy of intermolecular interaction.

Data on the sorption of phenols by capron fibers [2] also showed that equilibrium sorption changes little as the result of drawing. However, it is well known that the mechanical properties of undrawn and drawn capron fibers and of fibers subjected to heat treatment vary very considerably, and the rates of various sorption processes vary to an equal extent [3]. Evidently the intermolecular structure undergoes further condensation during drawing or heat treatment of capron fibers. This increase of the density of the structure has little influence on the aggregate, equilibrium processes, but the kinetic processes, which are primarily associated with the loose portion of the material, are very greatly changed.

Therefore, for evaluation of changes in the intermolecular structure of capron fibers, as the result of various heat treatments, we determined the kinetic heat of solution, i.e., the quantity of heat liberated in a calorimeter in 15 minutes, which characterizes the solution rate of the macromolecules in the loose structure of the fibers. It was presumed that this would give greater differences of the heat effects than are found in determinations of total heats of solution [4].

For a fuller characterization of the changes of molecular structure, the densities of the fibers were determined at the same time, Such data are also lacking at the present time. The literature only contains data on densities of undrawn and drawn nylon fibers and nylon plates [5].

EXPERIMENTAL

The kinetic characteristics of the heat of solution of capron fibers were determined by means of an isothermal microcalorimeter of the Schottky type [6]. With this calorimeter it is possible to measure small heat effects with good reproducibility and with small relative errors. The heat effects were measured to within 0.3 cal. The duration of the determinations was 15 minutes. During this time the solution became quite clear, and the subsequent change of temperature was much slower.

In order to find the most suitable solvent, preliminary experiments were carried out with an ordinary calor-

---

*23rd communication in the series of investigations on the intermolecular structure of high polymers.

TABLE 1

Kinetic Characteristics of the Heats of Solution of Undrawn and Drawn Capron Fibers in Various Solvents

Solvents	Undrawn fiber, Q'_K	Drawn fiber, Q''_K
20% HCl solution	5.9	4.9
40% H_2SO_4 solution	8.3	6.5
85% HCOOH solution	10.8	8.3
85% phenol solution	19.6	15.5

Note: The accuracy of the determinations was ± 0.5 cal/g.

imeter to determine the kinetic characteristics of the heats of solution of undrawn and drawn capron fibers in 20% HCl, 40% H_2SO_4, 85% HCOOH, and 85% phenol.

The results of these determinations are given in Table 1.*

Visual observations showed that the rate of solution of capron fibers decreases in these solvents in the following sequence: 20% HCl, 40% H_2SO_4, 85% HCOOH, 85% phenol. The differences of the kinetic heats of solution ($Q'_K - Q''_K$) between undrawn and drawn fibers decrease in the opposite sequence. It seems that in 20% HCl solution the solution process is more rapid and the measured heat effect of solution approximates to the limiting value Q_0, and therefore in 20% HCl the difference between the heats of solution of the undrawn and drawn fibers ($Q'_K - Q''_K$) is not large. When 85% HCOOH or 85% phenol are used as solvents, in which the solution rate is considerably lower, only the heat effects of solvation of the more loose domains is measured, and the difference between the heat effects $Q'_K - Q''_K$ for undrawn and drawn fibers becomes considerably greater.

Maximum solvation, i.e., the passage of all the macromolecules into solution, occurs very slowly, during several hours, with only a small additional heat effect, which can be determined with sufficient accuracy only by an adiabatic calorimeter [1].

As the result of the preliminary experiments, 85% solution of chemically pure HCOOH and 85% aqueous solution of phenol were used as the solvents in the subsequent experiments. The fibers studied were: samples of capron yarn No. 34, the same yarn subjected to dry heat in skeins and on bobbins for 5, 20 and 70 minutes, samples of yarn boiled in water in skeins and on bobbins for 0.5, 1 and 3 hours, samples of yarn steamed in an autoclave in skeins and on bobbins at 140° for 0.5, 1 and 3 hours, and samples of yarn additionally stretched in the heated state.

The results of measurements of the kinetic characteristics of the heats of solution, in the form of average values for 3-4 experiments, are given in Table 2. The solution concentration was approximately the same, 0.5-0.6%, in all cases. Table 2 shows that the kinetic characteristic of the heat of solution Q_k is lower for capron yarns subjected to various heat treatments than for the original No. 34 yarn. Therefore heat treatment of capron yarn produces denser molecular packing.

The greatest change in structure is produced by the action of steam on the fibers. It seems that with the high mobility of the molecular segments which results from the high temperature and the action of steam the macromolecules become rearranged into a denser form of packing in the fiber. It must also be pointed out that heat treatment of the fibers in the free state not only does not decrease the molecular density, as might have been expected, but increases it still more than does treatment on a rigid bobbin, especially by steaming. This is in good agreement with the results obtained by Lipatov [7] and Rogovin and Zazulina [8], who showed that in a number of cases changes of the degree of orientation on relaxation do not follow the same course as the total intermolecular interaction. Equal values were obtained for the kinetic characteristics of the heat of solution of fibers subjected to the same kind of heat treatment but for different times. The condensation of the molecular structure therefore proceeds very rapidly.

The Q_k values for the fibers studied are in good agreement with the results of density determinations for the same fibers.

The densities were determined as follows: a small skein of the yarn to be tested was placed in a bulb which was then evacuated down to $(1.25\text{-}1.34) \cdot 10^{-3}$ mm Hg and sealed. The sealed bulb was transferred to a cylinder containing a mixture of benzene and nitrobenzene, and broken. The cylinder with the fibers was placed in a thermostat maintained at 25 ± 0.005°. The mixture in the cylinder was occasionally stirred by hand. Ben-

---

* The results given in Table 1 were obtained by A.F. Kolbashova. The measurements were also continued for 15 minutes, to complete visible solution of the fibers.

TABLE 2

Kinetic Characteristics of the Heats of Solution of Capron Fibers Subjected to Various Heat Treatments

Fibers	Q_k cal/g	
	85% HCOOH	85% phenol
Undrawn yarn (old)	8.5	–
Drawn capron yarn No. 34	6.6	20.2
Ditto, heated on bobbin at 160°, 5 minutes	5.9	–
" , heated on bobbin at 160°, 20 minutes	5.9	–
" heated on bobbin at 160°, 70 minutes	5.9	19.2
" heated in skein at 160°, 5 minutes	5.9	–
" heated in skein at 160°, 70 minutes	6.0	19.1
" additionally stretched at 160°	5.5	18.7
" boiled in water on bobbin, 0.5 hour	5.7	–
" boiled in water on bobbin, 3 hours	5.6	18.6
" boiled in water in skein, 0.5 hour	5.1	–
" boiled in water in skein, 3 hours	5.1	17.5
" steamed on bobbin in autoclave at 140°, 0.5 hour	4.5	–
" steamed on bobbin in autoclave at 140°, 1 hour	3.8	–
" steamed on bobbin in autoclave at 140°, 3 hours	4.0	14.9
" steamed in skein in autoclave at 140°, 0.5 hour	2.5	–
" steamed in skein in autoclave at 140°, 3 hours	2.5	13.4

Note: The accuracy of the determinations was ± 0.2 cal/g.

TABLE 3

Densities of Fibers after Various Types of Heat Treatment

Fibers	Density in g/cc
Undrawn yarn No. 34	1.1303
Drawn yarn No. 34	1.1449
Ditto, additionally stretched at 160°	1.1437
" heated on bobbin at 160°, 70 minutes	1.1456
" heated in skein at 160°, 70 minutes	1.1471
" boiled in water on bobbin, 3 hours	1.1464
" boiled in water in skein, 3 hours	1.1479
" steamed in autoclave on bobbin at 140°, 3 hours	1.1533
" steamed in autoclave in skein at 140°, 3 hours	1.1598

Note: The accuracy was ± 0.00042 g/cc.

zene or nitrobenzene was added until the skein began to float within the liquid. The density of the benzene-nitrobenzene mixture was then determined pycnometrically; this was equal to the density of the fiber specimen.

The results of the density determinations, which are the average values of three separate experiments, are given in Table 3. As was stated earlier, the density data in Table 3 are in good agreement with the kinetic characteristics of the heat of solution, Q_k, thereby confirming that heat treatment results in an increase of the molecular packing density in the fibers.

SUMMARY

1. The kinetic characteristics of the heat of solution of capron fibers after different types of heat treatment differ considerably. These results are in agreement with other kinetic data and are a good measure of the change in the molecular structure of capron fibers caused by heat treatment.

2. Heat treatment of capron fibers on bobbins or in the free state results in a denser packing of the intermolecular fiber structure.

LITERATURE CITED

[1] N.V. Mikhailov, E.Z. Fainberg and S.M. Skuratov, Colloid J. 15, 271 (1953) (T.p. 279)*; S.M. Skuratov, N.V. Mikhailov and E.Z. Fainberg, Colloid J. 16, 58 (1954) (T.p. 65)*; N.V. Mikhailov and E.Z. Fainberg, Colloid J. 18, 44 (1956) (T.p. 41).*

[2] V.D. Tetyushkina, A.N. Pkashver and S.S. Frolov, Colloid J. 17, 63 (1955) (T.p. 57).*

[3] A.B. Pakshver and E.K. Mankash, J. Appl. Chem. 24, No. 2, 182 (1954); E.K. Mankash and A.B. Pakshver, Colloid J. 16, 451 (1954) (T.p. 429)*; V.A. Myagkov and A.B. Pakshver, Colloid J. 17, 120 (1955) (T.p. 109).*

[4] E.K. Mankash, Trans. Ivanovo Inst. Chem. Technol. 5, 127 (1956).

[5] G. Clark, M. Mueller and L. Scott, Ind. Eng. Chem. 42, No. 5, 831 (1950); N. Abbot and A. Gottings, J. Text. Inst. 40, No. 4, 232 (1949).

[6] H. Schottky, Z. Phys. Chem. 64, 425 (1908); K.P. Mishchenko, M.Z. Pronina and A.M. Sukhotin, J. Appl. Chem. 27, No. 9, 1003 (1954).

[7] Yu.S. Lipatov, Candidate's Dissertation (1954).

[8] Z.A. Zazulina and Z.A. Rogovin, Colloid J. 17, 343 (1955) (T.p. 327).*

Received November 6, 1956

The Ivanovo Institute of Chemical Technology
The All-Union Correspondence Institute for
the Textile and Light Industries

---

*T.p. = C.B. Translation pagination.

PERIODIC DEFORMATION OF COLLAGEN IN SOLUTIONS OF ELECTROLYTES AND TANNING AGENTS

A.G. Pasynsky and A.M. Tongur

The technical raw hide of the leather industry is a complex histological structure formed from bundles of collagen fibers (from 30 to 130μ in diameter) consisting consecutively, of collagen fibers (7-10μ), fibrils (tenths of a micron) and finally protofibrils (50-100 mμ), each containing some dozens of molecular chains. The interstices between the structural elements of the hide (up to several microns in size) are filled with interstitial materials (albumins, globulins, mucins, extractable matter) which are removed from the hide during the processes which precede tanning [1].

The permeability of hide to tanning agents largely depends on the histological rather than the molecular structure of the hide. Therefore, to accelerate penetration of tanning agents into hide, a suitable procedure seemed to be to influence the histological structure by periodic mechanical deformation of the hide. For this, a more detailed study of its relaxation properties was needed.

Zubov, Zhurkina and Kargin [2] discovered only short relaxation times for elastic gelatin gels (up to 20-30% gels); long relaxation times were found only under conditions in which some of the cross links of the network were broken and relative displacement of the molecules became possible. Gelatin gels are examples of histologically uniform structure, formed by molecular protein chains. Therefore, the variation of the deformation of raw hide in various media with the deformation frequency was also of interest in relation to the special deformation characteristics of histologically inhomogeneous structures, in the case of such a material as collagen (which comprises up to 98% of the fibrous protein of hide) [1]. In the present investigation a study was made of these characteristics, in order to determine the possibility of using them for acceleration of the tanning process.

EXPERIMENTAL

The relaxation properties of collagen were studied with the Aleksandrov-Kargin apparatus [2], at deformation frequencies from 1 to 1000 cycles per minute. Heavy cowhide specimens ~6 mm thick were used for the tests.

The clean hide (inner layer of fresh hide, with flesh side scraped and hair mechanically removed), in the loose and dense regions, behaves like an elastic gel up to 60°, with only short relaxation times in this range (Figure 1). Long relaxation times are found only at higher temperatures, corresponding to partial "fusion" of the hide structure. This behavior is similar to the properties of 30-40% gelatin gels [2], which have a similar content of dry protein (~ 35%) [1], but a sharp increase in the deformation of hide occurs at 60° (Figure 1), while for gelatin gels it occurs at 30°, which shows that the cross links of the network are stronger in collagen. At the same time, the existence of only short relaxation times below the "fusion" point of the gels indicates that the interaction between the chain segments between the cross links in the network is weak in both systems.

Alteration of the interchain bonding in the collagen structure may occur both as the result of temperature changes, and in presence of various dissolved substances. The effects of solutions of: KCNS, NaCNS, LiCl, KCl, $(NH_4)_2SO_4$ and urea, of various concentrations on periodic deformation behavior at different temperatures were therefore studied. Sets of curves similar to those shown in Figure 1 were obtained; the inflexion points on these curves varied for media of different composition, in general accordance with the thermal shrinkage temperatures in the same solvents. For example, after the hide specimens had been kept for 12 hours in the solutions, the

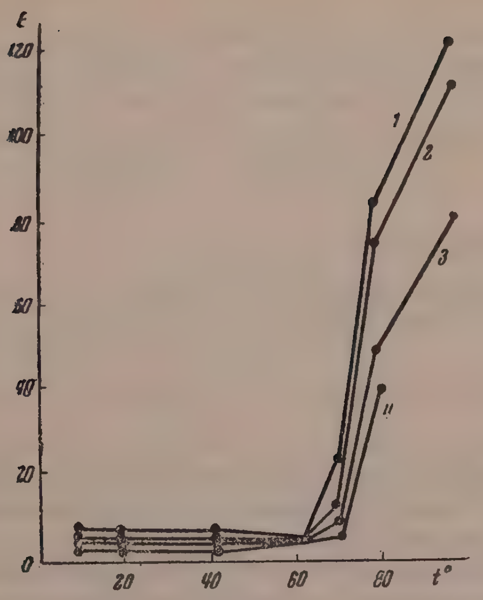

Fig. 1. Deformation-temperature curves for clean hide, for various frequencies: 1) 1 cycle/minute; 2) 10 cycles/minute; 3) 100 cycles/minute; 4) 1000 cycles/minute.

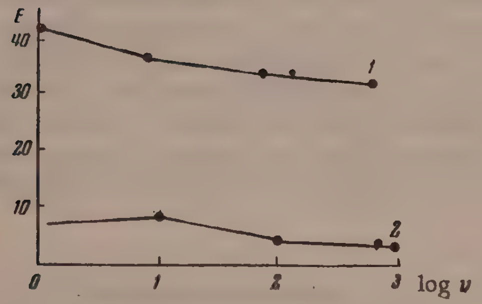

Fig. 2. Deformation of hide as a function of frequency, at the liming stage: 1) dense; 2) loose region of hide.

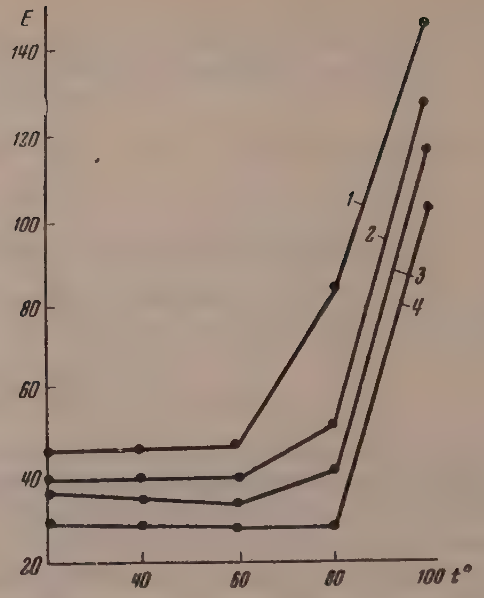

Fig. 3. Deformation-temperature curves for hide at the liming stage, for various frequencies: 1) 1 cycle/minute; 2) 10 cycles/minute; 3) 100 cycles/minute; 4) 1000 cycles/minute.

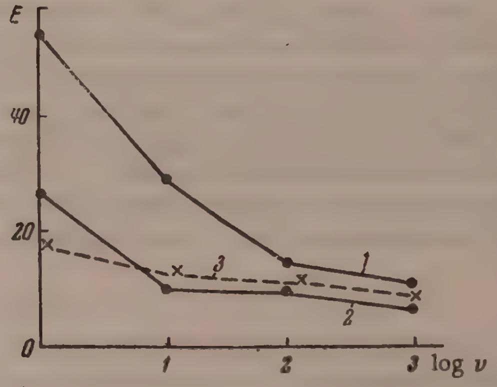

Fig. 4. Deformation of hide as a function of frequency, at the chroming stage: 1) dense region; 2) loose region; 3) deformation-frequency curve for leather.

points of inflexion on the curves were shifted to 20-22° in 2 M NaCNS and KCNS, to 38-40° in 5 M urea, were unchanged in 2 M LiCl, and were shifted by 10-20° in the direction of higher temperatures (i.e., up to 70-80°) in 2 M KCl and 25% solution of $(NH_4)_2SO_4$.[†] The shrinkage temperature of the collagen was marked in all cases by a sharp increase of deformation (as shown in Figure 1) and the appearance, beyond the inflexion point, of long relaxation times, which are detected by the clear dependence of the magnitude of deformation on the temperature. As was to be expected, the greatest increase of deformation is found at low vibration frequencies. At temperatures below 40°, at which tanning of collagen is usually carried out, clean hide shows only short relaxation times.

The relaxational properties of hide change in the course of technological processing. At the liming stage,

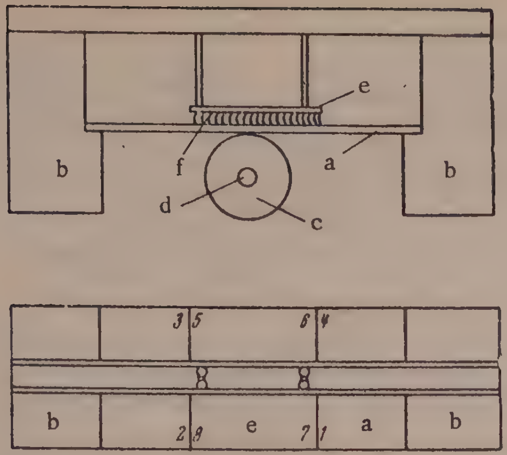

Fig. 5. Diagram of vibrator; below – diagram of control points.

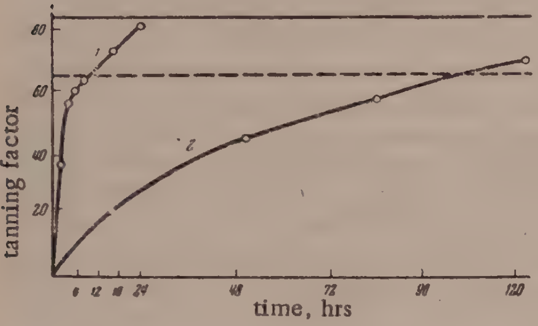

Fig. 6. The dynamics of tanning heavy hides: 1) during periodic compression 80 cycles/min; 2) in factory drum.

with the use of $Ca(OH)_2$ and Na_2S solutions, the deformation at 20° becomes almost independent of the frequency (Figure 2), but the deformation-temperature curves (Figure 3) begin to differ appreciably from the curves in Figure 1, both in the magnitude of deformation, and in the position of the inflexion points for various frequencies. At the liming and pickling stages (treatment with hydrochloric acid solution), deformation at 20° was almost independent of the frequency, both for the elastic and the soft portions of the hide, but at the liming stage the inflexion points on the deformation-temperature curves lay in the range of 60 to 90°, while at the pickling stage these curves again became similar to those shown in Figure 1, with a common inflexion point at 60°. It seems that at the liming and deliming stages additional stable bonds are formed in the collagen structure (possibly by calcium), which are completely destroyed in pickling.

At the chrome tanning stage the picture changes; as is seen in Figure 4 (Curves 1 and 2) the deformation of both the dense and the loose regions of the hide at 20° clearly depends on the frequency, especially at frequencies below 100 cycles/minute. This indicates that the hide has special mechanical properties at the chrome tanning stage, and it is significant that long relaxation times are found in this instance for the system in which relative displacement of the molecules is completely excluded as the result of a superposition of a network of additional stable bonds during chrome tanning, which results in a shift of the thermal shrinkage temperature to above 100°. An interesting fact is that even in the next operation (vegetable tanning in standard oak extract and syntans) the deformability of the leather again decreases considerably and the deformation becomes much less dependent on frequency (Figure 4, Curve 3).

We took advantage of the appearance of long relaxation times at the chrome tanning stage, before vegetable tanning, to influence the kinetics of the tanning process , the duration of which is determined primarily by the low rate of diffusion of the tanning solution into the hide. In our opinion, by means of periodic deformations of the hide, accompanied by contractions and extensions of the collagen fibers, equivalent to alternate condensation and rarefaction of the structure, it should be possible to accelerate the penetration of the tanning liquor into the hide. Naturally, this result could be expected only at deformation frequencies corresponding to long relaxation times, as at very high deformation frequencies the penetration of the tanning liquor into the structure could not keep pace with the changes in the field. As has been shown, at most stages in the production of leather, from the fresh hide up to the pickling stage, the hide has only short relaxation times at low temperatures, and it is only at the chroming stage, just before vegetable tanning, that the long relaxation times appear which could be used for accelerating the tanning process.

This possibility was explored in experiments on tanning of heavy and medium chromed hide (3 to 10 mm thick) with periodic deformation of the hide in the tanning liquor.

First we used vibrators operating at frequencies between 10 and 100 cycles/second. The vibrator (Figure 5) consists of two concrete supports b, with a plate a resting upon them, with an off-balance motor c attached to its under side. Vibrations of the body of the motor, induced by rotation of the eccentric pulley d mounted on the rotor, are transmitted to the plate a. The vibration conditions were controlled by means of an "Askania" recording dynamometer, which recorded the vibration amplitude and frequency at eight points in the vibrator,

TABLE 1

Results of Tanning in a Vibrator and in a Laboratory Drum (Without Heating)

Specimen No.	Tanning conditions	Moisture, %	% Contents in dry substance of					Bound tannins, %	Tanning factor, %
			ash	water-extractable substances		fats	hide material, from total nitrogen		
				inorganic	organic				
I	Vibrator, 50 cycles/ /sec, 6 hours	12.0	10.5	9.6	22.5	0	48.0	19.0	40
	Laboratory drum, 24 hours	13.8	10.7	9.0	21.6	0	52.7	15.0	28.5
II	Vibrator, 50 cycles /sec, 5 hours	12.7	7.6	6.8	14.7	0	59.9	18.2	31
	Laboratory drum, 5 hours	15.0	5.7	3.5	14.0	0	66.4	15.6	20

TABLE 2

Results of Tanning Under Periodic Compression at 80 cycles/minute and in a Factory Drum

Tanning time, hrs.	Moisture, %	% Contents in dry substance of					Bound tannins, %	Tanning factor, %
		ash	water-extractable substances		fats	hide material		
			inorganic	organic				
		Periodic compression at 80 cycles/minute						
2	11.2	10.2	9.3	29.8	0	44.5	15.5	35
4	12.0	9.1	8.7	26.3	0	41	23.7	57.7
6	10.6	9.7	8.8	24.6	0	41	24.7	60
12	10.15	9.85	9.0	29.2	0	37.4	23.55	63
18	10.0	9.9	9.05	28.6	0	35.4	26.1	74
24	9.7	9.3	8.35	27.8	0	35.0	27.9	80
		Factory drum						
48	12.8	6.7	6.0	11.5	0	56.5	27.4	45.0
82	12.2	7.8	6.9	11.8	0	53.0	25.3	52.0
125	11.7	6.9	5.0	10.8	0	49.2	33.1	67

indicated in the lower part of Figure 5. Specimens of chromed hide (6 x 6 cm) with tanning liquor were put into a thin rubber bag f (made from a surgical glove), placed between the vibrating plate a and the pressure plate e. The vibration amplitude of the pressure plate was considerably less than that of the vibrating plate (for example, 0.02 and 0.21-0.27 mm) in order to increase the relative deformation of the hide, and the deforming force was applied directly to the hide in order to create a vibration phase difference between the solid and the liquor. Simultaneously with the tanning in the vibrator, a specimen cut from the same portion of hide was tanned in a laboratory drum in standard oak tannin extract with additions of up to 20% of syntans, at a 1:4 ratio between the tanning agents in the volume of liquor used and the weight of the hide, and at pH of 4.25 to 4.5 of the diluted extract. The tanning was carried out at room temperature in both cases. The leather samples after tanning were analyzed according to GOST 938-45 for percentage fat, moisture, ash, easily removable low molecular substances, ash content of the extractable substances, and total nitrogen. The analytical data were used to calculate the total contents of nonhide material (percentage of bound tannins) and the tanning factor (ratio of bound tannins to total nitrogen in percent). The results for two heavy hide specimens (of the shoe sole type) are given in Table 1.

It is seen in Table 1 that periodic deformations accelerate the tanning of hide, and the process was further accelerated when the temperature was increased to 40° and the deformation frequency decreased to 25 cycles/second. However, it was difficult to reduce the frequency on the vibrator to below 100 cycles/minute, as required by the data in Figure 4. Therefore, in the following experiments the tanning was performed under periodic compression at a frequency of 1 cycle/second, effected by means of a plate with a rod with an eccentric drive. In this series of experiments (the control experiments for which were carried out in a factory drum) the liquors were heated to 38-40°. The results for the elastic region of heavy oxhide (5 mm thick) are given in Table 2 and Figure 6.

Table 2 and Figure 6 show clearly that tanning is accelerated on periodic compression of chromed hide, the standard degree of tanning (65% by GOST) being replaced in 12-13 hours instead of the 125 hours required in the factory drum. An interesting fact is that in experiments on vegetable tanning of unchromed hide, which shows only short relaxation times directly after pickling (see above), periodic deformation was found not to accelerate tanning. A negative result was also obtained in an experiment on vegetable tanning of a 15% chrome-treated gelatin gel, the deformation of which does not depend on the frequency..

DISCUSSION OF RESULTS

Gel structures are characterized by a spatial macromolecular network, cross linked by means of bonds of the valency or intermolecular type. The elastic properties of gels are determined by the flexibility of the macromolecular segments between cross links in the network, which fix the relative positions of the macromolecules. Characteristic features of typical gels are absence of fluidity and presence of elastic properties; in these gels only short relaxation times are found at temperatures below the gelation point. In such gels large relaxation times are found only after breakdown of some of the cross links of the network, when relative displacement of the macromolecules becomes possible [2]. Our data on the effect of frequency on the deformation of hide showed that the behavior of clean hide in water (Figure 1) and in various media (2 M solutions of KCNS, NaCNS, LiCNS, KCl, 5 M urea, 25% $(NH_4)_2SO_4$) is similar to that of an elastic protein gel, in which only short relaxation times are found below the heat shrinkage point, while the position of the inflexion points on the deformation-temperature curves (i.e., the appearance of long deformation times) is displaced in accordance with changes in the heat shrinkage temperature.

Interesting behavior is shown by chrome-tanned hide (Figure 4), in which long relaxation times are found in the gel state in presence of a network of additional bonds in the collagen structure, i.e., in conditions in which relative displacement of the macromolecules is excluded. This is not the consequence of an increased number of cross links in the network and interaction between the chains, as is shown by the fact that after vegetable tanning, during which the chrome cross links are retained and the absorption of vegetable tannins is added, long relaxation times are not found (Figure 4, Curve 3); neither are they found for chrome-treated gelatin gels. Therefore, the appearance of long relaxation times for chrome-tanned hide must depend on certain structural characteristics of the hide at this stage of treatment.

The characteristic in question is probably increased porosity of the structure. Owing to the removal of interstitial substances at the stages preceding tanning, the permeability of the hide increases sharply as has been shown by Frenkel and Mihailov [3], at the chroming stage, while during the subsequent vegetable tanning the permeability decreases again because the pores become filled with tannin particles [1]. Thus, at the chroming stage the structure of the leather acquires a peculiar character, which distinguishes it from the ordinary microscopically homogeneous gels, of the gelatin gel type, studied by Zubov, Zhurkina and Kargin [2].

In a histologically inhomogeneous porous structure, deformation of bundles of fibers or fibrils, even if the gel network is retained, leads to the appearance of longrelaxation times, associated with the deformed fibers entering and leaving the pores. This is the way in which the deformation of histologically porous structures differs in principle from the deformation of histologically homogeneous gels (such as gelatin gels), the heterogeneity of which is at the molecular structure level. This new effect in the deformation of collagen will probably be found in other polymeric substances with a submicroscopically heterogeneous structure. This effect disappears in collagen when the pores are filled with interstitial matter (in the raw hide) or with tannin (in vegetable tanning), on decrease of porosity as the result of fiber swelling (in unchromed hide) etc.

The appearance of long relaxation times in chromed hide is not only of theoretical but also of practical interest, in view of the possibility of accelerating the vegetable tanning stage, which is normally limited by the low rate of penetration of the tanning agent into the hide. It was to be expected that, on periodic deformation of chromed hide in tanning liquors at a frequency corresponding to its long relaxation periods, the alternating filling and emptying of the pores in the course of deformation of the collagen fibers should accelerate the penetration of the tanning liquor into the hide and assist repeated filling of the pores with fresh tanning liquor. We therefore carried out tanning tests in vibrators at frequencies from 25 to 100 cycles/second, and also under periodic compression at a frequency of 1 cycle/second, i.e., at fairly low deformation rates. Specimens of chromed hide were treated directly in the tanning liquor. Tables 1 and 2 and Figure 6 show that this method results in considerable acceleration of the tanning process in comparison with tanning either in a laboratory or in a factory drum. However, for materials which do not show long relaxation times – unchromed hide, chromed gelatin gel – periodic deformation does not accelerate tanning. It is possible that the use of periodic deformation at frequencies close to the long relaxation periods of the material in question may serve as a general method for accelerating the diffusion of liquids into materials of histologically inhomogeneous structure.

SUMMARY

1. The effect of frequencies from 1 to 1000 cycles/minute on the deformation of collagen (hide) in water and various media (2M solutions of KCNS, NaCNS, LiCl, KCl, 5M urea, 25% $(NH_4)_2SO_4$) has been studied at various temperatures and at different stages of the technological process. It is shown that with the exception of the chrome tanning stage (before vegetable tanning) hide has only short relaxation periods and shows behavior similar to that of an elastic protein gel.

2. In chromed hide, which has a histologically inhomogeneous porous structure, a new effect has been discovered; the appearance of long relaxation times in a polymeric material in absence of relative displacements of the molecules.

3. This effect was used to accelerate penetration of tanning agents into collagen by periodic deformation of chromed hide in tanning liquor at a frequency corresponding to the long relaxation times of the material. It is shown that by this method it is possible to accelerate the tanning of chromed hide considerably in comparison with tanning in a factory drum.

This work was performed in scientific cooperation with the Central Research Institute for the Leather Industry. The authors express their deep gratitude to Prof. A.N. Mikhailov and A.L. Zaides, and also to Academician V.A. Kargin and Z.N. Zhurkina for much valuable advice and help in this work.

LITERATURE CITED

[1] A.N. Mikhailov, Chemistry of Tanning Agents and Tanning Processes (State Light Industry Press, 1953), p. 794.

[2] P.I. Zubov, Z.N. Zhurkina and V.A. Kargin, Colloid J. 9, 109, 367 (1947).

[3] P.Ya. Frenkel and A.N. Mikhailov, Collected Papers of the Central Sci. Res. Inst. Leather Ind. No. 17, 50 (1950).

Received September 13, 1956

The A.N. Bakh Institute of Biochemistry
Academy of Sciences, USSR - Moscow

EFFECT OF ATMOSPHERIC TURBULENCE ON THE KINETICS OF AEROSOL COAGULATION

O.M. Todes and A.A. Chekunov

Turbulent pulsations in the atmosphere continuously decrease the particle concentration of an aerosol cloud for two reasons. Small scale pulsations intensify the chaotic motion of the particles and accelerate their coagulation. Large scale pulsations dilute the cloud and increase the volume occupied by the aerosol particles. The first of these factors decreases the particle concentration by a simultaneous increase of the particle size, while the latter does not affect the particle size.

The constant of turbulent coagulation. The influence of mass flow on the coagulation rate was considered even by Smoluchowski [1] and Muller [2]. Coagulation in turbulent flow was studied by Wigand and Frankenberger [3], Tunitsky [4], Teverovsky [5] and Levich [6, 7]. As the result of all these investigations it may be regarded as established that the influence of turbulence on coagulation rate increases very sharply with increasing particle size. In the case of aerosols with particles of the order of 10^{-6} to 10^{-5} cm turbulent diffusion does not play any important part, and the coagulation rate is determined entirely by the laws of Brownian movement. This view is challenged only by Teverovsky. However, Teverovsky's interpretation of his experimental data gives rise to a number of serious objections. Let us consider this important question in greater detail.

It was shown by Smoluchowski [8, 9] that in coagulation resulting from collisions between particles in Brownian movement the rate of change of the particle concentration N with time t is given by the expression

$$-\frac{dN}{dt}=KN^2\,. \tag{1}$$

The coagulation rate constant in this case is $K=\frac{8}{3}\frac{kT}{\eta}$, where η is the viscosity of air; k is the Boltzmann constant; and T is the absolute temperature. Integration of Equation (1) gives the well known law for the linear increase of the particle volume with time

$$\frac{1}{N}=\frac{1}{N_0}+K\cdot t. \tag{2}$$

Equations (1) and (2) remain valid even if the polydispersity of the coagulating sol is taken into account, and only the coagulation rate constant is about 10% greater than the value calculated by the Smoluchowski equation [10, 11].

The theory of turbulent scattering of impurities in the atmosphere has been developed fairly fully by Laikhtman [12] and others. In the case of a linear source perpendicular to the wind direction, the volume of the aerosol cloud increases in direct proportion to the distance x from the source. Hence it may be concluded that 1/N increases linearly with x and that

$$-\frac{dN}{dx}=\frac{1}{\Lambda}N^2, \tag{3}$$

where

$$A = \frac{Q}{\frac{2}{3}\pi^{3/2} S_z \delta r^3 u}. \tag{4}$$

Q is the output of the source per unit length (in g/m · second); r is the particle radius (in m); δ is the density of the particles (in g/m³); S_z is the vertical component of the turbulent diffusion coefficient (in m²/second); u is the wind velocity (in m/second); and N is the particle concentration of the aerosol (1/m³).

When the aerosol cloud is moved by the wind, x = ut and the coagulation rate Equation (1) can be written in the form

$$-\frac{dN}{dx} = \frac{K}{u} N^2. \tag{5}$$

Assuming that coagulation in the atmosphere is wholly determined by turbulent pulsations, Teverovsky replaces Equation (5) by the analogous equation

$$-\frac{dN}{dx} = \frac{K_T}{u} N^2 \tag{6}$$

and introduces, for the turbulent coagulation constant K_T, the relationship

$$K_T = 4\pi r \left(\frac{\lambda'}{l}\right)^4 \left(\frac{Lu}{\nu^2}\right)^3, \tag{7}$$

where L is the turbulence scale; l is the length of the path of mixing; λ' is the average free path of the particles coagulating on collision; D = Lu is the coefficient of turbulent diffusion, and ν is the kinematic viscosity of the air.

If both turbulent coagulation and scattering are present, Teverovsky considers the two factors to be additive, and proposes the following equation for the rate of change of the particle concentration during motion of the cloud:

$$-\frac{dN}{dx} = \left(\frac{K_T}{u} + \frac{1}{A}\right) N^2. \tag{8}$$

Integrating this equation, he finds that

$$\frac{1}{N} = \frac{1}{N_0} + \left(\frac{K_T}{u} + \frac{1}{A}\right) x \tag{9}$$

and compares the resultant theoretical N(x) relationship with his experimental determinations of the particle concentration at various distances from the source. Hence he calculates the value of K_T and compares it with the value calculated from Equation (7), obtaining satisfactory agreement between the theory and the experimental results. However, this agreement is purely apparent. The reason is that in the integration of Equation (8) the turbulent coagulation constant was assumed to retain a constant value. In fact, however, the values of λ' and r contained in it increase with decreasing particle concentration as follows:

$$\lambda' = N^{-1/3} \text{ and } r = \sqrt[3]{\frac{3c}{8\pi\delta}} N^{-1/3}. \tag{10}$$

Consequently

$$K_T = 4\pi \sqrt{\frac{5c}{8\pi\delta} \frac{D^3}{l^4 \gamma^2}} N^{-5/3} = BN^{-5/3}.$$

Substituting (10) into (8), and assuming, with Teverovsky, that $K_T/u \gg 1/A$, we find

$$-\frac{dN}{dx} = \frac{K_T}{u} N^2 = BN^{1/3}. \tag{11}$$

Integration of Equation (11) leads to a totally different expression for the particle concentration as a function of distance

$$N^{2/3} = N_0^{2/3} - \frac{2}{3} \cdot \frac{B}{u} x. \tag{12}$$

It follows from Equation (12) that at a certain distance

$$x_{\max} = \frac{3}{2} \frac{u}{B} N_0^{2/3} \tag{13}$$

coagulation ceases completely and the particle concentration N becomes zero. Substitution of the numerical values given by Teverovsky into Equation (13) gives $x_{\max} \approx 150$ m. This was not the case in reality, and in Teverovsky's experiments the aerosol continued to coagulate at considerably greater distances, and the coagulating particles, when conveyed by wind of $u \approx 3$ m/second to a distance of 1000 m, increased in size from $2 \cdot 10^{-5}$ to $4 \cdot 10^{-5}$ cm. Thus, Teverovsky's experiments do not provide convincing proof of his theory concerning the significant influence of atmospheric turbulence on coagulation, and we may, together with the other authors cited earlier, assume that for particles of the order of 10^{-5} cm, $K_T \ll K$.

Kinetics of the variation of particle concentration. For the derivation of a fundamental equation for the coagulation kinetics of a scattering cloud it is also necessary to examine critically Teverovsky's second assumption concerning the additivity of the coagulation and scattering processes. Consider a certain isolated volume V of the moving cloud and denote the total number of particles in it by n; then the particle concentration N in this volume will be

$$N = n/V. \tag{14}$$

If the cloud does not expand (V = const), N and n will vary synchronously; multiplying both sides of Equation (1) by V, we have:

$$-\frac{dn}{dt} = \frac{K}{V} n^2 . \tag{15}$$

Equation (15) gives the change in the total number of particles in the cloud caused by coagulation, and it remains valid if the volume of the cloud changes with time. On the other hand, Equation (1) ceases to be valid when $V \neq$ const. To find the rate of change of the particle concentration we must differentiate Equation (14)

$$-\frac{dN}{dt} = -\frac{d}{dt}\left(\frac{n}{V}\right) = -\frac{1}{V}\frac{dn}{dt} + \frac{n}{V^2}\frac{dV}{dt}. \tag{16}$$

Substituting the value of dn/dt from Equation (15) into Equation (16), and replacing the time of existence of the cloud t by the distance traversed by it, x = ut, we have

$$-\frac{dN}{dx} = \frac{K}{u} N^2 + \frac{1}{V}\frac{dV}{dx} N. \tag{17}$$

For a linear source the volume V of the cloud increases linearly with the distance x. Since near the source the concentration changes in the cloud should be determined by more complex relationships, we introduce an interpolation formula

$$V = c \cdot (x + x_0), \tag{18}$$

valid only for a certain distance $x > x_0$ from the origin of the cloud. Taking logarithms and differentiating Equation (18) we have

$$\frac{1}{V}\frac{dV}{dx} = \frac{1}{x + x_0}, \tag{19}$$

and the final equation for the process involving coagulation and scattering takes the form

$$-\frac{dN}{dx}=\frac{K}{u}N^2+\frac{N}{x_0+x}. \tag{20}$$

This equation is easily integrated by separation of the variables. The general integral of Equation (20) has the form

$$\frac{1}{N}=\frac{1}{N_0}+\frac{x}{N_0x_0}+\frac{K}{u}(x+x_0)\ln\frac{x+x_0}{x_0}. \tag{21}$$

Analysis of Equation (21). For analysis of the relationship derived in the form of Equation (21) let us consider the limiting cases of small and large distances.

1. For small distances when $x \ll x_0$ it is possible to resolve the logarithm into series and to use only the first term $\ln(1+x/x_0) \approx x/x_0$. Then, with an accuracy up to terms of the second order, we have from Equation (21) that

$$\frac{1}{N}=\frac{1}{N_0}+\left(\frac{K}{u}+\frac{1}{N_0x_0}\right)x. \tag{22}$$

It is thus seen that Teverovsky's assumption of the additive influence of coagulation and scattering on the particle concentration is valid only for very small distances, when the dimensions of the cloud are only slightly greater than the original.

2. At large distances when $x \gg x_0$ we may replace $x + x_0$ by x, and Equation (2) takes the form

$$\frac{1}{N}=\frac{1}{N_0}\cdot\frac{x}{x_0}\left(1+\frac{Kx_0N_0}{u}\cdot\ln\frac{x}{x_0}\right). \tag{23}$$

In this case simple additivity no longer applies and the variation of the particle concentration with distance depends considerably on the dimensionless parameter

$$\frac{KN_0x_0}{u}=\frac{KN_0}{u/x_0}, \tag{24}$$

which represents the ratio of the coagulation rate to the rate of scattering.

When $u = 5$ m/second and $x_0 \approx 50$ m, the rate of scattering $u/x_0 \approx 10^{-1}$ sec^{-1}. The coagulation constant $K = 3\cdot10^{-10}$ cc/second, at a low initial concentration $N_0 = 10^6$ cm^{-3}, the rate of scattering $KN_0 \approx 3\cdot10^{-4}$ sec^{-1} and the ratio of the rates $\frac{KN_0}{u/x_0} \approx \frac{1}{300} \ll 1$. In this case, even when $x/x_0 \approx 1000$ the value of $\ln x/x_0$ does not exceed 7 and coagulation may be neglected with an error of 2%; from Equation (23) we have that

$$N = N_0\cdot x_0/x. \tag{25}$$

Consequently, at low initial concentrations of the aerosol cloud the decrease of particle concentration is mainly determined by scattering of the cloud, and coagulation, even at large distances, produces not more than ~0.5% increase in the average particle size.

At a higher initial aerosol concentration, $N_0 \approx 10^9$ cm^{-3}, the ratio $\frac{KN_0}{u/x_0} \approx 3$ and at large distances the digit 1 in the parenthesis of Equation (23) may be neglected in comparison with the second term. In this case

$$\frac{1}{N}\approx\frac{1}{N_0}\,\frac{x}{x_0}\,\frac{Kx_0N_0}{u}\ln\frac{x}{x_0}=\frac{K}{u}x\cdot\ln\frac{x}{x_0}. \tag{26}$$

Comparison of Equations (26) and (2) shows that even if the rate of scattering is low in comparison with the coagulation rate ($u/x_0 < KN_0$), nevertheless at large distances scattering has a significant influence on the particle concentration N, which decreases $\ln x/x_0$ times as rapidly as in an enclosed space.

Since at large distances the volume of the cloud increases in direct proportion to the distance

$$V \approx V_0 \cdot x/x_0, \tag{27}$$

the total number of particles in the cloud will decrease according to the law

$$n = NV = \frac{uV_0}{Kx_0} \cdot \frac{1}{\ln (x / x_0)} \approx \frac{n_0}{\ln (x / x_0)}, \tag{28}$$

i.e., relatively slowly. Since the average radius of the particles is inversely proportional to the cube root of their number ($\bar{r} \sim n^{-1/3}$), as coagulation proceeds and the cloud expands, $\bar{r}$ will increase still more slowly with the distance, according to the relationship

$$\frac{\bar{r}}{r} = \sqrt[3]{\ln \frac{x}{x_0}}. \tag{29}$$

If, for instance, $x/x_0 = 1000$ and $\ln x/x_0 \approx 7$, the total number of particles n will decrease by a factor of 7, and the particle concentration N will decrease by a factor of 7000, while the average radius of the particles will become only $(7)^{1/3} \approx 2$ times as large. In the case of a point source, scattering of an aerosol cloud in the atmosphere occurs not only in a vertical but also in a horizontal direction at right angles to the wind. The particle concentration then decreases still more rapidly, while the particle size increases more slowly.

SUMMARY

1. In the motion of an aerosol cloud consisting of small particles of the order of 10^{-6} to 10^{-5} cm in size, small scale turbulent pulsations do not significantly increase the coagulation rate constant.

2. Large scale turbulent pulsations scatter and extend the cloud and thereby decrease the absolute rate of coagulation. Therefore, the particle size in an aerosol cloud in the atmosphere increases much more slowly than in an enclosed space.

LITERATURE CITED

[1] M. Smoluchowski, Zeit. Phys. Chem. 92, 129 (1917).

[2] H. Muller, Koll. chem. Beih. 27, 223 (1928).

[3] A. Wigand and E. Frankenberger, Phys. Zeit. 31, 204 (1930).

[4] N.N. Tunitsky, J. Phys. Chem. 20, 1137 (1946).

[5] E.N. Teverovsky, Symposium, New Ideas in the Study of Aerosols (1949), p. 108.

[6] V.G. Levich, Proc. Acad. Sci. USSR 94, No. 5, 809 (1954).

[7] V.G. Levich, Proc. Acad. Sci. USSR 94, No. 6, 1041 (1954).

[8] M. Smoluchowski, Phys. Zeit. 17, 587 (1916).

[9] M. Smoluchowski, Zeit. Phys. Chem. 92, 129 (1917).

[10] O.M. Todes, Coll. Papers Phys. Chem. 138 (1948).

[11] O.M. Todes, Symposium, Problems of Kinetics and Catalysis 7, 137 (1949).

[12] D.L. Laikhtman, Bull. Acad. Sci. USSR, Ser. Geog. and Geophys. 8, No. 1 (1944).

Received July 9, 1956 Leningrad

SETTLING OF AEROSOL PARTICLES ON THE WALLS OF AN ENCLOSED SPACE

I. Todorov and A. Sheludko

The settling of aerosol particles from the volume of a sphere on its walls is theoretically considered in this paper. It is assumed that the aerosol particles approach the walls by diffusion and sedimentation, and that no convection occurs in the gas. The coefficient of adhesion of the particles to the walls is assumed to be less than unity. This value is probably close to unity [1], but it nevertheless depends on the presence of surface-active substances [2], so that there are no grounds for assuming that it is equal to unity.

Our chosen model of a spherical space, with convection ignored, is of practical significance, for example, in calculations relating to dust removal by foam, and also as the limiting case of dust removal by filtration of aerosols through porous filters at a low rate of flow. In the latter instance, with a random arrangement of capillaries in the filter, such a filter will correspond to a certain spherical space the effective radius of which is determined by the capillary diameters. The question of the exact relationship between this effective radius and the actual capillary diameter is not considered here.

The following simplifying assumptions are made in solving the problem.

a) The aerosol concentration is taken to be fairly low, so that the coagulation rate is low in comparison with the rate of settling on the walls. This is a significant case, because if coagulation prevailed the walls would not influence the rate at which the aerosol particles are removed from the space. For a low particle concentration it can be assumed that the behavior of any given particles does not depend on the presence of other particles in the system, and also that the particles always settle on unoccupied regions of the wall surface and the adhesion coefficient does not change with time.

b) The adhesion coefficient is assumed to be independent of particle size.

c) The spherical space is fairly large relative to the free path of the gas molecules, so that it is possible to use the ordinary diffusion equations and to assume that the velocities of the aerosol particles throughout the volume, right up to the walls, have a Maxwellian distribution.

A preliminary qualitative examination of the problem on the assumption that the adhesion coefficient $\alpha = 1$ shows that particles of medium size will be the slowest to settle. Larger particles will mainly settle by sedimentation to the bottom under the force of gravity, and the smaller particles, by diffusion to the walls. The maximum time t_s in which a particle will settle to the bottom is evidently given by the expression $t_s = 2aB/P$, where a is the radius of the sphere; B is the coefficient of friction of the particle; P is its weight. The order of magnitude of the maximum time t_d in which a particle will reach the wall by diffusion can be calculated from its mean square displacement $\overline{\Delta}^2 = 2Dt$, if we assume that $\overline{\Delta}^2 = a^2$, so that $t_d = a^2B/2kT$, as

$$D = kT/B, \tag{1}$$

where k is the Boltzmann constant and T is the absolute temperature. It is obvious that t_s decreases and t_d increases with increasing particle size. Therefore, for the smaller particles the time for settling by diffusion is less than the time for settling by gravitation, while the converse is true for the larger particles. Particles for which $t_s \approx t_d$ will remain longest in the suspended state. It follows from this approximate condition that the weight of the most "stable" aerosol particles will be

$$P_0 = 4kT/a. \tag{2}$$

It is interesting to note that P_0 is determined only by the mean kinetic energy of the particles and the size of the space from which they are removed, and is independent of the viscosity of the gas. The time during which the suspended particles will be removed by the walls is determined by the time for the removal of particles with $P = P_0$, and is given by the expression $t_0 = a^2B_0/2kT$, where B_0 is calculated from P_0 for a given shape of the aerosol particles. Thus, the rate of settling of aerosol particles in an enclosed space depends on the behavior of particles with $P = P_0$. The order of magnitude of these particles can be determined from Equation (2). For example, for $a \geq 10^{-2}$ cm the effective radius of these particles R_0 is comparable to the mean free path of air molecules under atmospheric pressure and at room temperature. Therefore the Cunningham-Millikan equation should be used for B:

$$B = \frac{6\pi\eta R}{1 + A\lambda / R}. \tag{3}$$

The quantitative treatment of the problem is as follows: suppose the aerosol is contained in an enclosed spherical space of radius $\underline{a}$. We use a system of coordinates with the origin in the center of the sphere and the OZ axis directed downward. The particles fall under the action of their own weight at constant velocity $\underline{v}$ according to Stokes' law

$$v = P/B \tag{4}$$

and undergo random thermal motion. The weight of a spherical particle will be

$$P = \frac{4\pi}{3} \cdot R^3 \rho g, \tag{5}$$

where $\rho = \rho_1 - \rho_2$ is the difference between the density of the particle ρ_1 and of the gas ρ_2; $\underline{g}$ is the acceleration due to gravity. Let $U(\mathbf{r}, t) = U(x, y, z, t)$ be the concentration of the aerosol particles. By condition (c) the average number of particles meeting unit surface per second is $\sqrt{kT/2\pi m}\, U(\mathbf{r}, t)$, where $m = 4\pi/3\, R^3\rho$. $U(\mathbf{r}, t)$ for particles of one type satisfies the forced diffusion equation

$$\frac{\partial U}{\partial t} = D\Delta U - v\frac{\partial U}{\partial z}. \tag{6}$$

At the surface of the sphere ($\sqrt{x^2 + y^2 + z^2} = r = a$) the following boundary condition is satisfied

$$-D\frac{\partial U}{\partial n} = \alpha\sqrt{\frac{kT}{2\pi m}}\, U(\mathbf{r}, t).$$

If we put

$$\varkappa = \sqrt{\frac{2\pi m}{kT}}\,\frac{D}{a} = \frac{\sqrt{2\pi m k T}}{Ba}, \tag{7}$$

the boundary condition is written in the form

$$U = -\varkappa\frac{\partial U}{\partial r}. \tag{8}$$

Suppose at instant $t = 0$ the initial concentration distribution is symmetrical with respect to $\underline{z}$

$$U(\mathbf{r}, 0) = U_0(\mathbf{r}) = U_0(r, \theta). \tag{9}$$

We can put $U_0(\mathbf{r}) = c_0$ or

$$U_0(\mathbf{r}) = c_0 e^{k_1 z}, \quad (k_1 > 0). \tag{10}$$

We first solve Equation (6) for the boundary Conditions (8-10), and then show how it can be used for approximate solutions. We solve the problem, in the first approximation, for small values of κ. We determine the settling rate for this approximation and find the weight P_α and the corresponding radius R_α of the most "stable" particles.

a) By the substitution

$$U(\mathbf{r}, t) = V(\mathbf{r}, t)\, e^{-\frac{v^2}{4D}t + \frac{v}{2D}z} \tag{11}$$

Equation (6) becomes

$$\frac{\partial V}{\partial t} = D\Delta V. \tag{6'}$$

In spherical coordinates $\underline{r}$, θ, φ (θ is the angle included between $\underline{r}$ and $\underline{z}$), on the assumption that axial symmetry is maintained ($\partial V/\partial\varphi = 0$),

$$\Delta V = \Delta_{r\theta} V = \frac{1}{r^2}\frac{\partial}{\partial r}\left(r^2 \frac{\partial V}{\partial r}\right) + \frac{1}{r^2 \sin^2\theta}\frac{\partial}{\partial \theta}\left(\sin\theta \frac{\partial V}{\partial \theta}\right).$$

Equation (8) is obtained in the form $\varkappa \frac{\partial V}{\partial r} = -\left(1 + \frac{\varkappa v}{2D}\cos\theta\right)V$

Separation of the variables gives the auxiliary equation

$$\Delta_{r\theta} g_\lambda(r, \theta) + \lambda^2 g_\lambda(r, \theta) = 0; \tag{12}$$

for the boundary condition

$$\varkappa \frac{\partial g_\lambda}{\partial r} = -\left(1 + \frac{\varkappa v}{2D}\cos\theta\right) g_\lambda, \quad (r = a). \tag{13}$$

The solution of Equation (12), corresponding to its proper value of λ, has the form [3]:

$$g_\lambda(r, \theta) = \sum_{n=0}^{\infty} C_n^\lambda S_n(\lambda r)\, P_n(\cos\theta), \tag{14}$$

where $S_n(z) = \sqrt{\frac{\pi}{2}}\,\frac{I_{n+\frac{1}{2}}(z)}{\sqrt{z}}$; $I_k(z)$ is the k-th Bessel function

$$I_{\frac{1}{2}}(z) = \sqrt{\frac{2}{\pi z}}\sin z; \quad I_{\frac{3}{2}}(z) = \sqrt{\frac{2}{\pi z}}\left(\frac{\sin z}{z} - \cos z\right);$$

$$I_{p+1}(z) = \frac{2p}{z} I_p(z) - I_{p-1}(z) \;\; ([3]);$$

$P_n(z)$ are Legendre polynomials.

The Boundary Condition (13) gives:

$$\varkappa \sum_n C_n^\lambda \lambda S_n'(\lambda a)\, P_n(\cos\theta) =$$

$$= -\sum_n C_n^\lambda \left[S_n(\lambda a) + \frac{v\varkappa}{2D} S_n(\lambda a)\cos\theta\right] P_n(\cos\theta).$$

With the aid of the identity $zP_n(z) = \frac{n}{2n-1}P_{n-1}(z) + \frac{n+1}{2n+1}P_{n+1}(z)$ [3] the boundary condition may be written in the form:

$$C_0^\lambda [\varkappa\lambda S_0'(\lambda a) + S_0(\lambda a)] + C_1^\lambda \frac{\varkappa v}{6D} S_1(\lambda a) +$$

$$+ \sum_{n=1}^{\infty} \left\{ C_{n-1}^\lambda \frac{n}{2n-1} \frac{\varkappa v}{2D} S_{n-1}(\lambda a) + C_n^\lambda [\varkappa\lambda S_n'(\lambda a) + S_n(\lambda a)] + \right.$$

$$\left. + C_{n+1}^\lambda \frac{n+1}{2n+3} \frac{\varkappa v}{2D} S_{n+1}(\lambda a) \right\} P_n(\cos\theta).$$

Since this equation is identical with respect to θ, all the coefficients before $P_n(\cos\theta)$ are equal to zero:

$$\left.\begin{array}{c}
[\varkappa\lambda S_0'(\lambda a) + S_0(\lambda a)]\, C_0^\lambda + \frac{1}{3}\frac{\varkappa v}{2D} S_1(\lambda a)\, C_1^\lambda = 0 \\
\frac{\varkappa v}{2D} S_0(\lambda a)\, C_0^\lambda + [\varkappa\lambda S_1'(\lambda a) + S_1(\lambda a)]\, C_1^\lambda + \frac{2}{5}\frac{\varkappa v}{2D} S_2(\lambda a)\, C_2^\lambda = 0 \\
\cdots\cdots\cdots\cdots\cdots\cdots\cdots\cdots\cdots\cdots \\
\frac{n}{2n-1}\frac{\varkappa v}{2D} S_{n-1}(\lambda a)\, C_{n-1}^\lambda + [\varkappa\lambda S_n'(\lambda a) + S_n(\lambda a)]\, C_n^\lambda + \\
+ \frac{n+1}{2n+3}\frac{\varkappa v}{2D} S_{n+1}(\lambda a)\, C_{n+1}^\lambda = 0 \\
\cdots\cdots\cdots\cdots\cdots\cdots\cdots\cdots\cdots\cdots
\end{array}\right\} \qquad (15)$$

The Expression (15) is an infinite linear homogeneous system for unknown coefficients C_n^λ. From the condition that the system (15) has a nontrivial solution we determine the proper values λ_k of the parameter λ. We shall denote the coefficients $C_n^{\lambda k}$ by C_n^k and the proper function, corresponding to the proper values of λ_k, by $g_k(r, \theta)$. It is convenient to represent $g_k(r, \theta)$ by the standardized condition

$$\int_0^\pi \int_0^a g_k^2(r, \theta)\, r^2 \sin\theta \, dr d\theta = 1.$$

The solution of Equation (6') is obtained in the form:

$$V(r, \theta; t) = \sum_k B_k g_k(r, \theta)\, e^{-D\lambda_k^2 t}. \qquad (16)$$

The coefficients B_k are determined by the initial condition. According to Equations (9) and (11), $V(r,\theta;\, 0) =$ $= U_0(r, \theta)\, e^{-\frac{v}{2D} r\cos\theta}$, so that

$$B_k = \int_0^\pi \int_0^a U_0(r, \theta)\, e^{-\frac{v}{2D} r\cos\theta} g_k(r, \theta)\, r^2 \sin\theta \, dr d\theta. \qquad (17)$$

Especially,if $U_0(r, \theta) = C_0 e^{k_1 r\cos\theta}$ (10), i.e., $V(r, \theta;\, 0) = C_0 e^{k_2 r\cos\theta}$, $(k_2 = k_1 - v/2D)$, then according to Equations (14) and (4),

$$B_k = 2C_0 \sum_n C_n^k (i)^n \int_0^a S_n(\lambda_k r)\, S_n(-ik_2 r)\, r^2 dr.$$

From Equation (11) we have for the required concentration:

$$U(r, t) = \sum_k B_k g_k(r, \theta)\, e^{-D\lambda_k^2 t} e^{-\frac{v^2}{4D} t + \frac{v}{2D} r\cos\theta} \qquad (18)$$

b) We break off Equation (14) at the p-th term: $g_k(r, \vartheta) = \sum_{n=0}^{p} C_n^k S_n(\lambda_k r) P_n(\cos\vartheta)$. The boundary condition is then obtained in the form:

$$
\begin{gathered}
[\varkappa\lambda_k S_0'(\lambda_k a) + S_0(\lambda_k a)]\, C_0^k + \frac{1}{3}\frac{\varkappa v}{2D} S_1(\lambda_k a)\, C_1^k = 0 \\
\frac{\varkappa v}{2D} S_0(\lambda_k a)\, C_0^k + [\varkappa\lambda_k S_1'(\lambda_k a) + S_1(\lambda_k a)]\, C_1^k + \frac{2}{5}\frac{\varkappa v}{2D} S_2(\lambda_k a)\, C_2^k = 0 \\
\cdots\cdots\cdots\cdots\cdots\cdots\cdots\cdots\cdots\cdots \\
\frac{p}{2p-1}\frac{\varkappa v}{2D} S_{p-1}(\lambda_k a)\, C_{p-1}^k + [\varkappa\lambda_k S_p'(\lambda_k a) + S_p(\lambda_k a)]\, C_p^k = 0
\end{gathered}
$$

the term $\frac{p+1}{2p+1}\frac{\varkappa v}{2D} S_p(\lambda_k a) P_{p+1}(\cos\vartheta) C_p^k$ is neglected .

Cancellation of the coefficient determinant is necessary, and it is sufficient that this system of p + 1 equations with p + 1 unknowns C_n^k should have a nontrivial solution:

$$
\begin{vmatrix}
\varkappa\lambda_k S'_0(\lambda_k a) + S_0(\lambda_k a) & \frac{1}{3}\frac{\varkappa v}{2D} S_1(\lambda_k a) & 0 & \ldots\ 0 \\
\frac{\varkappa v}{2D} S_0(\lambda_k a) & \varkappa\lambda_k S_1'(\lambda_k a) + S_1(\lambda_k a) & \frac{2}{5}\frac{\varkappa v}{2D} S_1(\lambda_k a) & \ldots\ 0 \\
\cdots & \cdots & \cdots & \cdots \\
0 & 0\ \ldots & \frac{p}{2p-1}\frac{\varkappa v}{2D} S_{p-1}(\lambda_k a) & \varkappa\lambda_k S_p'(\lambda_k a) + S_p(\lambda_k a)
\end{vmatrix} = 0 \tag{19}
$$

The approximation made gives reason to assume that from the system of Equations (19) it is possible to determine the first p + 1 proper values (in order of increasing modulus) and consequently expansion of Equation (18) can be appropriately stopped at the (p + 1)-th term.

c) In order to find an expression for the aerosol concentration which is more convenient for calculations, we make the simplifying assumption

$$\varkappa \ll a, \tag{20}$$

which, as will be shown, is justified for the cases with which we are concerned.

We solve the problem in the first approximation, taking the first terms from the expansion of Equations (14) and (18). If we limit ourselves to accuracy of the first order with respect to κ, then the proper values of λ_k are determined from the System (19) as the roots of the equations $\kappa\lambda_k S_n'(\lambda_k a) + S_n(\lambda_k a) = 0$ [the Determinant (19) tends to zero together with κ^2 if at least one of the terms along the main diagonal cancels].

Suppose, for first orientation that $\kappa = 0$. The smallest positive root of the equations $S_n(\lambda a) = 0$, $n = 0, 1, 2 \ldots$ will be $\lambda_1 = \pi/a$ (root of the equation $S_0(\lambda'_1 a) \equiv \sin\lambda_1 a/\lambda_1 a = 0$ [4]). In the general case the least proper value is determined from the equation $\kappa\lambda_1 S_0(\lambda_1 a) + S_0(\lambda_1 a) = 0$, or

$$\frac{\varkappa}{a} = \frac{\sin\lambda_1 a}{\sin\lambda_1 a - \lambda_1 a\cos\lambda_1 a}. \tag{21}$$

Since according to the Assumption (20), κ/a is small, $\lambda_1 a$ is close to π. ($\lambda_1 a < \pi$). Expansion of $\lambda_1 a$ by powers of κ/a gives

$$\lambda_1 a = \pi - \pi\frac{\varkappa}{a} + \frac{\pi^3}{3}\frac{\varkappa^3}{a^3} + \ldots$$

We confine ourselves to terms of the first degree with respect to κ/a, as terms of higher degrees have already been omitted (19); this gives:

$$\lambda_1 \approx \frac{\pi}{a}\left(1 - \frac{\varkappa}{a}\right). \tag{22}$$

From Equations (14), (17) and (18) we have in the first approximation

$$U(r, t) = c_0 \frac{\sin \lambda_1 r}{\lambda_1 r} e^{\frac{v}{2D} r \cos 0} e^{-\left(\frac{v^2}{4D} + D\lambda_1^2\right) t}, \tag{23}$$

where c_0 is a measure of the initial concentration of the aerosol particles. It is seen from Equation (23) that in the first approximation the concentration distribution at time t does not depend on the exact form of the initial Distribution (9). Equation (23) is the exact solution of the problem for the initial condition $U(r, 0) = = c_0 \frac{\sin \lambda_1 r}{\lambda_1 r} e^{\frac{v}{2D} r \cos 0}$, which corresponds to an axial symmetry of distribution of the aerosol with the center of gravity displaced downward along the OZ axis. The fact that even this approximation has a physical basis and is nontrivial is evidence that the general form of solution is acceptable. The subsequent calculations are based on Equation (23).

d) According to Equation (23), the value

$$K = \frac{v^2}{4D} + D\lambda_1^2 \tag{24}$$

can be regarded as a measure of the settling rate. By means of Equations (1, 3, 4, 5, 7 and 22) it is possible to express this rate as a function of the radius R of the aerosol particles and of the parameters T, a, ρ and η. Replacing v, D and λ_1 by the quantities equal to them as given by these relationships, we have

$$K = \frac{\pi k T}{6\eta a}\left[\left(\frac{2\rho g a}{3kT}\right)^2 (R^5 + A\lambda R^4) + \right.$$
$$\left. + \left(\frac{1}{R} + \frac{A\lambda}{R^2}\right)\left(1 - \frac{2\sqrt{R}}{3\eta a \alpha}\sqrt{\frac{2kT\rho}{3}}\left(1 + \frac{A\lambda}{R}\right) + \frac{2kT\rho}{27\eta^2 a^2 \alpha^2}\left(1 + \frac{A\lambda}{R}\right)^2\right)\right],$$

where $K \to \infty$ when $R \to 0$ or $R \to \infty$, so that for a certain radius $R_\alpha > 0$ we have maximum stability. To find R_α, we first assume as an approximation that $\kappa = 0$. When $\alpha = 1$, κ is very small, as will be shown later. Then $K = \frac{\pi k T}{6\eta a^2}\left[\left(\frac{2\rho g a}{3kT}\right)^2 (R^5 + A\lambda R^4) + \frac{1}{R} + \frac{A\lambda}{R^2}\right]$. Put

$$\mu = \frac{2\rho g a}{3kT}. \tag{25}$$

After simple transformations of the equation $\partial K/\partial R = 0$ we have

$$5\mu^2 R^7 + 4\mu^2 A\lambda R^6 - R - 2A\lambda = 0. \tag{26}$$

Introducing also the shortened forms

$$f = (\sqrt{5}\cdot\mu)^{\frac{1}{3}} R \tag{27}$$

and

$$\tau = \frac{2}{5} A\lambda (\sqrt{5}\mu)^{\frac{1}{3}}, \tag{28}$$

we obtain Equation (26) in the form $\tau = \frac{f^6 - 1}{5 - f^6} f$. The analytical expression for $f(\tau)$ will be

$$f(\tau) = \sqrt[6]{\frac{1+5\tau}{1+\tau}}\,(1 - g(\tau)), \tag{29}$$

where, approximately (we make use of the fact that $g(\tau)$ is small)

$$g(\tau) = \tau \frac{1 - \sqrt[6]{\dfrac{1+\tau}{1+5\tau}}}{{}^{3}/_{2} + 10\,\tau + {}^{15}/_{2}\,\tau^2}\,. \tag{30}$$

The function $f(\tau)$ increases and $f(0) = 1$; $\lim f(\tau) = \sqrt[6]{5} = 1{,}308..$ Detailed investigation, omitted here, shows that Equations (29) and (30) are exact. The correction for $g(\tau) < 1/10$.

Finally, for the radius of the most "stable" particles we have, according to Equation (27)

$$R_0 = \left(\frac{3}{2\sqrt{5}}\,\frac{kT}{\rho g a}\right)^{\frac{1}{3}} \left(\frac{1+5\tau}{1+\tau}\right)^{\frac{1}{6}} [1 - g(\tau)] \tag{31}$$

where τ is given by Equation (28). The weight of these particles will be

$$P_0 = \frac{4\pi}{3} R_0^3 \rho g = 2{,}81 \sqrt{\frac{1+5\tau}{1+\tau}}\,[1 - 3g(\tau) + 3g^2(\tau)]\,\frac{kT}{a}\,. \tag{32}$$

The coefficient of kT/a depends little on T or a. In fact, $\tau \sim (a/T)^{1/3}$ while $f^3(\tau)$ increases very slowly with τ: for $0 < \tau < 2$; $1 < f^3(\tau) < 1.81$.

Let us now consider the more general case when $\kappa \neq 0$, but small. The condition for the minimum rate of settling is obtained in the form

$$(5\mu^2 R^7 + 4\mu^2 A\lambda R^6 - R - 2A\lambda) + \frac{\varepsilon}{a\sqrt{R}}\,(R^2 + 6A\lambda R + 5A^2\lambda^2) = 0, \tag{33}$$

where

$$\varepsilon = \sqrt{\frac{2kT}{3}\rho}\,\frac{1}{3\eta a}\,. \tag{34}$$

The term in the first set of parentheses coincides with the left side of Equation (26), while the second term represents a small correction, as κ/a is small relative to $\epsilon\sqrt{R}/\alpha$. We can therefore put for the radius of the most "stable" particles

$$R_\alpha = R_0(1 - \xi), \tag{35}$$

where R_0 is given by Equation (31) and ξ is a small correction. For approximate calculations we neglect the terms ξ^2 and $\xi\epsilon$, which corresponds to the approximations in calculation of λ_1; from the Condition (33) we have

$$-7R_0 f^6(\tau)\,\xi - \frac{24}{5} A\lambda f^6(\tau)\,\xi + R_0\xi + \frac{\varepsilon\sqrt{R_0}}{\alpha}\left(R_0 + 6A\lambda + 5\frac{A^2\lambda^2}{R_0}\right) = 0,$$

i.e.,

$$\xi = \frac{\varepsilon\sqrt{R_0}}{\alpha}\;\frac{R_0 + 6A\lambda + 5A^2\dfrac{\lambda^2}{R_0}}{\left(7P_0 + \dfrac{24}{5} A\lambda\right) f^6(\tau) - R_0}\,. \tag{36}$$

Finally

$$R_\alpha = R_0(1-\xi) = R_0\left(1 - \frac{\sqrt{2kT\rho}}{3\sqrt{3}\eta a}\,\frac{R_0 + 6A\lambda + 5\frac{A^2\lambda^2}{R_0}}{\left(7R_0 + \frac{24}{5}A\lambda\right)f^6(\tau) - R_0}\,\frac{1}{\alpha}\right) \tag{37}$$

and correspondingly:

$$P_\alpha = P_0(1-\xi)^3 \approx P_0(1-3\xi) \equiv P_0\left(1 - \frac{\zeta}{\alpha}\right), \tag{38}$$

where P_0 is given by (32) and ξ by (36);

$$\zeta = 3\frac{R_0 + 6A\lambda + 5\frac{A^2\lambda^2}{R_0}}{\left(7R_0 + \frac{24}{5}A\lambda\right)f^6(\lambda) - R_0}\sqrt{R_0}\varepsilon \tag{39}$$

together with $\sqrt{R_0\epsilon}$, a small quantity.

Let us consider the concrete example of the settling of quartz dust ($\rho = \rho_1 - \rho_2 = 3$ g/cm^2) in air at atmospheric pressure and room temperature [$\lambda = 10^{-5}$ cm; $A = 0.9$; $\eta = 1.816 \cdot 10^{-4}$ (g cm/second)]. Let $a =$ $= 2 \cdot 10^{-2}$ cm; then we have

$$(\sqrt{5}\mu)^{\frac{1}{3}} = \left(2.236\,\frac{2}{3}\,\frac{\rho g a}{kT}\right)^{\frac{1}{3}} = 1.27 \cdot 10^5 \text{ cm}^{-1}$$

$$\tau = \frac{2}{5}A\lambda(\sqrt{5}\mu)^{\frac{1}{3}} = 0{,}457,$$

$$f(\tau) = \left(\frac{1+5\tau}{1+\tau}\right)^{\frac{1}{6}}\left(1 - \tau\frac{1 - \left(\frac{1+\tau}{1+5\tau}\right)^{\frac{1}{6}}}{{}^3/_2 + 10\tau + {}^{15}/_2\,\tau^2}\right) = 1{,}136,$$

$$R_0 = \frac{f(\tau)}{(\sqrt{5}\mu)^{\frac{1}{3}}} = 0.894 \cdot 10^{-5} \text{ cm}$$

$$P_0 = \frac{4}{3}\pi R_0^3\rho g = 8.8 \cdot 10^{-12} \text{ dyne}$$

and, approximately, at a and T close to those used

$$P_0 = \frac{2\pi}{\sqrt{5}}f^3(\tau)\frac{kT}{a} \approx 4{,}12\,\frac{kT}{a}$$

(this is in almost complete agreement with Equation (2) derived by a semiquantitative method).

When $\alpha = 1$ $\varkappa_0 = \frac{1}{3\eta}\sqrt{\frac{2kT\rho}{3}}\left(\sqrt{R_0} + A\frac{\lambda}{\sqrt{R_0}}\right) = 3{,}23 \cdot 10^{-6}$ cm.

Therefore, in this instance Assumption (20) is justified, as $\varkappa_0/a = 1.615 \cdot 10^{-4}$ is small.

$$\sqrt{R_0}\cdot\varepsilon = \frac{\varkappa_0}{a}\,\frac{1}{1 + A\frac{\lambda}{R_0}} = 0{,}805 \cdot 10^{-4} \text{ and } \alpha\xi = \frac{\zeta}{3} = 4{,}02 \cdot 10^{-5}.$$

The coefficients of $1/\alpha$ in (37) and (38) are small, so that this is not a convenient way of calculating the adhesion coefficient α.

The fact that R_α or P_α depend little on α, at approximately $\alpha > 0.1$, justifies the approximations Ia and Ib. Our chosen value for a corresponds in order of magnitude to the dimensions of the capillaries in the lungs. Consequently, when air containing quartz dust is breathed in, particles $2 \cdot 10^{-5}$ cm in diameter are retained least effectively in the lung capillaries and penetrate into the depth of the lung. It is interesting to note that according to some reports particles of this size are met most frequently in the lungs of silicosis victims. This result confirms the views of Vigdorchik [5] on the absorption of dust by the lungs. It should also be pointed out that the formulas derived by Buchwald [6] are readily obtained from our Equation (18) if sedimentation is ignored ($v = 0$) and the concentration at the walls is assumed to be vanishingly small ($\kappa = 0$).

SUMMARY

1. It is shown theoretically that the settling rate of aerosol particles on the walls of an enclosed space containing them depends on the particle size and reaches a minimum value for an optimum particle size. A relationship has been derived between the optimum particle size and the temperature, radius of the enclosed spherical space, adhesion coefficient, and viscosity of the gas.

2. It is proved that the distribution of settling rates according to particle size depends little on the adhesion coefficient if this coefficient is not too small.

3. It is proved that the weight of the particles settling at the lowest rate can be calculated fairly accurately by the approximate equation $P_0 = 4kT/a$, where a is the radius of the spherical space.

In conclusion, we wish to thank Professor Khr.Ya. Khristov for much valuable advice.

LITERATURE CITED

[1] N.A. Fuks, Mechanics of Aerosols (Moscow, 1955), p. 175.

[2] P.A. Rebinder, N.N. Serb-Serbina and S.A. Kordyukova, The Struggle Against Silicosis, Collected papers, Vol. 1 (Moscow, 1953), p. 57.

[3] R. Courant and D. Hilbert, Methods of Mathematical Physics, Vol. 1 (Moscow-Leningrad, 1951), pp. 80, 269, 413.[Russian translation.]

[4] V.I. Smirnov, Course of Higher Mathematics, Vol. 3, Pt. 2 (Moscow-Leningrad, 1951), pp. 527, 563.

[5] E. Vigdorchik, Retention of Aerosols in Respiration (Leningrad Sci. Res. Inst. Labor Organization and Industrial Safety, Leningrad 1948).

[6] E. Buchwald, Ann. Phys. 66, 1 (1921).

Received October 3, 1956

Institute of Physical Chemistry
Sofia State University

APPLICATION OF THE METHOD OF APPROXIMATIONS TO CALCULATIONS OF FLOW OF DISPERSE SYSTEMS

N.V. Tyabin and G.V. Vinogradov

The advantage of the method of approximations for technical calculations of flow processes in disperse systems lies in the fact that it is not necessary to know the law of flow in the form of a continuous relationship between the true velocity gradient (D) and the shearing stress (τ), $D = \varphi(\tau)$, and it is possible to perform calculations on the basis of viscosimetric data obtained by direct experiments.

In the previous communication [1] examples were given of the approximation of flow curves for solid greases, with variations of the velocity gradient over a range of five tenth-powers, in the form of three or four straight lines corresponding to Shvedov-Bingham equations. However, the number of Shvedov-Bingham equations approximating to the flow curve for a plastic disperse system can be decreased considerably if the actual flow conditions of the disperse system are taken into account. It is first necessary to select the scale of the graph used for approximation of the flow curves. The choice of the scale should be based on the values of the maximum velocity gradients and tangential stresses in the flow zone. We shall consider, as examples, approximation of the flow curves for a plastic grease and bitumen.

Plastic greases are widely used for lubrication of sliding bearings, when the flow velocity gradients reach high values (10^5-10^6 $\sec^{-1}$). A consecutive approximation to the flow equation for solidol grease at 20° [2]: $\tau_R = 3500 + 6\overline{D} + 2800\,\overline{D}^{1/3}$ was given in the previous communication [1].

If the graphical scale chosen for the approximation corresponds to a velocity gradient of $\sim 10^5$ $\sec^{-1}$, and the experimental error is assumed to be 5%, it is seen (Figure 1, where the error zone is indicated by broken lines) that the flow curve for solidol in the zone of high velocity gradients can be fairly satisfactorily approximated by one Shvedov-Bingham equation:

$$\tau = \pm\,\theta + \eta D, \tag{1}$$

where $\theta = 7.9 \cdot 10^4$ dynes/cm^2; $\eta = 5.2$ poises.

A plastic grease in the low velocity gradient region, where the nonlinear relationship $D = \varphi(\tau)$ is most pronounced, can for simplicity be regarded as a "continuous" solid body, while the flow of the grease in the bearing should be calculated on the basis of the Shvedov-Bingham Equation (1). There is no doubt that relative flow will occur in the continuous "solid" body region, but at a velocity 3-4 orders of magnitude lower than in the main mass of the grease, and it may be neglected. Thus, for describing the "deformation" process in the zone in which the tangential stress is less than the limiting (yield) stress which follows from the Shvedov-Bingham equation, it is not admissible to apply formally the theory of elasticity, as flow at very low velocity gradients occurs in this zone.

As a second example of the method of approximations, this time for a zone of low velocity gradients, let us consider the approximation of the curve for the flow of bitumen [3]. Bitumens and materials based on them are used for construction of hydroinsulation covers and roofs. The durability of such a covering depends on the ability of a thin layer of bitumen (2-3 mm) to resist flow down inclined surfaces when the air temperature rises [4]. To select the graphical scale for approximation of the flow curves for bitumen, we determine the maximum tangential stress at the roof surface:

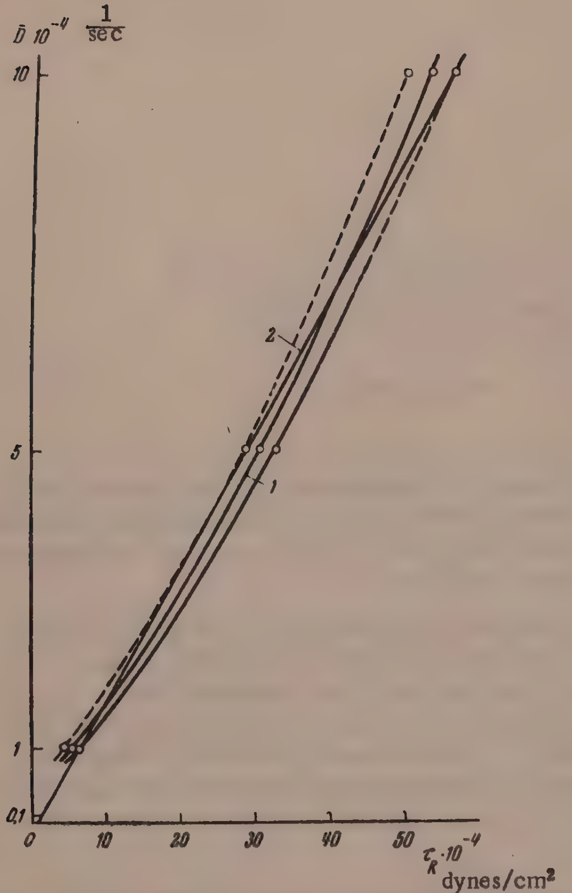

Fig. 1. Graph for the approximation of the flow behavior of solidol at 20° in the high velocity gradient region: 1) flow curve for solidol; 2) approximating straight line.

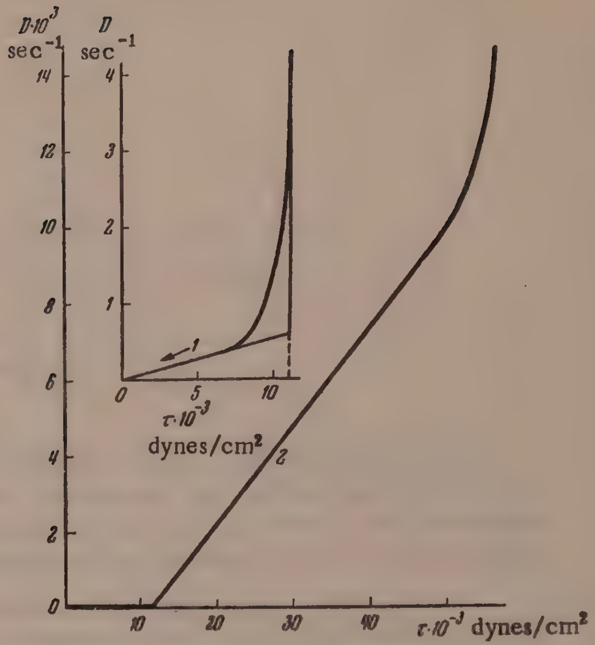

Fig. 2. Approximation curves for experimental data on the flow of bitumen III at 20° in the region of low tangential shearing stresses: 1) Newtonian straight line; 2) Shvedov-Bingham line.

$$\tau_{\max} = \gamma h (\sin \alpha)_{\max}, \tag{2}$$

where γ is the density of the bitumen; h is the thickness of the layer; α is the slope of the surface. Assuming $\gamma = 1000$ kg/m³ and $\alpha = 90°$, we find $\tau_{\max} \sim 10^3 \cdot h$ dynes/cm². Thus, a thin layer of bitumen on the surface of a roof is subjected to maximum tangential stresses of $\sim 10^2$-10^3 dynes/cm².

Approximation of the flow curve for bitumen at 20° [3, 5], shown on two scales in Figure 2, leads to two equations:

$$\tau = \eta_0 D\, (\tau < \tau_{01}) \text{and} = \theta_1 + \eta_1 D \ (\tau_{01} \leqslant \tau \leqslant \tau_{02}), \tag{3}$$

where $\eta_0 = 1.25 \cdot 10^{11}$ poises; $\tau_{01} = 1.1 \cdot 10^4$ dynes/cm²; $\theta_1 = 1.1 \cdot 10^4$ dynes/cm²; $\eta_1 = 3.9 \cdot 10^6$ poises; $\tau_{02} = 5 \cdot 10^4$ dynes/cm². It is seen that η_0 is greater than η_1 by five tenth-powers, and therefore in layers in which $\tau < \tau_{01}$ the bitumen will move as a continuous body, and its flow in the zone of small tangential stresses should be calculated by Equation (3).

As examples of application of the method of approximation of flow curves for plastic disperse systems, let us consider the flow in the gap between two coaxial cylinders and along an inclined plane under the force of gravity.

Let a plastic disperse system, the flow curve of which is approximated by n Shvedov-Bingham equations, flow in the gap between two coaxial cylinders as the result of rotation of the inner cylinder of radius R_1 at angular velocity ω_0. The tangential stress in the medium will be $\tau = M/2\pi h r^2$, where M is the torque; h is the height of the cylinders; r is the current radius of the cylindrical coordinate system (Figure 3). In the gap n coaxial layers are formed, and the radii of the surfaces of the limiting and boundary shearing stresses are given by the expressions

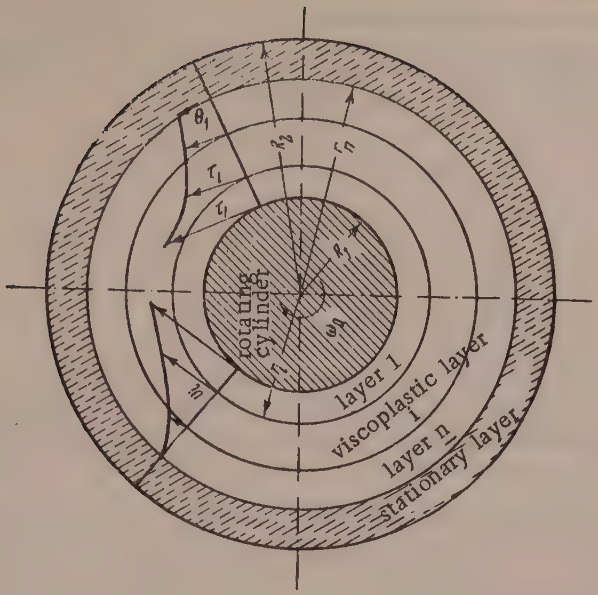

Fig. 3. Flow of a plastic disperse system in the gap between two coaxial cylinders.

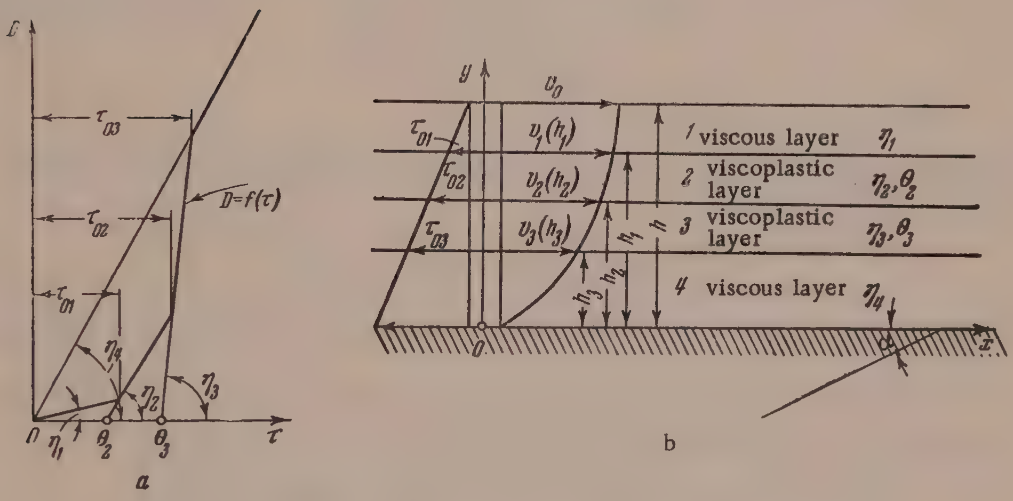

a

b

Fig. 4. Flow of a non-Newtonian liquid along an inclined surface.

$$r_i = \left(\frac{M}{2\pi h \tau_{0i}}\right)^{1/2}; \tag{4}$$

$$r_n = \left(\frac{M}{2\pi h \theta_i}\right)^{1/2}; \tag{5}$$

$$\tau_{0i} = \frac{\theta_i \eta_{i+1} - \theta_{i+1}\eta_i}{\eta_{i+1} - \eta_i}, \quad (i = 1, \ldots, n-1), \tag{6}$$

where τ_{0i} are the boundary shearing stresses; θ_1, θ_i, η_i are the limiting shearing stresses and plastic viscosities according to the approximate Shvedov-Bingham relationships.

As is known, the distributions of velocities and tangential stresses in a viscoplastic medium flowing in the space between coaxial cylinders are given by the expressions

$$v_i = \frac{\theta_i}{\eta_i} r \ln r + A r - \frac{B_i}{2r}; \tag{7}$$

$$\tau_i = -\theta_i + \eta_i\left(\frac{\partial v_i}{\partial r} - \frac{v_i}{r}\right) = \eta_i \frac{B_i}{r^2}, \quad (i = 1, \dots, n), \tag{8}$$

where A_i and B_i are integration constants, found from the boundary conditions. The medium adheres to the surface of the rotating cylinder; then $v_1(R_1) = \omega_0 R_1$, from the condition of continuity of velocities and tangential stresses at the boundary stress surfaces – $v_i(r_i) = v_{i+1}(r)$, $\tau_i(r_i) = \tau_{i+1}(r_i)$, where $(i = 1, \dots, n-1)$, $\tau_n(r_n = = -\theta_1$.

Let us assume that the shear does not extend to the surface of the outer cylinder; then at the limiting shearing stress surface $v_n(r_n) = 0$. On the basis of these boundary conditions we obtain, from Equations (7) and (8), a system of equations with 3n unknowns A_i, B_i, r_i. Solving these we find, in particular, that

$$B_1 = -\frac{2\omega_0 + 2\sum\limits_{i=1}^{i=n} \frac{\theta_i}{\eta_i} \ln \frac{r_i}{r_{i-1}}}{\sum\limits_{i=1}^{i=n} \frac{\eta_1}{\eta_i}\left(\frac{1}{r_{i-1}^2} - \frac{1}{r_i^2}\right)}, \tag{9}$$

where it should be assumed that at $i = 1$, $r_{i-1} = R_1$. The torque which must be applied in order to rotate the cylinder at angular velocity ω_0 is given by

$$v_i = \frac{\theta_i}{\eta_i} r \ln r + A r - \frac{B_i}{2r}; \tag{10}$$

From Equation (8) at $i = 1$, $\tau_1 = \eta_1 B_1 / R_1^2$, and then, substituting the value of B_1 from Equation (9), we find

$$\tau_i = -\theta_i + \eta_i\left(\frac{\partial v_i}{\partial r} - \frac{v_i}{r}\right) = \eta_i \frac{B_i}{r^2}, \quad (i = 1, \dots, n), \quad (8) \tag{11}$$

In calculations by this equation it should be taken, in accordance with Equation (4), that

$$r_i^2 / r_{i-1}^2 = \tau_{0i-1} / \tau_{0i},$$

while

$$\tau_{0i\,-1} = M / 2\pi h R_1^2.$$

If the shear extends to the outer cylinder, then at $i = n$, $r_n = R_2$. When $i = 1$, then the medium flowing in the gap between the cylinders obeys a single Shvedov-Bingham equation, Equation (11) gives the known Reiner-Rivlin equation.

Bitumens at temperatures between 40 and 140° are typical non-Newtonian liquids [4, 5], the flow curves for which can be approximated by two Newton equations and two Shvedov-Bingham equations (Figure 4a) [6].

For calculations of the thermostability of bitumens and materials based on them, let us consider the flow of a non-Newtonian liquid along an inclined plane under the action of gravity. In this instance the stress will be greatest at the inclined surface and the whole stream will separate into two viscous and two viscoplastic layers. The coordinate system and notation are given in Figure 4b.

The laws of velocity and tangential stress distributions, both in the viscous and the viscoplastic layers, are given by the expressions:

$$v_i(y) = -\frac{\gamma}{2\eta_i}\sin\alpha y^2 + C_i'y + C_2''; \tag{12}$$

$$\tau_i(y) = -\theta_i + \eta_i\frac{\partial v_i}{\partial y} = -\theta_i - \gamma\sin\alpha y + C_i'\eta_i, \tag{13}$$

where $(i = 1, \ldots, 4)$, $\theta_1 = \theta_4 = 0$.

The integration constants and the unknown coordinates of the boundary shearing stream surfaces h_i are found from the boundary conditions. The liquid adheres to the inclined surface: $v_4(0) = 0$; from the condition of continuity of velocities and tangential stresses we have:

$$v_i(h_i) = v_{i+1}(h_i), \quad \tau_1(h) = 0;$$
$$\tau_i(h_i) = \tau_{i+1}(h_i) = -\tau_{0i}, \quad (i = 1, 2, 3),$$

where τ_{0i} are the boundary shearing stresses determined by Equation (6), if it is assumed that $\theta_1 = \theta_4 = 0$. On the basis of the boundary conditions, we obtain, from Equations (12) and (13), eleven equations with eleven unknowns; solving these, we have:

$$h_i = h - \frac{\tau_{0i}}{\gamma\sin\alpha}, \quad (i = 1, 2, 3) \tag{14}$$

$$C_i' = \frac{\gamma\sin\alpha}{\eta_i}h - \frac{\theta_i}{\eta_i}, \quad (i = 1, 2, 3, 4); \ (\theta_1 = \theta_4 = 0) \tag{15}$$

$$C_i'' = \frac{\gamma\sin\alpha}{2}\sum_1^3 h_i^2\left(\frac{1}{\eta_i} - \frac{1}{\eta_{i+1}}\right) + \sum_i^3 (C_{i+1} - C_i')h_i, \quad (i = 1, 2, 3) \tag{16}$$

$$C_4'' = 0. \tag{17}$$

The rate of flow at the surface of the layer is found from Equations (12) and (14-17) when i = 1

$$v_0 = \frac{\gamma\sin\alpha}{2}\left[\frac{1}{\eta_1}h^2 + \left(\frac{1}{\eta_1} - \frac{1}{\eta_2}\right)h_1^2 + \left(\frac{1}{\eta_2} - \frac{1}{\eta_3}\right)h_2^2 + \left(\frac{1}{\eta_3} - \frac{1}{\eta_4}\right)h_3^2\right] +$$
$$+ \gamma\sin\alpha h\left[\left(\frac{1}{\eta_2} - \frac{1}{\eta_1}\right)h_1 + \left(\frac{1}{\eta_3} - \frac{1}{\eta_2}\right)h_2 + \left(\frac{1}{\eta_4} - \frac{1}{\eta_3}\right)h_3\right] -$$
$$-\frac{\theta_2}{\eta_2}h_1 - \left(\frac{\theta_3}{\eta_3} - \frac{\theta_2}{\eta_2}\right)h_2 - \frac{\theta_3}{\eta_3}h_3,$$

where $h_1 = h - \frac{\tau_{01}}{\gamma\sin\alpha}$; $h_2 = h - \frac{\tau_{02}}{\gamma\sin\alpha}$; $h_3 = h - \frac{\tau_{03}}{\gamma\sin\alpha}$.

This expression can be used to calculate the flow rate at the surface of the bitumen layer, i.e., to evaluate its thermostability in relation to γ, α, $\underline{h}$ and the six rheological constants η_1, η_2, θ_2, η_3, θ_3, η_4 (Figure 4b).

It must be noted in conclusion that the flow curves can be approximated not only in the form of Shvedov-Bingham equations in the usual coordinate system, but also in the form of exponential functions $D = k\tau^N$ in logarithmic coordinates, when these functions are represented by linear intercepts.

SUMMARY

1. The flow of plastic greases in sliding bearings, and of bitumens along inclined planes, has been used to demonstrate the necessity of evaluating the actual values of the maximum tangential stresses and velocity

gradients in approximating the flow curves for disperse systems.

2. An expression has been derived for the torque as a function of the angular velocity of rotation in the flow of a plastic disperse system in an annular gap between coaxial cylinders, when the flow curve can be approximated by n Shvedov-Bingham equations.

3. The flow of a layer of non-Newtonian liquid along an inclined surface has been considered. The laws governing the flow velocity distributions in the layers and on the surface of a non-Newtonian liquid have been determined; the flow curves can be approximated by two Newton equations and two Shvedov-Bingham equations.

LITERATURE CITED

[1] N.V. Tyabin and G.V. Vinogradov, Colloid J. 19, 352 (1957) (T.p. 353)*

[2] V.P. Pavlov, Candidate's Dissertation (Moscow, 1948).

[3] N.V. Mikhailov, Doctorate Dissertation (Moscow, 1955).

[4] N.V. Mikhailov, Roof and Hydroinsulation Coverings (Machinery Constr. Press, 1950).

[5] S.Ya. Shalyt, Candidate's Dissertation (Moscow, 1955).

[6] N.V. Tyabin, J. Tech. Phys. 26, 1994 (1956).

Received June 19, 1956

Institute of Petroleum
Academy of Sciences, USSR - Moscow

---

* T. p. = C. B. Translation pagination.

EFFECT OF ELECTROLYTES ON THE STRUCTUROMECHANICAL PROPERTIES OF BENTONITE SUSPENSIONS

I.A. Uskov

Despite the large number of rheological studies of structure formation in bentonite suspensions [1], some important questions still remain unsolved. In particular, the mechanism of the action of electrolytes present in the dispersion medium is not clear; the influence of these electrolytes is often attributed to cation exchange effects [2], although there are no convincing grounds for this.

The present paper reports a study of the variations of the structuromechanical properties of aqueous askangel (a bentonite of Caucasian origin) suspensions under the action of various electrolytes. The purified material contained particles $< 50\mu$ in diameter. Most of the insoluble impurities were removed by dialysis through a collodion membrane at 50-70°. The electrical conductivity of a 6.91% suspension was $1 \cdot 10^{-4}$ ohm^{-1} cm^{-1}. To eliminate aging effects, the original 6.91% suspension was kept for 6 months; it was subsequently diluted with water or the appropriate electrolyte solution down to 3.12% concentration.

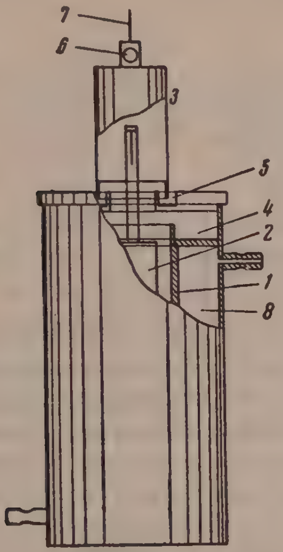

Fig. 1. Diagram of the main part of the instrument used for studying structuromechanical properties: 1) outer cylinder; 2) inner cylinder; 3) load on inner cylinder; 4) annular space for excess liquid displaced by immersion of the inner cylinder; 5) hydraulic seal to prevent evaporation during the experiment; 6) mirror; 7) torsion wire; 8) thermostat liquid.

The structuromechanical properties of the suspensions were studied by means of a coaxial cylinder instrument (Figure 1) of the Shvedov type [3]. Measures were taken to prevent evaporation of the suspension during the experiments and to ensure a constant liquid level in the outer cylinder. The temperature was kept constant by means of a circulating thermostat set to 25°.

The method for obtaining a group of deformation-time curves, developed by Rebinder and his associates [4], requires several hours for each experiment; this restricts its use to systems in which no appreciable changes occur during this time. This method is not applicable in this form to askangel suspensions containing considerable amounts of electrolytes, when syneresis effects hinder the experiment. However, it is possible to shorten the time required for obtaining the groups of deformation curves. Trapeznikov [5] made a detailed study of the effect of a constant load on deformation of adsorption layers of saponin; it follows from his results that the time required to reach a constant deformation rate is shortened tens of times as stresses corresponding to breakdown of the structure are approached. We obtained similar results for bentonite suspensions. It was found experimentally that at stresses close to the strength limit of the structure practically steady flow is established in 1-2 minutes. The approximate strengths of the structure were first determined in the experiments, and the exact values of the structuromechanical constants were then calculated from curves plotted for fresh samples of the suspensions. The time of structural buildup in the suspensions (after filling of the instrument) was 1 hour in all experiments. The average deviations in repeated experiments from the average values of the measured quantities did not exceed 7%.

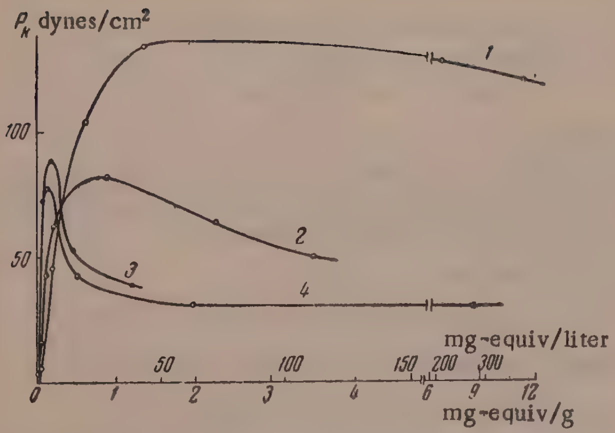

Fig. 2. Variations of the limiting shearing stress (yield value) of a 3.12% askangel suspension with electrolyte concentration: 1) sodium chloride; 2) sodium sulfate; 3) calcium sulfate; 4) calcium chloride.

The effects of electrolytes most commonly met in oil well drilling – sodium and calcium chlorides and sulfates – were studied. It was found by preliminary experiments that the variation of the structuromechanical properties of the suspensions under the influence of added electrolytes continues for a long time. This effect was quantitatively studied for a suspension containing 0.053 mg-equiv sodium chloride per 1 g of bentonite (see table).

Variations of the Structuromechanical Properties of an Askangel Suspension after Addition of Sodium Chloride

Time in hours after addition of electrolyte	E_0 dynes/cm^2	E_τ dynes/cm^2	P_k dynes/cm^2	η_r poises	$\lambda = E_0/E$
0.02	0	0	0	0	0
0.1	1.6	1.5	0	0	0.52
1.0	5.2	5.8	0.7	600	0.47
4.5	15.5	21	2.4	3400	0.42
16.5	30	54	5.8	6050	0.36
25	33	78	6.4	6950	0.30
300	51	146	9.5	9000	0.26
576	55	151	11.5	9800	0.27

It is seen from these results that during the first day the elasticity and viscosity of the system show very large increases. Subsequently, the rate of increase of the structuromechanical characteristics diminishes, but they continue to increase even a month after addition of the electrolyte. The possibility is not excluded that in our experiments partial exchange of the calcium ions sorbed by the bentonite for sodium ions took place, but this exchange could not have been considerable. The amount of NaCl added was 0.053 mg-equiv per 1 g of bentonite containing 0.354 mg-equiv of adsorbed calcium, which was nearly 7 times the total amount of sodium added. If, moreover, it is considered that calcium is adsorbed much more vigorously than sodium [6], it becomes evident that practically no cation exchange occurs in these conditions. The observed changes in the mechanical properties of the suspensions were caused by the coagulating action of the electrolyte present in the dispersion medium, resulting in coagulational structure formation.

The increase of all the structuromechanical constants is accompanied by a decrease of the elasticity of the system, indicating strengthening of the structural bonds between the particles. Not all the bonds between the particles which arise in the course of thixotropic structure formation are broken down when the suspension is shaken. The number of such bonds of higher strength increases with increasing time of electrolyte action.

The influence of the concentration and nature of the electrolytes was studied 46-48 hours after addition of the electrolytes to the askangel suspension. Figure 2 shows the variation of the most important constant, P_k, with salt concentration. The other structuromechanical constants varied in the same way as P_k and are therefore not given. The system was not structurized before addition of the electrolytes. All the electrolytes studied caused structure formation even at very low concentrations. Coagulational structure formation greatly increased with additions of successive amounts of electrolytes.

As the salt concentration increases, P_k increases at first, reaches a maximum, and then decreases. The amounts of added sodium salts in the region of the maximum – 1.4 mg-equiv/g of NaCl and 0.9 mg-equiv/g of Na_2SO_4 – are sufficient for appreciable changes to take place in the composition of the adsorbed cations. However, here also the determining role is played by the coagulating action of the electrolyte, increasing concentration of which may lead to formation of a compact coagulate with lower mechanical characteristics.

The hypothesis that cation exchange plays a decisive role in processes involving the action of nonhydrolyzing electrolytes is entirely unsubstantiated in relation to calcium salts. The development of elasticity on addition of negligibly small amounts (relative to the capacity of the exchange complex) of calcium salts and the extremely rapid increase of P_k with increasing concentration of added electrolytes cannot be attributed to cation exchange.

The proportions of electrolyte concentrations required to produce equal degrees of structure formation in the ascending branches of the curves are in qualitative agreement with the Schulze-Hardy rule. Bentonite particles are negatively charged, and therefore the effects produced by salts depend on their cations. Calcium salts have 3-5 times the coagulational structure formation effect of the corresponding sodium salts. The effects of anions on the structuromechanical properties of bentonite suspensions can be judged by the effects of the different electrolytes studied. The data for calcium salts, for which the difference between the anions is masked by the strong bivalent cation, are not convenient for judging this effect. Sodium salts are more suitable in this respect. Sodium chloride at low concentrations causes less strengthening of the structure than sodium sulfate, but starting with 15 mg-equiv/liter it assists the formation of a stronger structure than that produced by the action of other electrolytes. The concentration corresponding to the strength maximum is considerably higher for sodium chloride than for the corresponding sulfate, so that the sulfate ion can be regarded as the more powerful coagulant.

SUMMARY

1. Electrolytes, even at low concentrations, cause structurization of aqueous askangel suspensions. During the first day after addition of electrolytes to the suspension, the strength, elasticity and viscosity characteristics increase tens of times, Subsequently these characteristics increase less rapidly, but continue to change even after a month.

2. Low concentrations of calcium and sodium chlorides and sulfates produce sharp increases in the structuromechanical constants of askangel suspensions owing to formation of coagulation structures. The electrolyte concentrations required to produce equal degrees of structurization conform to the Schulze-Hardy rule. Sodium and calcium sulfates are more powerful agents of coagulational structure formation than the corresponding chlorides.

The author expresses his deep gratitude to A.V. Dumansky for his guidance, and thanks to F.D. Ovcharenko, I.A. Dumansky and R.V. Voitsekhovsky for discussion of the work and critical comments.

LITERATURE CITED

[1] N.N. Serb-Serbina, In Viscosity of Liquids and Colloidal Solutions, Vol. 1 (1941); N.N. Serb-Serbina and P.A. Rebinder, Colloid J. 9, 381 (1947); H. Braune and J. Richter, Koll.-Z. 113, 20 (1949); N.N. Serb-Serbina and T.M. Polonsky, Proc. Acad. Sci. USSR 96, 103 (1954).

[2] P. Vageler, Cations and Water in Mineral Soils (Agric. Press, 1938); I.V. Popov, Fundamentals of Engineering and Geological Soil Science (State Geol. Press, 1941).

[3] F.N. Shvedov, J. phys. theori et appl. 2, 341 (1889).

[4] E.E. Segalova and P.A. Rebinder, Colloid J. 10, 223 (1948); P.A. Rebinder, In New Methods of Physicochemical Investigations of Surface Phenomena (Izd. AN SSSR, 1950), p. 3.

[5] A.A. Trapeznikov, In New Methods of Physicochemical Investigations of Surface Phenomena (Izd.

AN SSSR, 1950) p. 20; Trans. All-Union Conf. on Colloid Chem. (Acad. Sci. Ukrainian SSR Press, 1952), p. 175.

[6] K.K. Gedroits, The Absorptive Capacity of Soils (Agric. Press, 1933).

Received June 3, 1956

The T.G. Shevchenko State University
Kiev

RELATIONSHIP BETWEEN THE INTRINSIC VISCOSITY AND MOLECULAR WEIGHT OF BUNA S RUBBER*

Chien Jen-Yuan, Ching Wen and Cheng Yung-Shih

The intrinsic viscosity-molecular weight relationship for Buna S rubber has been studied by numerous workers [1-5] (Table 1). However, hitherto it was not taken into account that the fractions used for the viscosity and osmotic pressure determinations might contain branched macromolecules, which would result in a $[\eta] - M$ relationship different from the relationship for linear molecules. The presence of branched molecules, formed in high temperature polymerization at high degrees of conversion, or during fractionation, influences the viscosity [6, 7], and increases the value of the Huggins constant k', which represents the slope of the $[\eta]$ line relative to the abscissa axis [8, 9].

TABLE 1

Relationship Between Intrinsic Viscosity and Molecular Weight of Buna S; $[\eta] = KM^{\alpha}$

Polymerization temperature	$K \times 10^4$	α	Solvent	Temperature in °C	Reference
50	5.4	0.66	Toluene	30	[1]
50	5.4	0.66	Benzene	25	[2]
50	5.25	0.67	Toluene	25	[3]
Low-temperature (SKS-30A)	2.96	0.71	Benzene	25	[4]
5	1.8*	0.76*	Benzene	25	[5]

*Estimated from the influence of polymerization temperature on the value of α for polybutadiene and chloroprene.

The viscosity of Buna S polymerized at lower temperatures, with molecules of a lower degree of branching [4, 5], also has high values owing to increases of the value of α in the equation $[\eta] = KM^{\alpha}$. Moreover, in the published papers on the osmotic pressure of Buna S solutions in toluene or benzene use was made of linear extrapolation of the $\pi/c - c$ relationship. It is shown in the present paper that the $\pi/c - c$ relationship is represented by curves convex toward the concentration axis, and therefore linear extrapolation gives incorrect molecular weight values.

Data on the viscosity and osmotic pressure of 9 Buna S fractions are given in Tables 2 and 3. The curves for the $\pi/c - c$ relationship (Figure 1a) are represented by the equation

$$\pi / c = RT\,(1/M_n + A_2c + A_3c^2), \qquad (1)$$

or, according to Flory,

---

*This paper was published in Chinese in Acta Chimica Sinica 22, 249 (1956).

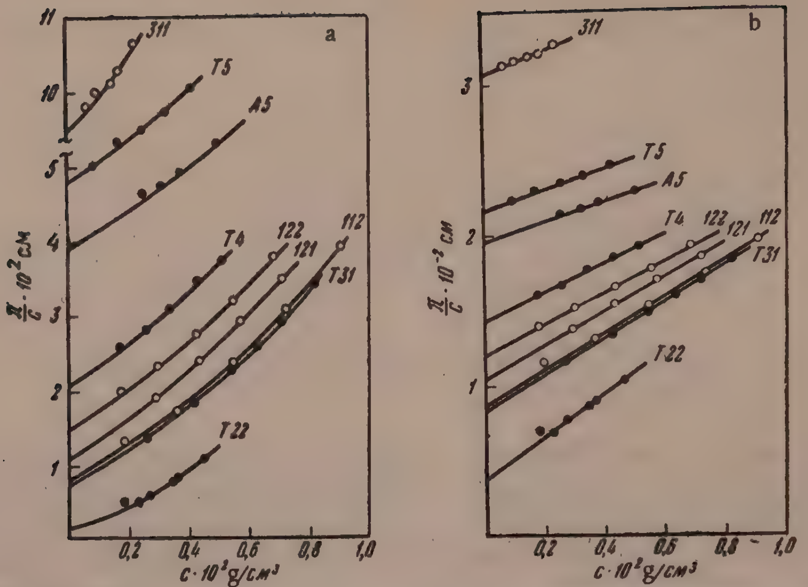

Fig. 1. $\pi/c - c$ (Figure a) and $(\pi/c)^{1/2} - c$ (Figure b) curves for Buna S fractions in toluene at 25°.

TABLE 2

Viscosity Data for Buna S Fractions in Toluene at 30°

$$\frac{\eta_r - 1}{c} = [\eta] + k'[\eta]^2 c; \quad \frac{\ln \eta_r}{c} = [\eta] - \beta\,[\eta]^2 c$$

Buna S fraction	Range of η_r	$[\eta]$	k'	β	$k' + \beta$
T22	1.80—1,20	4.76	0.76	—0.17	0.59
T31	2.48—1,49	2.72	0.52	0,05	0.57
T4	2.02—1,28	1.54	0.41	0,12	0.53
A5	1.99—1,37	0.92	0.40	0.14	0.54
T5	1.92—1,34	0.76	0.39	0.14	0.53
112	1.52—1,15	3,21	0.46	0.06	0.52
121	1.63—1,18	2.46	0.42	0.09	0.51
122	1.67—1,19	1.97	0.37	0.13	0.50
311	1.49—1,15	0.50	0.34	0.17	0.51

(2)

If we take $\Gamma_3 = g\Gamma_2^2$ at $g = \frac{1}{4}$, then a graphical plot of $(\pi/c)^{1/2}$ will also be linear [10]. This is confirmed by Figure 1b. Values of $(\pi/c)_0$, M_n, Γ_2 and RTA_2 obtained in this way are given in Table 3.

Cassasa [11] considered that polymer molecules dissolved in a good solvent the value of $A_2\overline{M}_w/[\eta]$ should be constant and independent of M. Schultz [12] obtained the value $A_2\overline{M}_w/[\eta] = 1.39$ for polyvinyl acetate in butanol at 25°. From the data obtained in the present investigation, the value of $A_2\overline{M}_w/[\eta]$ for Buna S in toluene at 30° (Figure 2) is 0.87. Apart from fractions T22 and T31, the molecules of which are apparently strongly branched, the $[\eta] - M$ relationship is represented by the equation (Figure 3):

TABLE 3

Osmotic Pressure Data for Buna S Fractions in Toluene at 25° (π in g/cm^2; c in g/cc)

Buna S fraction	$c \times 10^2$	h, см		$\pi/c \times 10^{-2}$	$(\pi/c)_0$	$\overline{M}_n \times 10^{-4}$	$\Gamma_2 \times 10^{-2}$	$RTA_2 \times 10^{-4}$
T22	0.1809	0,10	0 10	0.48	0.15	174	7.5	1.12
	0.2262	0,12	0.13	0.48				
	0.2714	0.18	0.19	0.60				
	0 3393	0.30	0.28	0.75				
	0.3619	0,34	0.32	0.80				
	0,4524	0.56	0.57	1.08				
T31	0.2609	0.40	0,42	1.36	0.71	34.9	2.9	2.06
	0,4170	0,87	0.89	1.82				
	0.5415	1,40	1,42	2.24				
	0.6256	1,86	1.89	2,58				
	0.7089	2.37	2.41	2.91				
	0.8160	3.17	3.24	3 39				
T4	0.1687	0.50	0.50	2,54	2.02	12,5	1,38	2.79
	0.2531	0,82	0.81	2.78				
	0.3375	1,20	1.21	3,07				
	0.5218	1.67	1.68	3.42				
	0.5062	2,17	2.17	3.70				
A5	0.2495	1,34	—	4.61	3.84	6.6	0.69	2.65
	0.3125	1.72	—	4.72				
	0.375	3.13	—	4.88				
	0.499	3,06	—	5.27				
T5	0.0817	0.46	0.49	4,99	4.75	5.3	0.61	2.90
	0.1634	0.99	1.02	5.29				
	0.2451	1.53	1.59	5.47				
	0.3268	2.15	2.21	5.72				
	0.4085	2.84	2,90	6.03				
112	0.1807	0.27	—	1.30	0.76	33.4	3.13	2.37
	0.3614	0.71	—	1.70				
	0.5420	1.45	—	2.33				
	0.7227	2.54	—	3.05				
	0.9034	4.01	—	3.86				
121	0.2849	0.62	—	1.88	1.10	23.0	2.17	2.39
	0.4273	1.16	—	2.37				
	0.5698	1.91	—	2.90				
	0.7123	2.83	—	3.45				
122	0.1704	0.38	—	1.95	1.47	17.2	1.72	2.53
	0.2922	0,78	—	2,31				
	0.4260	1.34	—	2,73				
	0.5453	1,99	—	3,16				
	0.6816	2,94	—	3,74				
311	0.0562	0.64	—	9.80	9,49	2.67	0,49	4.62
	0.0964	1.07	1.15	9.98				
	0.1406	1 63	1.66	10,09				
	0.1799	2.12	2.14	10,23				
	0.2249	2.75	2,78	10,62				

The higher value of α indicates that the fractions studied contain molecules of a lower degree of branching, as is shown by the values of α for polybutadiene samples polymerized at the same temperature but with different degrees of conversion [13]. The linear extrapolation of the $\pi/c - c$ relationship used by some workers would give high values of M. The higher the molecular weight, the greater would be the deviations of c and the lower the value of α.

EXPERIMENTAL

Fractionation. The material studied was emulsion-polymerized butadiene-styrene copolymer obtained at 50° with 80% conversion, with 71 : 29 butadiene : styrene ratio. The sample was extracted with acetone and fractionated three times by toluene-methanol mixture. Fractions T22, T31, T4, A5 and T5 were obtained from a sample which was dried under vacuum at 50° for 8.5 hours after acetone extraction. The fractions ob-

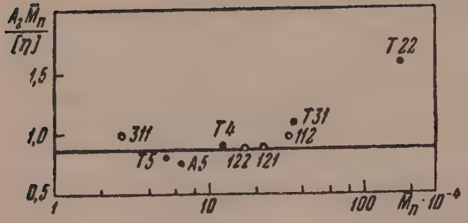

Fig. 2. Values of $A_2\overline{M}_n/[\eta]$ for Buna S fractions in toluene.

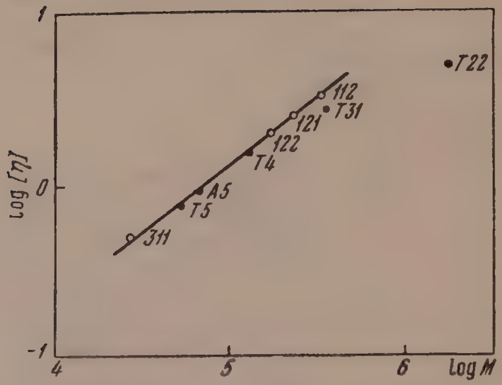

Fig. 3. log[η] – log M curves for Buna S in toluene.

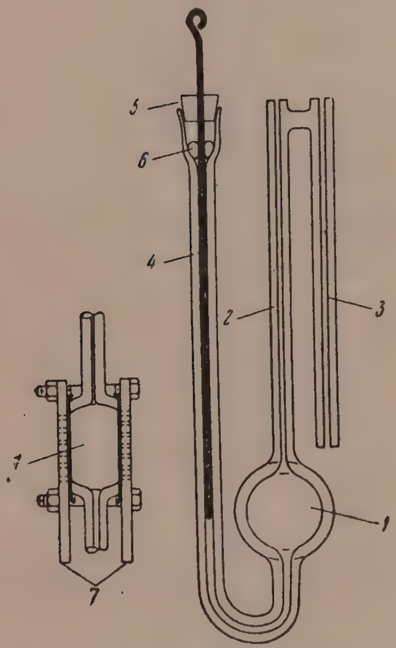

Fig. 4. Osmometer: 1) osmometric cell; 2) osmometric cell capillary; 3) reference capillary; 4) stainless steel wire; 5) bung; 6) mercury seal; 7) bronze plates.

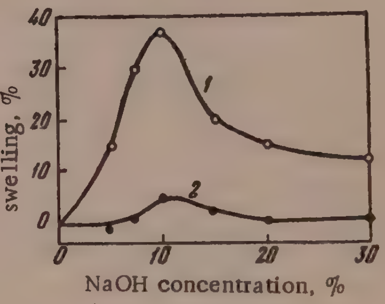

Fig. 5. Swelling of cellophane film in solutions: 1) parallel; 2) at right angles to the direction of winding.

tained after the second fractionation were kept in darkness in a nitrogen atmosphere for over seven months before the last fractionation. The final fractions were dried under vacuum at 30° for 8 hours, and then dissolved in toluene. Fractions 112, 121, 122 and 311 were not dried during purification and fractionation, and the precipitant-solvent mixture was driven off under vacuum. The viscosity and osmotic pressure were measured immediately after preparation of the solutions.

Osmotic pressure measurements. The osmometer used [14] (Figure 4) was a modification of the Zimm-Meyerson osmometer [15]. The measuring and control capillaries were chosen so that the difference of the capillary rise of the solvent did not exceed 0.015 cm. The semipermeable membrane was a cellophane film which had been consecutively swollen for half a minute in 20, 10 and 5% NaOH solutions. The film was then washed in water and kept for 2 hours in 50 and 95% ethanol solutions, 1 hour in absolute alcohol, and 2 hours in anhydrous ethanol-toluene mixture (50:50). As the film must not be allowed to dry, it was kept in toluene before use.

The swelling of cellophane film in NaOH solutions of various concentrations was studied. Figure 5 shows swelling curves for the film. It is seen that the swelling of the film is considerably greater in the longitudinal direction than at right angles to the direction of winding. The maximum swelling occurred in 10% NaOH solution. Equilibrium swelling was reached after several hours. The semipermeable membrane prepared in this way

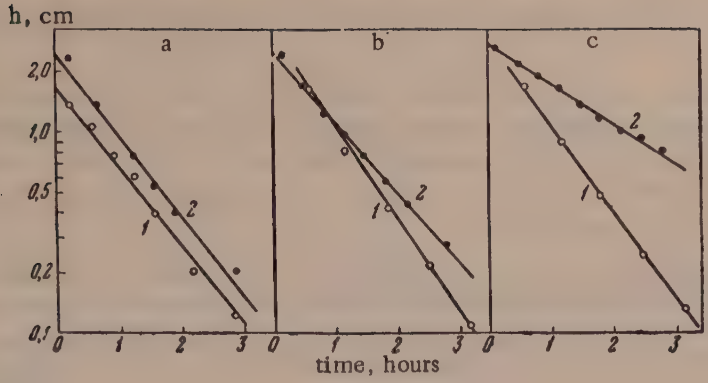

Fig. 6. Permeability of the membrane to the solvent after repeated use: a) kept in solvent; b) after use with sample of $\overline{M}_n = 7.5 \times 10^4$; c) the same, with sample of $\overline{M}_n = 3.3 \times 10^4$; 1) osmometer immediately after assembly; 2) after use during three months.

showed appreciable asymmetry at first, up to several millimeters of solvent column, but after the membrane had been kept in the solvent for a week the asymmetry did not exceed 0.02 cm. The membrane was tested for Buna S fractions of $\overline{M}_\eta = 33{,}000$ and 22,000. In the former case the osmotic pressure did not decrease for 5 days, while in the latter case it fell by 5% in the first day and then continued to decrease, but at a lower rate. Evidently membranes prepared in this way can be used for determination of molecular weights above 30,000.

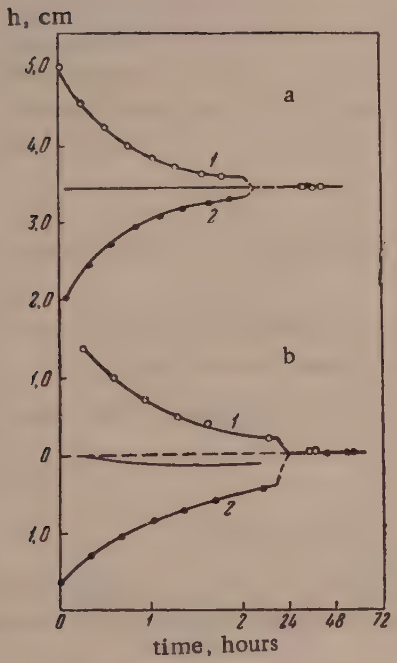

Fig. 7. Determination of osmotic pressure (a) and membrane asymmetry (b) by the half-sum method: 1) descending curve; 2) ascending curve.

7-11 osmometers were put into a thermostat at 25°, ± 0.01°. The osmotic pressure was measured by the static method. The difference between the heights of the liquid columns in the capillaries was read off by means of a cathetometer with an accuracy of 0.01 cm. Equilibrium became established in 24-48 hours, after which the liquid levels in the capillaries varied only as the result of temperature fluctuations, within ± 0.01-0.02 cm. Most of the readings were taken after equilibrium had been reached. In the molecular weight determinations the osmometers were first filled with the less concentrated solutions. When the solution was changed, the osmometer was rinsed out with the next more concentrated solution and kept in it for 15 minutes. When the fraction was changed, the osmometer was placed in the solvent for 2-3 days, the solvent being changed 3-4 times, until the asymmetry did not exceed 0.02 cm.

Variation of membrane permeability during use. The permeability of the membrane to a solvent may be represented by the equation [16]

$$a\,dh/dt = sAh,$$

or

$$\ln h = A/a \cdot st + \text{const},$$

where h is the difference between the liquid column heights in the measuring and control capillaries for time t; a is the capillary cross section; A is the effective membrane surface; s is the permeability constant for the membrane.

For a given osmometer, s can be characterized by the slope of the straight lines on $\ln h - t$ plots. An osmometer kept in a solvent for 3 months showed no change in the value of s for the membrane. However, the value of s decreased considerably after the membrane had been used with a polymer solution, especially with fractions of lower molecular weight, as is shown in Figure 6. This is probably the result of adsorption of polymer molecules in the pores of the membrane.

Deformation of the membrane during the experiment. The half-sum method is often cited in the literature [17] for the determination of osmotic pressure. It is then assumed that the semipermeable membranes are not deformed during the experiment. We found in determinations of asymmetry in solvents that, for the same difference of levels of the solvent moving through the membrane, the rate of rise was always greater than the rate of fall, although ultimately the rise and fall curves always met at the same equilibrium height. This shows that if the half-sum method is used for evaluation of membrane asymmetry a negative value would always be obtained as shown in Figure 7, and the osmotic pressure values would increase with increasing difference between the initial levels. However, in measurements of the osmotic pressure of polymer solutions both the half-sum method and the statistical method gave the same results; this can be explained by deformation of the membrane during the experiment. If the hydrostatic pressure outside the cell was higher than inside, the membrane could be bent into the cell. Thus, as the liquid level rose within the cell, the membrane would gradually expand with decrease of the rate of rise. If the hydrostatic pressure was greater inside than outside the cell, the membrane could not be deformed, as the cell was clamped between two bronze plates. In experiments with polymer solutions, although equilibrium was reached with rise and not fall of the liquid, the solution level within the cell was always higher than the solvent level outside the cell, and therefore deformation could not occur.

SUMMARY

1. An osmometric method for determination of molecular weight is described; the molecular weights of nine Buna S fractions have been determined.

2. The kinetics and maximum swelling of Cellophane membranes in 5-30% NaOH solutions have been determined. It is shown that the permeability of the membranes changes during repeated rise.

3. The $\pi/c - c$ relationship for the system studied is nonlinear. Linear extrapolation for determination of $\overline{M}_n$ and A_2 is possible if $(\pi/c)^{1/2}$ curves are plotted.

The A_2M_n/η ratio for Buna S is constant, irrespective of M.

4. The variation of $[\eta]$ with M is represented by the equation $[\eta] = 1.65 \cdot 10^{-4} M^{0.78}$.

The somewhat higher values of α obtained by previous workers are attributed to linear extrapolation of the $\pi/c - c$ plots, which does not take into account the presence of branched structures in the polymer solutions.

LITERATURE CITED

[1] D.M. French and R.H. Ewart, Ind. Eng. Chem. Anal. Ed. 19, 165 (1947).

[2] J.A. Yanko, J. Polymer Sci. 3, 576 (1948).

[3] R.L. Scott, W.C. Carter and M. Magat, J. Am. Chem. Soc. 71, 220 (1949).

[4] A.S. Novikov, M.B. Khaikina, T.V. Dorokhina and M.I. Arkhangelskaya, Colloid J. 15, 51 (1953) (T.p. 55).*

[5] W.C. Mochel and J.B. Nichols, Ind.Eng. Chem. 43, 154 (1951).

[6] L.H. Cragg and A.T. Brown, Can. J. Chem. 30, 1033 (1952).

---

*T.p. = C.B. Translation pagination.

[7] L.H. Cragg and G.R.H. Fern, J. Polymer Sci. 10, 2 (1953).

[8] R. Speiser and R. Whittenberger, J. Chem. Phys. 13, 349 (1945).

[9] J.A. Manson and L.H. Cragg, Can. J. Chem. 30, 482 (1952).

[10] U. Berglund-Larssen, cf. P.J. Flory, Principles of Polymer Chemistry (Cornell Univ. Press, Ithaca, 1953), p. 280.

[11] E.F. Cassasa, Thesis, MIT (1953), cf. ref. 12.

[12] A.R. Schultz, J. Am. Chem. Soc. 76, 3422 (1954).

[13] B.L. Johnson and R.D. Wolfangel, Ind. Eng. Chem. 44, 752 (1952).

[14] J.Y. Chien, W. Ching and I.H. Chuang, Reported in the First Conference on High Polymer Chemistry (Peking, October 1954).

[15] B.H. Zimm and I. Meyerson, J. Am. Chem. Soc. 68, 911 (1946).

[16] H.J. Philipp and C.F. Bjork, J. Polymer Sci. 6, 383 (1951).

[17] R.M. Fuoss and D.J.Mead, J. Phys. Chem. 47, 59 (1943).

Received November 2, 1956

Institute of Applied Chemistry
Academy of Sciences, China
Changchun

LETTERS TO THE EDITOR

THE EXTERNAL FRICTION OF RUBBER

V.V. Lavrentyev

There is no agreed opinion on the nature of the friction of rubber and the laws of friction.

Ratner and Sokolskaya [1] use the relationship:

$$F = \mu_{\infty} P + BP^{1-h}, \tag{1}$$

based on Deryagin's binomial law for solids. In Equation (1) F is the frictional force; P is the normal pressure; μ_{∞} and B are constants; μ_{∞} depends only on the micro- and macroroughness of the surface. The term $\underline{h}$ accounts for the hardness of the rubber. Ratner assumes that Equation (1) is valid for any normally applied loads; he determines the coefficient μ_{∞} by extrapolation of the $\mu - 1/P$ plot to $1/P \to 0$.

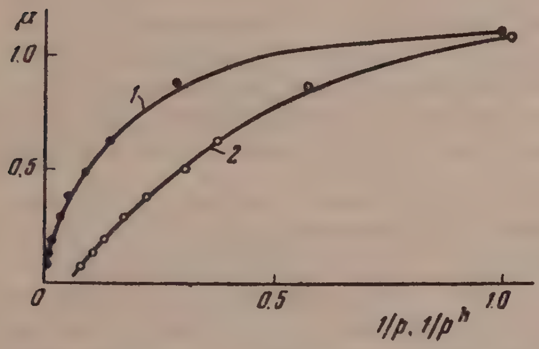

Fig. 1. Variation of the coefficient of friction with the normal nominal pressure in the friction of SKN-26 rubber against polished steel; 1) plotted in μ, $1/P$ coordinates; 2) plotted in μ, $1/P^h$ coordinates, where $h = 0.46$.

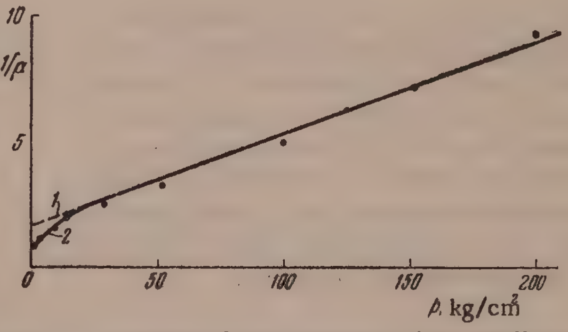

Fig. 2. Variation of the reciprocal of the coefficient of friction with normal nominal pressure, for the same data as in Figure 1. Curves calculated from: 1) Thirion's equation; 2) Bartenev's equation, with the following values for the constants: $C = 27.4$; $\alpha = 0.0023$; $S_0^A = 0.048\, S^N$; $S^N = 0.4$ cm².

According to Bartenev [2], the frictional force F for the sliding of rubber along smooth solid surfaces, calculated with the actual contact area S^A taken into account, is given by the following expression:

$$F = CS^A = CS^N(\nu_0 + \alpha P)\,/\,(1 + \alpha P). \tag{2}$$

where C, ν_0 and α are constant, and $\nu_0 = S_0^A/S^N$, P is the normal pressure in kg/cm²; S^N is the nominal contact area in cm². This equation for a residual contact area S_0^A after removal of the load, becomes the Thirion equation [3].

It follows from Equation (1) that the experimental data* should lie on a straight line, whereas the corresponding experimental relationship is nonlinear (Figure 1). Consequently the coefficients μ_∞ and B in Equation (1) are not constants.

---

*The testing method is described in [1]. In this method the force of initial friction is measured after a definite time of static contact.

By the Thirion equation

$$1/\mu_\infty = a + bP. \tag{3}$$

a straight line should be obtained in $1/\mu$, P coordinates. Figure 2 shows that deviations from linearity are found only at small loads. The theoretical Curve (2) corresponds to Equation (2); it describes the data over the whole range of loads. Therefore, the Thirion equation is in agreement with experimental data over a wide load range. The deviations at low loads are explained by the influence of the residual area of actual contact S_0^A, taken into account in Bartenev's equation.

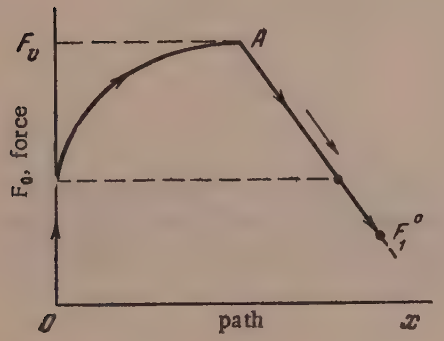

Fig. 3. Variation of tractive force with the sliding path of a rubber specimen on polished steel in a pendulum tribometer: F_0) initial or "static" friction at 20°; F_v) steady friction at sliding velocity v = 100 mm/minute; point A) traction stopped; F^0) frictional force when the specimen stops after the tractive force is removed; F_1^0) further decrease of tractive force owing to increase of temperature.

The molecular-kinetic nature of rubber friction is confirmed by our experiments on the influence of temperature on the force of friction on stopping. Figure 3 shows variations of tractive frictional force F as a function of the sliding path x (the experimental procedure is described in detail in [1]). At the point F^0 the solid support was heated above room temperature. The experiments showed that when the temperature was increased, even by 10°, the rubber specimen began to move with increased speed. At the point F^0 the specimen is either in very slow motion, or is retarded to a state of rest by the stronger bonds which arise between the rubber and the support on prolonged contact. Heating could either decrease F^0 (by rupture of the stronger bonds) or could simply increase the mobility of the contacting rubber molecules and hence the sliding rate of the rubber. To settle this question, we measured the frictional forces at temperatures from 23 to 90° under different normal loads.

In these experiments the decrease of the frictional force caused by the temperature increase was measured. To eliminate this effect, the possible decrease of the frictional force at a definite temperature and under normal load was compensated by an additional normal load. Nevertheless there was an appreciable shift of the specimen from the point F^0 on increase of temperature. This clearly shows that at the point F^0 the specimen was still in slow motion under normal conditions. Heating increases the sliding velocity of the rubber specimen. It must be taken into account that under the influence of prolonged thermal aging stable bonds are formed at the rubber-metal contact surface; to overcome these, large negative normal loads are sometimes required, greater than the strength of the rubber. This indicates that a certain number of more stable bonds may be formed during prolonged periods of contact at ordinary temperatures. Our experiments show in this case that the additional frictional force resulting from the influence of the contact time depends on the experimental conditions (roughness of the support, temperature, etc.).

The molecular nature of the friction of rubber and the conventional character of static friction are most predominantly seen at high temperatures (with short contact times) and under large normal loads. Formation of stable bonds on prolonged contact, and large amounts of filler in the rubber, mask the molecular nature of rubber friction.

LITERATURE CITED

[1] S.B. Ratner and V.D. Sokolskaya, Proc. Acad. Sci. USSR 99, 431 (1954).

[2] G.M. Bartenev, Proc. Acad. Sci. USSR 96, 1161 (1954); 103, 1017 (1953).

[3] P. Thirion, Rubb. Chem. Techn. 21, 505 (1948).

Received December 11, 1956

The V.M. Potemkin Moscow
Pedagogic Institute
Chair of Theoretical Physics

CURRENT EVENTS

NINTH CONFERENCE ON COMPOUNDS OF HIGH MOLECULAR WEIGHT

The Ninth Conference on Compounds of High Molecular Weight, devoted to general questions of chemistry and physics of high polymers, took place in Moscow from January 28 to February 1, 1957. The range of participants at the Conference, the diversity of the problems considered, and the depth of the discussions reflect not only the importance of the problems confronting polymer science, but also the broad sweep of the research which is proceeding in this field in our country.

About 1500 delegates took part in the Conference, including foreign scientists from the People's Republic of China, the German Democratic Republic, Poland, Rumania, Federal Republic of Germany, Israel, and Yugoslavia. Academician V.A. Kargin, in opening the Conference, reviewed the present state of polymer science and emphasized the urgent necessity for extending research work with the aim of finding new methods of polymer production and new classes of polymers, and of development of deep studies of the phenomena and mechanisms of processes which occur in the synthesis, conversion and utilization of polymeric materials.

About two hundred papers were presented at the meetings of six sections of the Conference.

The Section on Polymer Synthesis included 44 papers; in addition, 10 papers in the Section on Chemical Properties and Modification of Polymers also dealt with synthesis. A.N. Nesmeyanov, R.Kh. Freidlina and a group of their associates reported on the reaction of telomerization of CCl_4 and C_2H_4 and on new possibilities of obtaining monomers of great practical interest from the products of this reaction. In the paper by B.A. Dolgoplosk et al., a number of new systems which initiate polymerization reactions were described and the mechanism of their action examined. The papers by S.S. Medvedev et al., and by A.I. and S.T. Yurzhenko dealt with the mechanism of emulsion polymerization. A.N. Pravednikov and S.S. Medvedev gave convincing proofs for their proposed peculiar mechanism of the formation of the ω-polymer of chloroprene.

A.S. Semenova and E.V. Kuvshinsky reported the results of an investigation of the influence of pressure (up to 4000 kg/cm^2) on the polymerization kinetics of styrene. The paper by S.E. Bresler and his co-workers described the determination of free radical concentrations by means of the Hg^{203} radioactive isotope and by a radiospectroscopic method. Questions of diene hydrocarbon polymerization formed the subject of the papers by K.B. Piotrovsky and by teams of authors headed by A.A. Korotkov, N.I. Nikolaev and others. A.R. Gantmakher and S.S. Medvedev described in their paper the peculiarities of the kinetics of carbonium polymerization and copolymerization.

Interesting data on the synthesis and properties of certain polymers were reported in the papers by Yu.V. Mitin (on polymers containing aromatic rings in the chain), B.A. Dolgoplosk, E.I. Tinyakova, et al. (on carboxyl-containing rubbers), and I.A. Lifshits, S.I. Ilyina and V.N. Reikh (on piperylene polymers); the paper by S.A. Subbotin et al. gave the results of an investigation of isoprene rubber (synthesized under the guidance of A.A. Korotkov) similar to natural rubber in structure and properties. Polymerization of methyl methacrylate under the action of butyllithium yields a polymer of much higher heat stability than ordinary polymethyl methacrylate; this is the principal result of an investigation reported by A.A. Korotkov and his associates. Polymers (and copolymers) of certain unsaturated esters of phosphinic acids, described by G. Kamai and V.A. Kukhtin, have high flame resistance.

The papers by V.V. Korshak and his co-workers gave the results of studies of the polymerization and copolymerization of unsaturated organosilicon and organogermanium compounds, synthesis of polyesters of various dicarboxylic acids and glycols, and polycondensation of phosphine and phosphinic acid derivatives. M.F. Shostakovsky described methods of preparation and polymerization, and the properties of vinyl organosilicon compounds. The paper by O.Ya. Fedotova, M.A. Askarov and I.P. Losev dealt with synthesis and study of symmetrical diaminodiarylmethanes and polyamides derived from them. A.L. Klebansky and N.S. Vilesova reported interesting data on the synthesis of N-alkyl derivatives of hexamethylenediamine and their polycondensation with dibasic acids. T.S. Sogomonyants and M.V. Volkenshtein put forward experimental proofs of the influence of stereoisomerism on the properties of polymers (illustrated by certain polyamides and polyesters synthesized by them). Interesting papers were presented by the Czechoslovak scientists O. Wichterle and K. Vesely' on cationic polymerization of olefins.

At the Section entitled "Chemical Properties and Modification of Polymers" great interest and lively discussions were aroused by six papers on various aspects of rubber vulcanization (by B.A. Dogadkin and his coworkers, G.M. Bartenev, A.S. Priss and L.E. Vinnitsky); I.S. Okhrimenko reported some interesting results on the high pressure vulcanization of rubber. A.Ya. Drinberg and A.D. Yakovlev reported on the structurization of linear polymers. The paper by B.A. Dogadkin, A.V. Dobromyslova, et al. dealt with the influence of the structure of butadiene polymers on their chemical activity. Papers on various aspects of the chemistry and physical chemistry of cellulose and its derivatives comprised a considerable proportion of the Section (14 papers). These included descriptions of new derivatives of cellulose (papers by S.P. Danilov and A.A. Lopatenok, and by Z.A. Rogovin et al.) and of chitin (by E.A. Plisko); data were presented on the reactivity of primary and secondary hydroxyls (V.A. Derevitskaya et al., O.M. Klimova), and the results of studies of hydrolysis, oxidation, and thermal decomposition of cellulose and its derivatives were reported (V.I. Maiboroda and N.V. Mikhailov, O.P. Golova et al., O.P. Kozmina and V.I. Kurlyankina, M.M. Pavlyuchenko et al.). V.I. Ivanov and N.Ya. Lenshina reported on the properties of cellulose in relation to its use in chromatography.

Several papers dealt with polymer-analog conversions (of polyvinyl alcohol, by S.N. Ushakov and E.M. Lavrentyeva; of polyacrylonitrile, by A.A. Strepikheev, G.I. Kudryavtsev and E.A. Vasilyeva-Sokolova); E.A. Kurilchikov described the modification of certain fiber-forming polymers by proteins. Wan U Hey (People's Republic of China) gave an interesting paper on the study of caprolactam by end group titration.

The section on "Molecular Structure and Solutions of Polymers" contained papers giving the results of investigations of various materials by the most diverse methods. The paper by V.A. Kargin, S.Ya. Mirlina and N.F. Bakeev contained conclusions concerning the shape of the molecules of polyacrylic acid and its salts, based on electrochemical measurements and direct observations by means of the electron microscope. O.B. Ptitsyn reported on a detailed theory of light scattering by polymer solutions; the consequences of this theory are of considerable importance. Studies of light scattering, viscosity, diffusion, and flow birefringence of polymer solutions were described in a series of papers by V.N. Tsvetkov and his co-workers, and also by E.V. Frisman. The paper by I.Ya. Poddubnyi and E.G. Erenburg gave the results of a study of the connection between the conditions of rubber synthesis and the structure of the macromolecules formed, determined by studies of their solutions. S.M. Lipatov et al. and A.A. Tager reported results of thermodynamic investigations of polymer-solvent systems. In the paper by S.A. Glikman and L.A. Root reference was made to the possibility of studying intermolecular forces in polymer solutions by the dilatometric method. The paper by P.A. Rebinder and L.V. Ivanova-Chumakova was devoted to the general laws governing the viscoelastic properties of polymer solutions, and methods for studying them over a very wide concentration range — from very dilute solutions to the pure polymers. The papers presented by G.V. Vinogradov and his associates described methods and results of studies of the mechanical and optical polarization properties of concentrated polymer solutions.

In the paper by V.V. Korshak, S.A. Pavlova and G.L. Slonimsky a relationship was established between the molecular weight distribution function of polycondensation products and the polycondensation mechanism. I.Ya. Poddubnyi reported an investigation, which has practical significance, of the molecular weight distribution of divinyl-styrene rubbers. Teams of authors headed by V.V. Korshak and N.V. Mikhailov reported on the relationships between the properties and macromolecular structure of polyamides. S.S. Voyutsky et al. reported the results of a study of the relationship between the adhesive properties of polymers and macromolecular structure.

The controversial question of the structure of crystalline polymers was dealt with in papers by A.I. Kitaigorodsky and Yu.V. Mynukh, and by G.S. Markova and V.A. Kargin. Studies of internal rotation and rotational isomerism of polymeric molecules by the photoelastic method and by means of polarized infrared radiation were described in papers by teams headed by N.M. Bazhenov and V.N. Nikitin. Yu.Ya. Gotlib advanced a theory of birefringence in polymers and demonstrated that this theory is in satisfactory agreement with experimental data for several substances. Studies of dielectric properties were reported in papers by G.P. Mikhailov and T.I. Borisov (amorphous polymers), B.I. Sazhina (crystalline polymers), and O.D. Kurlienko (hydrophilic polymers). N.V. Mikhailov et al. reported the results of an investigation of polymer compatibility and the use of polymer mixtures for improving fiber properties. Several papers (S.N. Danilov and M.G. Okun, A.G. Pasynsky and A.M. Tongur, V.I. Kasatochkin, A.A. Alimov et al.) dealt with studies of natural compounds.

Interesting, but in many respects controversial views on the submicroscopic structure of polymers were advanced by K. Hess (Federal Republic of Germany). A.Katchalsky (Israel) gave two papers, on the principal properties of polyelectrolytes and on certain questions related to the direct conversion of chemical into mechanical energy.

At the Section entitled "Structure and Mechanics of Polymers" about thirty papers were presented and discussed. A very wide range of problems was covered by these papers. The papers by T.I. Sogolova and V.A. Kargin, and by A.A. Pozin et al., dealt with the mechanism and laws of the flow of polymers. High-elastic properties of polymers formed the subject of papers by G.M. Bartenev et al., G.L. Slonimsky, A.P. Kusov, G.A. Patrikeev, and E.V. Kuvhsinsky et al. The characteristics of relaxation processes in polymer glasses and the mechanical behavior of glassy polymers were discussed in the papers by M.V. Volkenshtein et al. and Yu.S. Lazurkin et al. Highly important questions of the strength and fatigue of polymer materials were considered in papers by A.A. Rogovina and V.A. Kargin, G.M. Bartenev et al., M.M. Reznikovsky et al., V.G. Epshtein, and V.E. Gul. S.B. Ratner and V.V. Lavrentyev reported the results of a study of the static friction of rubber, The value of the thermomechanical method of polymer investigation, in particular in relation to determination of the mechanism of hardening and the structure of three-dimensional polymers, was demonstrated in papers by L.A. Igonin and V.A. Kargin, B.M. Kovarskaya et al., and L.E. Kalinina, V.I. Alekseenko and S.S. Voyutsky. The paper by S.V. Vinogradov, G.L. Slonimsky and V.V. Korshak gave the results of a study of the mechanical properties of amorphous polyesters, and the relationship between the structure and molecular flexibility of these substances was discussed on the basis of the data obtained. V.P. Pavlov and G.V. Vinogradov described new apparatus by means of which it is possible to determine the instantaneous modulus and to study the relaxation behavior of easily deformed polymeric systems. N.A. Shchegolevskaya and S.N. Sokolov reported on the relationships established by them between the composition, structure and mechanical and optical (photoelastic) properties of certain multicomponent polymer systems. Chen Bao-Kun (People's Republic of China) devoted his paper to the viscoplastic properties of natural rubber. Prof. Porejko (Poland) dealt with some questions of the technology of polyvinyl chloride processing.

In the Section on "Aging and Degradation of Polymers" the papers reflected the attention paid by our investigators to studies not only of pure polymers but also of complex polymeric systems containing such components as solvents, fillers, etc. A series of papers dealt with questions of oxidation and photodegradation of vulcanizates and other systems containing rubber (by B.A. Dogadkin et al., T.G. Degteva and A.S. Kuzminsky, G.A. Patrikeev et al., Yu.S. Zuev and S.I. Pravednikova, N.N. Lezhnev,and A.S. Kuzminsky). The papers by V.V. Korshak et al., S.E. Bresler et al., N.V. Mikhailov et al., R.I. Gruz, and A.A. Vanshteidt gave the results of studies of the light and heat degradation of certain plastics and summarized work on the increase of their stability.

Papers by A.A. Berlin, G.L. Slonimsky et al., and N.K. Baramboim, dealing with problems of mechanochemistry, aroused great interest and lively discussions.

In the Section on "Applications and Methods of Polymer Control" more than 20 papers were presented. N.K. Moshchinskaya's paper dealt with the synthesis of diarylmethanes and the possibility of their use as plasticizers. S.A. Pavlov in his paper discussed the relationship between the chemical nature and properties of high polymers used in the production of artificial leather. Z.A. Rogovin and Z.A. Zazulina reported on a method for the production of a new fiber, ftorlon, which is of great practical interest. Several papers dealt with purification, utilization, and properties of cellulose and its derivatives and of starch. Interesting data on the sorption of dipolar ions by ion exchange resins were given by G.V. Samsonov and his associates. V.D. Bezuglyi and V.I. Dmitrieva reported on the successful use of a polarographic method in studying the production and processing of various plastics. G.N. Kukin devoted his paper to studies of the mechanical properties of textile materials, and B.I. Gengrinovich dealt with the plasticoelastic properties of rubbers and raw rubber compositions. L.A. Igonin and E.E. Glukhov described their new instruments, of great interest for studying the mechanical properties of polymeric materials. H. Klare (German Democratic Republic) presented interesting data obtained in studies of certain cellulose derivatives and viscose fibers. E. Correns (German Democratic Republic) devoted his paper to the reactivity of wood; C. Simionescu (Rumania) dealt with fractionation of cellulose. T. Rabek (Poland) reported the results of studies of the properties of ion exchange resins.

The participants at the Conference expressed the desire for the organization of a future series of meetings on individual questions — heat stability of polymers, some physical properties of polymer systems (viscosity and elasticity, thermodynamics of solutions, dielectric properties), aging and stabilization, mechanochemistry, artificial leather, polymerization and hardening at room temperatures, and apparatus for mechanical testing.

In closing the Conference, V.A. Kargin announced that, by the decision of the Commission on High Polymers of the Academy of Sciences USSR the next, 10th Conference, which is to be called in a year's time, will be devoted to biologically active polymers (proteins, nucleoproteins) and to models of such polymers.

Yu.M. Malinsky.

COLLOID JOURNAL OF THE U.S.S.R. IN ENGLISH TRANSLATION

July-August, 1957

TABLE OF CONTENTS

	Page	Russian page
Changes in the Structure, Degree of Dispersion and Yield Value of Peats as the Result of Complete Freezing. M.P. Volarovich, K.F. Gusev, S.N. Markov and V.P. Tropin	407	401
Investigation of Electroosmosis in Capillary Systems of Different Charge and Structure. O.N. Grigorov and K.P. Tikhomolova	411	406
Investigation of Adhesion Effects in Bonding Rubber to Metal by Leukonat Adhesive. A.M. Medvedeva, B.V. Deryagin and S.K. Zherebkov	417	412
Effect of Mercaptobenzothiazole on Structural Changes in Rubber on Oxidation, Heating and Plasticization. B. Dogadkin, A. Dobromyslova, L. Sapozhkova and I. Tutorsky	425	421
The Structure of Gels. 10. Globulization of Rubber Under the Action of Nonsolvents Added to Solutions. P.I. Zubov, Z.N. Zhurkina and V.A. Kargin	435	430
Sedimentation Volumes of Polydisperse Suspensions of $Ca_3(PO_4)_2$ in Electrolyte Solutions. G.G. Kandilarov	439	435
Gelatinized Emulsions. 14. Ethylcellulose as a Stabilizer of Emulsions of the W/O Type. L.Ya. Kremnev and G.A. Shadrin	443	440
Colloidochemical Processes in Reactions of Tetraalkoxysilanes with Aqueous Aluminate Solutions. A.P. Kreshkov, L.V. Myshlyaeva and L.M. Khananashvili	449	446
Study of the Colloidal Properties of Sulfosuccinic Acid Esters. 1. Esters of the Lower Aliphatic Alcohols. R.V. Kucher, A.A. Yavorsky and M.A. Kovbuz	457	454
Heat Evolution in the Initial Period of Hydration of Cement with Plasticizing Additions. O.I. Lukyanova, E.E. Segalova and P.A. Rebinder	461	459
Effect of Temperature on the Magnitude and Rate of Swelling of Agar. V.P. Mishin and N.D. Verderevskaya	467	472
Investigation of the Structure and Properties of Carbon Chain Polymers in Dilute Solutions. 3. Mixtures of Polyvinyl Chloride and Polyacrylonitrile. N.V. Mikhailov and S.G. Zelikman	473	465
Alteration of the Intermolecular Structure of Capron Fiber as the Result of Heat Treatment. L.I. Pokrovsky and A.B. Pakshver	479	478
Periodic Deformation of Collagen in Solutions of Electrolytes and Tanning Agents. A.G. Pasynsky and A.M. Tongur	483	483
Effect of Atmospheric Turbulence on the Kinetics of Aerosol Coagulation. O.M. Todes and A.A. Chekunov	489	490
Settling of Aerosol Particles on the Walls of an Enclosed Space. I. Todorov and A. Sheludko	495	496
Application of the Method of Approximations to Calculations of Flow of Disperse Systems. N.V. Tyabin and G.V. Vinogradov	505	505
Effect of Electrolytes on the Structuromechanical Properties of Bentonite Suspensions. I.A. Uskov	511	511
Relationship Between the Intrinsic Viscosity and Molecular Weight of Buna S Rubber. Chien Jen-Yuan, Ching Wen and Cheng Yung-Shih	515	515

TABLE OF CONTENTS (Continued)

	Page	Russian page

Letters to the Editor

The External Friction of Rubber. V.V. Lavrentyev	523	522

Current Events

Ninth Conference on Compounds of High Molecular Weight. Yu.M. Malinsky	527	524

SOVIET RESEARCH
in
CATALYSIS

Chemistry Collection No. 3. Covers all aspects of catalysis; papers selected from all Soviet chemical journals translated by Consultants Bureau, 1949-1955.

Sections may be purchased separately as follows:

I.	Theoretical and Sundry Associated Effects	262 pages	$50.-	
IIa.	General	250 pages	50.-	$125.-
IIb.	General	250 pages	50.-	
IIc.	General: Reduction-Oxidation and Fischer-Tropsch	214 pages	50.-	
III.	Hydrogenation Dehydrogenation Cracking	294 pages	50.-	
IV.	Isomerization Alkylation Dehydration	274 pages		$50.-
V.	Polymerization Friedel-Crafts Zeigler	128 pages		30.-

The Collection, comprising 1,672 pages, 262 papers may be purchased as a unit for **$200.00**

Individual papers are available separately – Table of Contents on request.

CONSULTANTS BUREAU, INC.

227 WEST 17TH STREET, NEW YORK 11, N. Y.

C B

Landau and Smorodinsky
LECTURES ON NUCLEAR THEORY
IN COMPLETE ENGLISH TRANSLATION

RUSSIAN–ENGLISH SOLID
STATE PHYSICS GLOSSARY

LECTURES ON NUCLEAR THEORY, by L. Landau and Ya. Smorodinsky is a concise presentation of some of the basic concepts of nuclear theory; based on a series of lectures to experimental physicists (by Landau) in 1954. Since there is no complete theory of nuclear forces at this time, conclusions about nuclear structure are limited to those based on experimental data, using only general quantum-mechanical relations. New experimental results are indicated.

English translation, 79 pages, $15.00

* * *

RUSSIAN-ENGLISH PHYSICS DICTIONARY AND SUBJECT GLOSSARIES

GLOSSARIES PUBLISHED — STILL AVAILABLE — $10.00 EACH

NUCLEAR PHYSICS AND ENGINEERING—Over 12,000 Russian terms. Contains all terms in USSR Academy of Sciences Dictionary of Nuclear Physics and Engineering. 195 pages

SOLID STATE PHYSICS—4,000 Russian terms. Covers solid state theory, crystallography, metallurgy, physics of metals, ferromagnetism, semiconductors, important general quantum theory, electronics. 90 pages

ELECTRONICS AND PHYSICS—Over 22,000 Russian terms. 11 page, 10 section appendix covers US–Soviet vacuum tube equivalents, unit equivalents, circuit components and notations, abbreviations. Specifies fields in which terms are used as explained. 343 pages

GLOSSARIES IN PREPARATION—$10.00 EACH—Electricity and Magnetism; Acoustics and Shock Waves; Liquids and Hydraulics; Mechanics and General Physics; Atomic Physics, Spectroscopy, Optics.

Glossary text clearly reproduced by multilith process from varitype copy; staple bound in durable paper covers.

Pre-publication subscribers to the up-to-date, comprehensive, authoritative, Russian-English Physics Dictionary, which will be published in permanently bound, indexed form in 1959, will also receive, as soon as it is published, a free copy of each of the 8 *interim* glossaries above ALL FOR ONLY $50.00

Consultants Bureau *cover-to-cover* translations by *bilingual physicists,* including all diagrammatic and tabular material; books staple bound in durable paper covers; text clearly reproduced by multilith process.

CONSULTANTS BUREAU, INC.

227 WEST 17th STREET, NEW YORK 11, N. Y. — U.S.A.
Telephone: Algonquin 5-0713 • Cable Address: CONBUREAU, NEW YORK